

ENHANCING THE COOLING SYSTEM OF A
RESIDENTIAL BUILDING USING INTEGRATED
BUILDING INFORMATION MODELLING WITH
SOLAR ABSORPTION SYSTEM

ALI ABDULQADER MUSTAFA AL-QAYSI

UNIVERSITI TUN HUSSEIN ONN MALAYSIA

UNIVERSITI TUN HUSSEIN ONN MALAYSIA

STATUS CONFIRMATION FOR THESIS
MASTER'S DEGREE

ENHANCING THE COOLING SYSTEM OF A RESIDENTIAL BUILDING
USING INTEGRATED BUILDING INFORMATION MODELLING WITH
SOLAR ABSORPTION SYSTEM

ACADEMIC SESSION : 2021/2022

I, **ALI ABDULQADER MUSTAFA AL-QAYSI**, agree to allow this Thesis to be kept at the Library under the following terms:

1. This Thesis is the property of the Universiti Tun Hussein Onn Malaysia.
2. The library has the right to make copies for educational purposes only.
3. The library is allowed to make copies of this report for educational exchange between higher educational institutions.
4. The library is allowed to make available full text access of the digital copy via the internet by Universiti Tun Hussein Onn Malaysia in downloadable format provided that the Thesis is not subject to an embargo. Should an embargo be in place, the digital copy will only be made available as set out above once the embargo has expired.
5. ** Please Mark (√)

CONFIDENTIAL

(Contains information of high security or of great importance to Malaysia as STIPULATED under the OFFICIAL SECRET ACT 1972) *Title and Abstract only*

RESTRICTED

(Contains restricted information as determined by the Organization/institution where research was conducted) *Title, Abstract and Introduction only*

EMBARGO

_____ until _____
(date) (date)

FREE ACCESS

Approved by,

ali

(ALI ABDULQADER MUSTAFA AL-QAYSI) (PROF. MADYA TS DR. ZAMRI BIN NORANAI)

Permanent Address:
35, KATHA, BAGHDAD
IRAQ

Date : 6/9/2022

Date: _____

NOTE:

** If this Thesis classified as CONFIDENTIAL or RESTRICTED, please attach the letter from the relevant authority/organization stating reasons and duration for such classifications.

This thesis has been examined on date 13th April 2022
and is sufficient in fulfilling the scope and quality for the purpose of awarding the
Degree of Master of Engineering.

Chairperson:

DR. WAN SAIFUL-ISLAM BIN WAN SALIM
Faculty of Mechanical Engineering and Manufacturing
Universiti Tun Hussein Onn Malaysia

Examiners:

DR. IR. TS. MOHD ZAID BIN AKOP
Faculty of Mechanical Engineering
Universiti Teknikal Malaysia Melaka

ASSOC. PROF. DR. MOHD FAIZAL BIN MOHIDEEN BATCHA
Faculty of Mechanical Engineering and Manufacturing
Universiti Tun Hussein Onn Malaysia



PUTRA UTHM
PUSHTAKAAN TUNKU TUN AMINAH

ENHANCING THE COOLING SYSTEM OF A RESIDENTIAL BUILDING
USING INTEGRATED BUILDING INFORMATION MODELLING WITH
SOLAR ABSORPTION SYSTEM

ALI ABDULQADER MUSTAFA AL-QAYSI

A thesis submitted in
fulfilment of the requirement for the award of the
Master of Degree in Mechanical Engineering

Faculty of Mechanical and Manufacturing Engineering
Universiti Tun Hussein Onn Malaysia

SEPTEMBER 2022

I hereby declare that the work in this thesis is my own except for quotations and summaries which have been duly acknowledged

Student: *ali*
.....
ALI ABDULQADER MUSTAFA AL-QAYSI

Date: 6/9/2022
.....

Supervisor:
PROF. MADYA TS DR. ZAMRI BIN NORANAI



PTTA ALUTHM
PERPUSTAKAAN TUNJUNGAN AMINAH

To who left me early My Father

To whom the Heaven under her feet ... My Mother

To the soulmate ... My Wife

To whom I live For ... Abdulqader and Rooh



PTTA UTHM
PERPUSTAKAAN TUNKU TUN AMINAH

ACKNOWLEDGEMENT

Thanks to Almighty ALLAH, whose grace and mercy have made this study a success. I wish to gratefully thank my supervisor Professor Dr. Zamri Bin Noranai for his guidance and support throughout this study. His outstanding supervision and knowledge, creative suggestions, unbreakable enthusiasm and patience through this long research program has added a new dimension to my research ability. I do not think that words are capable of describing his effort in making this research successful.

I also would like to express my deep gratitude and appreciation to (Dr. Adel Mohsen) for his contribution and continuous attention thorough comments, valuable advice, encouragement and support during the excellent supervision of this work. Deep appreciation to Mr. Ali Habeeb Askar, a kind person who gives without charge.



PTTA UTHM
PERPUSTAKAAN TUNKU TUN AMINAH

ABSTRACT

Building energy management is concerned with the energy consumption of the building. The used electricity in the residential building has the highest percentage when applying HVAC systems among all other building services installations and other electric appliances. For that, the present work focuses on the cooling load capacity issues and the methods to reduce the amount of electricity used in the building, particularly in air conditioning systems. In order to achieve this target, three main steps were applied; the first step was calculating the cooling load capacity by using the Cooling Load Temperature Difference method (CLTD) method. The second step was to find a sustainable wall material that could reduce the cooling load requirements using Building Information Model (BIM). The sustainable material was a new type of concrete block with a high insulation capability. The final step was to analyse the required energy of the cooling system device by using an applied Engineering Equation Solver (EES) to obtain accurate results. Two types of cooling systems were tested to determine the economic device based on the energy required to operate them under the same conditions. The two cooling systems were the conventional vapour-compression and solar absorption systems. The EES program evaluates the mathematical model and calculations for these systems to investigate the performance coefficient of the selected air-conditioning systems within (May, June, July and August) months in Iraq. This program evaluated the cooling systems by calculating the cost of used power. The results observed that the use of sustainable material reduces the building energy consumption by about 20%, and the solar absorption system is the best device for cooling systems. The solar absorption system provided the best COP in May, which was 0.8048.

ABSTRAK

Pengurusan tenaga bangunan adalah berkaitan penggunaan tenaga di bangunan. Penggunaan elektrik di bangunan kediaman memperolehi peratus yang tertinggi apabila sistem HVAC digunakan bersama pemasangan perkhidmatan dan perkakasan elektrik yang lain. Oleh itu, kajian ini tertumpu kepada isu beban pendinginan dan kaedah untuk mengurangkan jumlah penggunaan elektrik dalam bangunan terutamanya pada penyaman udara. Untuk mencapai sasaran ini, tiga langkah utama telah digunakan; langkah pertama ialah mengira kekuatan beban penyejukan dengan kaedah *Cooling Load Temperature Difference (CLTD)*. Langkah kedua melibatkan penentuan bahan dinding mampan yang mampu mengurangkan permintaan beban pendinginan dengan menggunakan *Building Information Model (BIM)*. Bahan mampan adalah bahan baru bongkah konkrit yang berkapasiti tebatan tinggi. Langkah akhir adalah untuk menganalisa permintaan tenaga untuk sistem peranti penyejukan dengan penggunaan *Engineering Equation Solver (EES)* untuk menghasilkan keputusan yang jitu. Dua jenis sistem pendinginan diuji untuk menentukan peranti ekonomi berdasarkan keperluan tenaga operasi di bawah kondisi yang sama. Dua sistem pendinginan tersebut adalah mampatan-wap lazim dan penyerapan tenaga suria. Model matematik dan pengiraan sistem ini dinilai dengan program EES untuk mendapatkan kecekapan penyaman udara diantara bulan yang terpilih (Mei, Jun, Jul dan Ogos) di Iraq. Perisian ini menilai sistem pendinginan dengan mengira kos penggunaan tenaga. Keputusannya penggunaan bahan mampan didapati dapat mengurangkan penggunaan tenaga bangunan sebanyak 20% dan sistem serapan suria adalah terbaik untuk sistem pendinginan. Sistem penyerapan suria memberikan COP yang terbaik pada bulan Mei dengan nilai 0.8048.

CONTENTS

	TITLE	i
	DECLARATION	ii
	DEDICATION	iii
	ACKNOWLEDGEMENT	iv
	ABSTRACT	v
	ABSTRAK	vi
	CONTENTS	vii
	LIST OF TABLES	xi
	LIST OF FIGURES	xiii
	LIST OF SYMBOL AND ABBREVIATIONS	xvi
	LIST OF APPENDICES	xviii
CHAPTER 1	INTRODUCTION	1
	1.1 Introduction	1
	1.2 Research Background	2
	1.3 Problem Statement	3
	1.4 Research Question	4
	1.5 Objective	4
	1.6 Scope of Research	5
	1.7 Research Gap Error! Bookmark not defined.	
	1.8 Significant of Research	5
	1.9 Thesis Organization	6
CHAPTER 2	LITERATURE REVIEW	7
	2.1 Introduction	7
	2.2 Air Conditioning System	7
	2.2.1 Refrigeration Cycle	8
	2.3 Cooling Load Temperature Difference	
	Method	10
	2.4 Building Information Modelling	12

2.4.1	BIM Scope	14
2.4.2	BIM and Energy Performance Analysis	15
2.5	Solar Energy	16
2.6	Application of Solar Energy	17
2.7	Types of Solar Collectors	17
2.7.1	Flat Plate Collector	19
2.7.2	Evacuated Tube Collectors	20
2.7.3	Parabolic Trough Collectors	21
2.7.4	Fresnel Solar Collectors	22
2.7.5	Composite Equivalent Solar Complex Collectors	23
2.7.6	Heliostat Field Collectors	24
2.8	Types of Solar Cooling Technologies	26
2.9	Solar Powered Absorption Cooling System	28
2.10	Theoretical Analysis and Simulation of Absorption System	29
2.11	Experimental Investigation of Absorption System	38
2.12	Solar Powered Absorption Cooling New Design Opportunities	42
2.13	System Optimization of Absorption System	45
2.14	Summary of previous research of the Solar Absorption System	47
2.15	Summary	52
CHAPTER 3	METHODOLOGY	53
3.1	Introduction	53
3.2	Research Flow Chart	54
3.3	Case Study Location	55
3.4	Climate Condition	57
3.5	Comfort Condition	59
3.6	Building Characteristic	60

3.7	Cooling Load Calculation	61
3.8	Load Component	61
3.9	Cooling Load Temperature Difference (CLTD)	63
3.9.1	Solar Heat Gain through Glass	64
3.9.2	Heat Gain from Occupants	65
3.9.3	Heat Gain from Lighting and Electric Equipment	66
3.9.4	Infiltration Heat Gain	68
3.10	Assumptions	70
3.11	BIM Model	70
3.11.1	As-built 3D BIM Model	71
3.12	Cooling System	73
3.12.1	System Design	73
3.13	Evaluation Method	74
3.14	Technical simulation of absorption system and vapour compression system	75
3.15	Engineering Equation Solver (EES)	78
CHAPTER 4 SIMULATION RESULTS AND DISCUSSION		81
4.1	Introduction	81
4.2	Design Condition	81
4.3	Cooling Load Temperature Results	83
4.3.1	Results of First Floor	84
4.3.2	Results of Second Floor	85
4.3.3	Results of Third Floor	86
4.3.4	Load Summation	87
4.4	Results of BIM Model	88
4.5	Results of Conventional Vapour Compression System	91
4.6	Result of Solar Absorption System	93
4.6.1	COP for Absorption System	93
4.6.2	Temperature Component Effect on Coefficient of Performance of Solar Absorption System	96

4.7	Evaluate Results of Power Consumption	98
4.8	Investment Cost for Vapour Compression System and Absorption System	99
4.9	Annual Operation Cost for Vapour Compression System and Absorption System	99
4.9.1	Annual Operation Cost at Rate 0.10 \$/kWh	99
4.9.2	Annual Operation Cost at Rate 0.066 \$/kWh	100
4.9.3	Annual Operation Cost at Rate 0.029 \$/kWh	100
4.9.4	Annual Operation Cost at Rate 0.016 \$/kWh	101
4.9.5	Summary of Analysis Cost	101
4.10	Discussion	102
4.11	Summary of Simulation Result	104
CHAPTER 5	CONCLUSION AND RECOMMENDATION	106
5.1	Introduction	106
5.2	Conclusion	107
5.3	Limitations of the Study	109
5.4	Recommendations	109
	REFERENCES	111
	APPENDIX A	121
	LIST OF PUBLICATIONS	134
	VITA	135

LIST OF TABLES

2.1	Conditions under which solar collectors operate (Real et al., 2014)	25
2.2	Absorption chiller: solar thermal collector matching (Shirazi et al.,2018)	26
2.3	The principal operational used parameters of the solar-powered single-effect absorption cooling systems (Zhai et al., 2011)	29
2.4	Summary of previous research of the absorption system	47
3.1	Average temperature guide (°C) for the city of Baghdad	58
3.2	Effective temperature day manual (°C) to the city of Baghdad	59
3.3	Building Characteristic	61
3.4	Components of Cooling Load	63
3.5	Number of Air Variations per Hour (Shubbar et al., 2017)	68
3.6	Electricity rates for Rosenthal building in Iraq (Iraqi ministry of electricity)	74
3.7	Cost Rate of key parameters of economic analysis	75
4.1	Design Criteria Data of Dry Bulb temperature (Iraqi metrological)	82
4.2	Design Criteria Data of wet Bulb temperature (Iraqi metrological)	82
4.3	Design Criteria Data of Humidity ratio (Iraqi metrological)	82
4.4	Numerical results of first-floor heat calculation	84
4.5	Numerical results of second-floor heat calculation	86
4.6	Numerical results of third-floor heat calculation	87
4.7	Summary of the CLTD results	87

4.8	The standard condition for the VCRS	92
4.9	Design temperature variables in August	93
4.10	Results of COP Absorption system in the hot season of Baghdad	94
4.11	The investment cost for the Vapour Compression system and Absorption system	99
4.12	Annual operation cost for VC system and Absorption system at a rate of 0.10\$/kWh	99
4.13	Annual operation cost for VC system and Absorption system at a rate of 0.066\$/kWh	100
4.14	Annual operation cost for VC system and Absorption system at a rate of 0.029\$/kWh	100
4.15	Annual operation cost for VC system and Absorption system at a rate of 0.016 \$/kWh	101
4.16	Payback periods versus electricity rate range	102
4.17	Payback period versus electricity rate range with 50% government subsidy	103
4.18	Summary of the simulation results for the Vapour Compression system and Absorption system	104



LIST OF FIGURES

1.1	Thermal insulation system for residential building (Ruuska & Häkkinen, 2014)	3
2.1	Compressive cooling cycle (Yang et al., 2022)	10
2.2	2D data exchange in comparison with BIM interoperability	13
2.3	BIM based energy analysis showing the windrose and solar path on the BIM model (Samuel et al., 2016)	16
2.4	Types of solar collectors	18
2.5	Flat plate collectors (Shirazi et al.2018)	19
2.6	Evacuated tube collectors (Suman et al., 2015)	20
2.7	Parabolic trough collectors (Shirazi et al., 2018)	21
2.8	Fresnel Solar collectors (Facão et al., 2011)	22
2.9	Composite equivalent solar complex collectors (Bellos et al., 2016)	24
2.10	Heliostat field collectors (Marc et al., 2010)	25
2.11	Types of solar cooling technologies	27
2.12	Emerald's impact on the annual solar fraction caused by hot water tanks (Baniyounes, Rasul, & Khan, 2013)	32
2.13	Annual solar fraction Gladstone as a function of hot water tank (Baniyounes, Rasul, & Khan, 2013)	33
2.14	Annual solar fraction Rock Hampton as a function of hot water tank (Baniyounes, Rasul, & Khan, 2013)	33
3.1	Flow chart of Research Study	54
3.2	Location of the residential building (Kithara city, Baghdad, Iraq)	55
3.3	Ground Floor of the residential building	56
3.4	First floor of the residential building	56
3.5	Second floor of the residential building	57

3.6	Climate Annual Condition (ASTM E2877)	58
3.7	Comfort Condition Based on Psychrometric Chart (Paoli., 2012)	60
3.8	Excel Sheet for result observation	64
3.9	Heat gain through glass sheet	65
3.10	Occupant Heat Gain Sheet	66
3.11	Lightning Heat Gain Sheet	68
3.12	Opaque surfaces heat gain sheet	70
3.13	BIM- Rivet drawing geometry result	72
3.14	BIM- Rivet drawing sun rise result	72
3.15	Solar absorption cooling process (Ayau & Coronas., 2020)	74
3.16	LiBr-H ₂ O absorption system	76
3.17	Input process in EES software	79
3.18	Results of EES Software	80
4.1	The main factors for building heat load calculation	83
4.2	First-floor rooms dimensions	84
4.3	Second-floor rooms dimensions	85
4.4	Third Floor Room Dimensions	86
4.5	Solar angle results	88
4.6	Effect of solar angle	89
4.7	Thermal evaluation by Rivet software	89
4.8	Solar heat effect (Case 1)	90
4.9	Solar heat effect (Case 2)	91
4.10	The solution window of the EES program for the Vapour Compression system	92
4.11	The solution window of the EES program for the absorption system in the condition of August	93
4.12	The coefficient of performance with temperature of generator	95
4.13	The coefficient of performance with temperature of condenser	95
4.14	The effects of the generator temperature of the solar system on the coefficient of performance	96

4.15	The effects of the condenser temperature of the solar Absorption system on the coefficient of performance	97
4.16	The effect of the absorber temperature of the solar Absorption system on the coefficient of performance	98
4.17	Payback periods by electricity rate	102
4.18	Payback periods by electricity rate with 50% government subsidy	103



LIST OF SYMBOL AND ABBREVIATIONS

<i>AC</i>	-	Air-conditioning
<i>ACF</i>	-	Annual cash flow
<i>CLF</i>	-	Cooling load factor
<i>CLTD</i>	-	Cooling load temperature change
<i>C.O.P</i>	-	Coefficient of Performance
<i>CO₂</i>	-	Carbon dioxide
<i>DMEU</i>	-	Di methyl ethylene urea
<i>h</i>	-	Enthalpy (kJ/kg)
<i>HCFC</i>	-	hydrochlorofluorocarbon
<i>HFC</i>	-	hydrofluorocarbon
<i>HVAC</i>	-	Heat ventilation air-conditioning
<i>IC</i>	-	Investment cost
<i>kWh</i>	-	kilowatt-hour
<i>Kg</i>	-	kilogram
<i>LiBr- H₂O</i>	-	Lithium Bromide- Water
<i>m</i>	-	mass flow rate (kg/s)
<i>NH₃- H₂O</i>	-	Ammonia- Water
<i>P_e</i>	-	Pressure of evaporator
<i>PBP</i>	-	payback period (year)
<i>PCM</i>	-	Phase-change material
<i>PHX</i>	-	plate heat exchanger
<i>PMV</i>	-	Predicted mean vote
<i>PPD</i>	-	Predicted percentage dissatisfied
<i>PTAC</i>	-	Package terminal air conditioning system
<i>PV</i>	-	Photovoltaic
<i>Q_C</i>	-	rate of heat input to condenser (kW)
<i>Q_E</i>	-	refrigeration effect (kW)

Q_G	-	rate of heat input to generator (kW)
S	-	Specific entropy, J/(kg K)
SCL	-	Solar cooling load
$TETD$	-	Time equivalent temperature difference
T_{abc}	-	Heat of absorber ($^{\circ}\text{C}$)
T_C	-	Heat of condenser ($^{\circ}\text{C}$)
T_g	-	Heat of generator ($^{\circ}\text{C}$)
T_{Win}	-	Internal water temperature ($^{\circ}\text{C}$)
T_{Wout}	-	Outer water temperature ($^{\circ}\text{C}$)
W_{Comp}	-	Work of compressor
X	-	Constant of solution

Greek Letters

η	-	Efficiency
--------	---	------------

Subscripts

e	-	evaporator
g	-	generator
r	-	refrigerant
ss	-	strong refrigerant-absorbent solution
ws	-	weak refrigerant-absorbent solution
$1-5$	-	system state points



LIST OF APPENDICES

APPENDIX	TITLE	PAGE
A	Investments cost	122
B	Coefficient of performance for VC system	126
C	Codes of EES program of absorption system and vapour compression system	128



PTTA UTHM
PERPUSTAKAAN TUNKU TUN AMINAH

CHAPTER 1

INTRODUCTION

1.1 Introduction

Improving energy efficiency is considered a cost-effective strategy for building economies. The total contribution of building energy consumption has risen and surpassed the other primary sectors, such as transport and industrial sectors. It makes up nearly 40% of emerging countries' energy consumption (Farah 2016). In order to control the energy used in residential buildings, the use of heating, ventilation, and air-conditioning (HVAC) systems are the central components which must be considered in the energy consumption. The researcher focused on this issue due to its importance in energy consumption. Realizing building energy efficiency is essential in calculating the cooling load of a building; this is the primary procedural approach to achieve this target. Cooling load computation is the first step in designing building air conditioning systems (Wang et al., 2018). It measures the required energy that consumes power based on Energy Efficiency Ratio, which represents the appliance's cost.



1.2 Research Background

The vast extent of residential buildings observed a problem of increasing demand for electricity due to the need to create a comfortable environment inside the building. A comfortable life involves various instruments and devices that are used by the people live day. The extent of these instruments and devices increases the electricity demand and causes a non-significance environmental effect such as a high rise in environmental temperature due to the ozone damage from CO_x and NO_x. The growth in the number of buildings that require summer air-conditioning are the augmented thermal load, the increase in living standards and the human needs of the occupants. In addition, the architectural features and trends of buildings include the growth in the percentage of transparent to solid surfaces in the cover of building and extend to ordinary buildings of glass covering.

In particular, in large systems ranging around (50 kW) and beyond, various techniques of heat-driven cooling exist on the market that could be utilized in combination with solar thermal collectors. Currently, 30% of used energy is utilized to cool or heat residential and commercial buildings that have received growing focus today (Chang, Lin, & Chung, 2013). In the 1980s, solar energy regimes for air-conditioning use evolved, especially in the U.S. and Japan. The evolution of the solar air conditioning (SAC) method is preferred due to its economic profit. In previous works (Bellos & Tzivanidis, 2017) concerning heating and cooling consumption analysis, it is proposed to consider an integrated tactic for energy saving assessment. Furthermore, in solar air-conditioning systems, performance is highly related to external circumstances and the dynamics of the cooling load (Bellos et al., 2017).

Many researchers have implemented several methods to decrease the effect of using conventional energy resources. They tried to change the types of used material in building construction and add insulation material to protect the residential occupants, as shown in Figure 1.1 (Ruuska & Häkkinen, 2014). Other researchers developed or suggested new methods to use natural resources to heat or cool the buildings, such as using earth heat (Jain et al., 2013). Nowadays, most international cooperative projects use solar energy as a promising renewable energy resource (Eicker et al., 2012).



Figure 1.1: Thermal insulation system for residential building (Ruuska & Häkkinen, 2014)

1.3 Problem Statement

Buildings in Iraq need to be improved due to the high ambient temperature. Improving energy efficiency will reduce the use of electricity and lowering energy expenses. Also, it provides a more comfortable life and lowers bad environmental effects, including CO₂ emissions. The overall potential benefits of technologies and policies targeted at reducing energy usage in buildings. In addition, Iraq suffers from providing electric power, which is essential for social needs. One of the solutions to this problem was to use renewable energy. Renewable energy sources for heating, cooling, and electricity are being examined, as well as changes to the building envelope, such as materials, natural ventilation, and daylighting, and enhancements to building services, such as heating, mechanical ventilation, and air conditioning. (Berardi & U, 2015; Yu, Evans, & Shi, 2014).

Several types of energy-saving buildings are given, along with progressive retrofitting criteria. Low-energy buildings, for example, with yearly thermal loads that include active solar collectors or solar heating, zero-energy houses, energy self-

sufficient households, and Plus-energy houses are all examples. ASHRAE's objective is that smart houses with intelligent energy management systems would develop market-viable NZE buildings (NZEBS) that are technically near to the zero-energy buildings performance target. For comparative value, the collected information by the audit team must specify the building operation characteristics and the technical characteristics of its various cooling parameters with a long-term analysis of the cost. Also, the team must investigate the available equipment that can be used in cooling the building and know the equipment specifications (Young et al., 2020; Menezes et al., 2014).

1.4 Research Questions

The research questions that are needed to highlight the problem of this study were as in below:

- i. What is the influence of using different materials on the cooling building capacity?
- ii. What is the impact of material properties on the environment and the economy?
- iii. How to decrease the impact of the cooling load on the economy and the environment?
- iv. What is the benefit of using solar absorption cooling systems?

1.5 Objective

The objectives of this study are:

- i. To determine the required cooling load based on effective factors of residential building characteristics by using a mathematical model.
- ii. To evaluate the solar effect on the cooling load differences based on different materials using BIM software.
- iii. To investigate the operation condition of two practical cooling systems (solar absorption system and vapour compression system) used in residential buildings and compare them to choose the best for the building.

1.6 Scope of Research

The scope of the present study is:

- i. The cooling load calculation method is the Cooling Load Temperature Difference (CLTD).
- ii. The building sample was taken in Iraq, Baghdad, which is in the coordinates: 33°20'N 44°23'E, 33°20'N 44°23'E (33.333°N 44.383°E)
- iii. The environmental data for the selected building was gathered from Climate Data for Cities Worldwide, Climate Data.org, and National Centers for Environmental Information, Iraqi electrical official office.
- iv. Building information modelling is used to evaluate the solar energy heat gain to the building.
- v. Engineering Equation Solver (EES) software is used to calculate the selected cooling system functions.
- vi. American Society of Heating, Refrigerating, and Air-Conditioning Engineers (ASHRAE) standard has been used as a reference book.

1.7 Significance of Research

The rate of energy consumption is increasing daily as Iraq is a developing country. The younger generation lives in a world full of state-of-the-art devices and equipment powered by electrical energy. These conditions have increased the demand for electrical energy. The energy issue has become less prioritized by Iraqis today, mainly due to a lack of awareness. It is necessary to raise their awareness regarding the consequences of extensive electricity usage on the natural environment. In addition, Iraq has experienced up to a 50% decrease in electrical power in the last thirty years due to war. Hence, it is crucial to identify and evaluate the energy consumption of a building.

By identifying the electrical equipment used in residential buildings, the energy consumption and electrical cost can be evaluated. This will help to raise awareness of energy expenditure. Through the proposal of potential energy saving, the number of utility bills every year can be reduced.

1.8 Thesis Organization

This thesis includes five chapters relating to this research, and each chapter summary is as follows:

Chapter one introduces the overview of the current research, which contains the introduction, brief background of the energy consumption, and the potential saving in the residential building located in Kithara city, Baghdad, Iraq. This is succeeded by the problem statement, objectives of the study, and the scope of research that will obtain the importance of the current study.

Chapter two shows the related literature of the previous similar research from key people in the energy field. It presents the relations depicted in the theoretical framework and the hypothesis formulation of the present research.

Chapter three explains the methodology of research and looks to clarify the method used in this work. Also, it illustrates the building identification, location, and user trend in addition to the procedure and collection of data collection to determine the initial data for the current study. Details of the utilized methods are explained in this chapter by the analysis of data.

Chapter four comprises the outcomes and discussion and outlines the performed analysis of data. Also, it illustrates the proposed solutions and recommendations after the results are found to improve this research in future works. Additionally, the chapter focuses on the analysis of data, where the results are listed in a table in the last part of the chapter.

Lastly, chapter five presents the conclusion and recommendation. The research of the results, discussion and clarification of the results of the analysis were briefed. It offers the researchers an understanding of the implications and limitations of this study; furthermore, it provides insights into how the researcher deals with a future study inside the scope of energy consumption and potential saving for intermittent.

CHAPTER 2

LITERATURE REVIEW

2.1 Introduction

The current chapter offers a survey study of journals, articles, theses, books, and other sources concerning the research topic. This is necessary to increase knowledge in a related research topic for the researcher to have a clear objective and expected outcome. The present work discussed the solar energy concept and applications. It provides the research with a clear idea about the solar energy system in the following chapters. Also, it presents the air conditioning systems used in residential buildings with all details, such as the efficiency of the systems and capacity with respect to the energy usage. The final important step of this chapter is the related studies of the building information system (BIM), which is used to calculate the number of used materials and solar effect. This provides the researcher with all the cooling load information needed in the building.

2.2 Air Conditioning System

Air conditioning eliminates heat and moisture within an occupied space to enhance occupant comfort. Air conditioning may be utilized in both local and commercial environments. This procedure is commonly utilized to obtain a further comfortable indoor environment, usually for humans and other animals; however, air conditioning is likewise utilized to cool and rooms dehumidification packed with heat-making electronic instruments, for example, computer servers and energy amplifiers, and to show and store some delicate goods, for example, the air conditioner regularly utilizes

a fan to spread the air conditioning over an employed space, for example, a building or car to enhance thermal comfort and interior air quality. Air conditioning units, according to electric coolers, vary from minor units that can cool small bedrooms and possible to be lifted by one mature man to huge units put on the rooftops of office towers that could cool the whole building. Cooling is usually done through the refrigeration cycle, but occasionally evaporation or free cooling is utilized. Air conditioning systems may also be manufactured depending on desiccants (chemicals that eliminate moisture from the air). Some AC systems refuse or store heat in underground pipes.

In a building, a whole system of heating, ventilation, and air conditioning is known as HVAC. Whether at houses, workplaces or means of transportation, its purpose is to offer relief by changing the characteristics of the air, generally by cooling the air inside. The key task of the air conditioner is to change opposing temperatures (Abdel-Salam, Ge, & Simonson, 2013).

2.2.1 Refrigeration Cycle

The Vapour Compression Refrigeration Cycle is almost 200 years old, but it does not look like it will be replaced anytime soon. Even though some researchers have shown this technique as environmentally harmful and ineffective, the cycle remains appropriate in the industrial field.

Natural gas factories, petroleum refineries, petrochemical factories, and lots of food and drink operations are some of the factories that use pressure steam cooling systems. The Vapour Compression Refrigeration Cycle includes four mechanisms: compressor, condenser, expansion valve/throttle valve, and evaporator. As shown in Figure 2.1, a compression process aims to increase the cooling pressure as it streams from an evaporator. The high-pressure refrigerant runs in a condenser/heat exchanger in advance to reach the primary low pressure and head back to the evaporator. Additional detailed clarification of the steps is described underneath (Tehrani et al., 2015).

2.2.1.1 Compression

Refrigerant (such as R-717) goes into the compressor at minimum temperature and pressure. It is in a gaseous state; at this time, pressure is utilized to increase the temperature and compress the coolant. The refrigerant departs the compressor and goes into the condenser. An electric motor might be utilized in this process because it needs work. Compressors themselves can be a scroll, screw, centrifugal or reciprocating kind.

2.2.1.2 Condensation

The condenser is basically a heat swap. Heat is transported from the coolant to the water flow. The water enters a cooling tower to be cooled in the state of water-cooled condensation. Observe that seawater and air-cooling approaches could similarly act in this part. Such as, the refrigerant flows into the condenser, and it is at a steady pressure.

The safety and efficiency of the capacitor cannot be ignored. In particular, pressure control is significant for safety and efficiency causes. There is numerous pressure-regulating equipment to take care of this need.

2.2.1.3 Throttling and Expansion

When the refrigerant goes into the throttle valve, it expands and liberates pressure. Thus, the temperature decreases at this phase. As a result of these changes, the cooling liquid vapours escape from the throttle as a mixture, usually about 75% and 25%, in that order.

Throttles valves play two critical roles in the vapour's pressure cycle. Initially, they preserve a pressure difference among lower and higher-pressure sides. Additionally, they regulate the volume of liquid refrigerant that goes into the evaporator

2.2.1.4 Evaporation

At this phase of the Vapour Pressure Refrigeration Cycle, the refrigerant is at a temperature lesser than its ambient temperature. Hence, it absorbs and evaporates within the heat of vaporization. Heat removal from the refrigerant occurs at low pressures and temperatures. The suction effect of the compressor helps to preserve low pressure.

There are different versions of evaporation on the market, but the main classification is liquid or air cooling based on if they cool liquid-or air correspondingly. Figure 2.1 show the compressive cooling cycle for the refrigeration system.

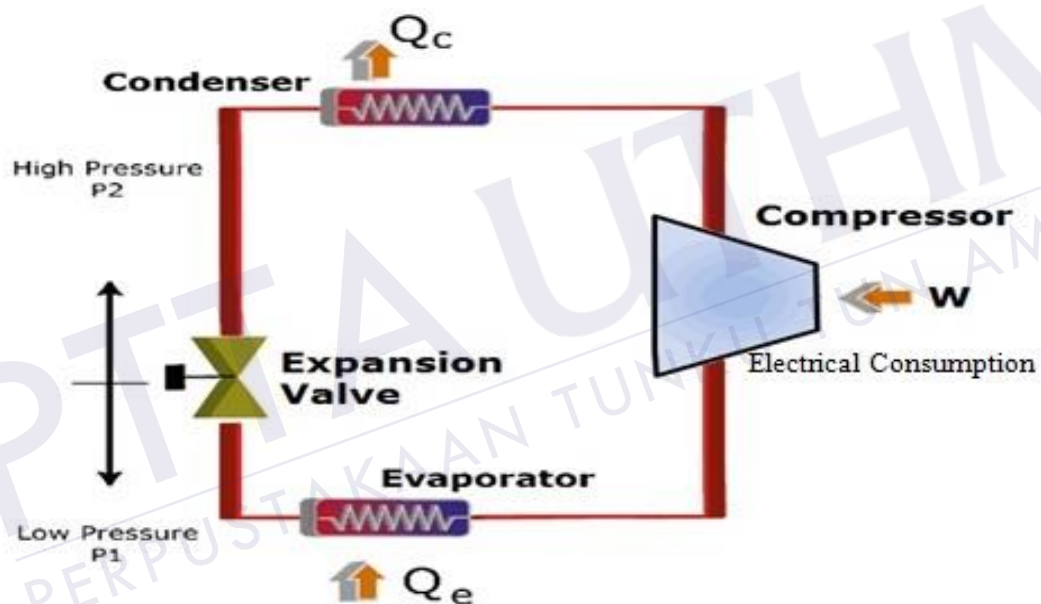


Figure 2.1: Compressive cooling cycle (Yang et al., 2022)

2.3 Cooling Load Temperature Difference Method

Currently, the meaning of continuing comfortable conditions in the home environment and reduced early investment, repairs and operating expenses, in addition to choosing a suitable cooling system, are significant in buildings. Capacity must rely on the building cooling load in choosing the cooling system. That cooling load is not calculated in a reliable way, causing the selection of a cooling system that does not fit the building, raises the cooling system price and exacerbates indoor environment comfort conditions. Thus, the dependability calculation technique would be used for

the calculation of building cooling loads. There are some approaches that calculate building cooling loads.

Nowadays, TEDT/TA, HB, TFM, CLTD/SCL/CLF and RTS approaches that are usually employed are compared according to their utilizing information, coefficients and calculation process. The elementary school positioned in İstanbul is chosen as a case in point for comparison of numerical differences between these approaches (Hashim et al., 2018). The factors that affect the cooling load calculations can be described below:

- i. **Dominations, Location and Climate:** Inside design condition for comfort is associated with the quantity of heat extracted from the room, where a greater number means additional cooling energy is required to cool the room. The building position is defined by its latitude and height. This position defines the values for the outdoor design conditions, for example, the height of the position, latitude, winter heating dry bulb temperatures, summer cooling dry bulb temperatures and relative humidity (RH) data (Solomon et al., 2020).
- ii. **Definition of Materials:** Walls and roofs of buildings are made of many layers of materials, and the construction and operating conditions of the walls and the roofs may vary considerably from one structure to another. Heat transmission into a wall or roof section is also impacted by the loading and radiation heat transference coefficients at the non-covered surfaces (Mukesh et al., 2020).
- iii. **Walls, Ceilings, and Roofs:** Roofs are generally joined through the combined loading and radiation heat transmission coefficients. Most structures have a mixture of a ceiling and a roof with attic space in between, and the determination of the R-value of the ceiling –attic–ceiling combination rests on if the attic is vented or not. For well-ventilated attics, the temperature of the attic air is practically the same as the outside air, so the heat transfer through the roof is governed by the R-value of the roof only. The main purpose of the ceiling in this situation is to work as radiation protection by stopping off solar radiation.
- iv. **Doors and Windows:** Windows are glass openings in a building facade that usually consist of single or multiple glazing (glass or plastic), frames and shading. In a structure facade, windows give the minimum resistance to heat transmission. Nearly 1/3 of the entire heat loss in winter happens over the windows. Similarly, most air infiltration happens at the edges of the windows.

The solar heat increase over the windows is responsible for much of the cooling load in summer. The net influence of a window on the heat balance of a structure relies on the features and orientation of the window in addition to the solar and weather information.

- v. **People, Lighting and Equipment:** Lighting constitutes around 7 percentage of the entire power employed in domestic buildings and 25 percentage in commercial buildings. Thus, lighting can have an essential influence on the heating and cooling loads of a structure. Not including the candlelight utilized for emergencies and passionate settings and the fuel lamps utilized throughout camping, all present lighting tools are powered by electricity. Also, the average amount of heat specified by one relies on the activity level and can range from around 100 W for a resting somebody to beyond 500 W for a physically very active person.

2.4 Building Information Modelling

Building Information Modeling or known as BIM is a numerical model of a building that consists of the digital equivalents of the real building parts and components used in the actual construction. These building elements, systems, parts and components have the exact attributes and enable the engineers to complete a virtual simulation of the entire, real building before the construction development begins. Furthermore, BIM includes the entire life cycle of a building, that is, the plan, manufacture, operation and maintenance of a building (Tristan et al., 2016). BIM has the opposite approach. It concentrates all information in one database and associates all data with those objects (building and building components). The BIM model is, therefore, a central database model, where all the information is correlated to each other in an intelligent way. Moreover, this centralized model assists in the collaboration between all involved disciplines (BIM interoperability). On the other side, traditional tools (such as CAD) require more traditional ways of communication between the various actors, as shown in Figure 2.2 (Ziwen et al., 2020). Figure 2-2 shows the 2D data exchange in comparison with BIM interoperability. The BIM system facilitates the data transferred between the designers and people who makes the decision in building design. As shown in the Figure, the traditional methods need to communicate between

people in the building design process. This method will be more costly and contain great mistakes due to the missing data between the designers. When the BIM was used, communication became less and easier, and the mistakes in design were fewer.

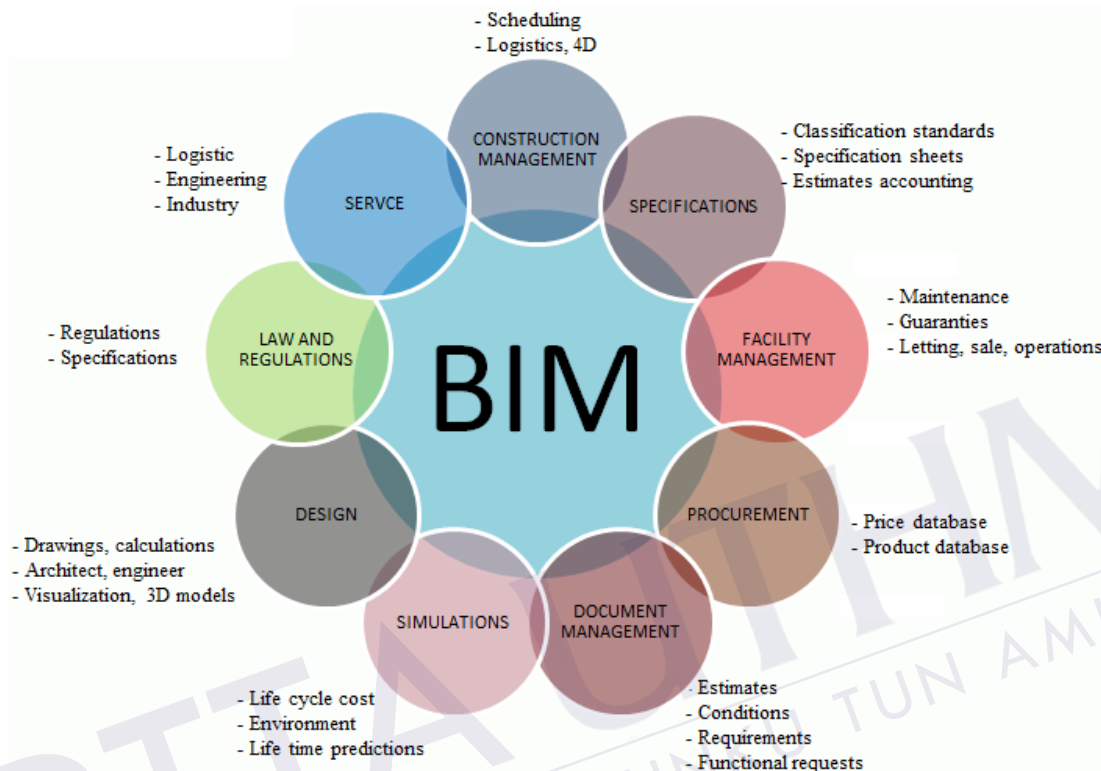


Figure 2.2: 2D data exchange in comparison with BIM interoperability

There are different BIM applications over the development and the lifecycle of a building. These applications are related to various dimensions of the BIM technology and how it is implemented. The ones that follow are only a portion of the uses of BIM that can be connected to each part of the development process through its design, planning and construction stages.

Building Information Modelling (BIM) is not only a complex process of managing design documents in 3D shape but also contains all the sequential stages of design analysis pursued by construction management and post-completion facility management. The success achieved by collaborating to unite the joint efforts of architects, builders and HVAC engineers will make the work of all stakeholders more fruitful because current information technology has provided this option for a long time. Since the beginning of the building life cycle in the construction industry, the

task of training to take advantage of BIM relatively new and highly complex approach has become more and more complex.

2.4.1 BIM Scope

The scope of BIM are as follows:

- i. BIM is the business process of creating and utilizing the building data that designs and manages a building in its lifecycle. BIM paved the way to all stakeholders to access the same information simultaneously through interoperability within the technology platform.
- ii. BIM is a digital representation of a facility's physical and functional features. Thus, they work as a well-known knowledge foundation for information about the facility and form a dependable basis for decisions through the life cycle from the beginning.
- iii. (BIM) is the organization and control of business processes that take advantage of the information contained in digital prototypes to influence information exchange throughout the asset lifecycle. Benefits include centralized and visual communication, a quick exploration of options, durability, efficient design, integration of disciplines, site control, ready documentation and more. An effective asset life cycle process and model are developed from idea to finish (national BIM standard). BIM covers engineering, spatial relationships, light analysis, geographic information, and the amounts and properties of building components (manufacturers' details). BIM can be utilized to show the whole building life cycle, as well as the construction and facility process procedures. Amounts and shared characteristics of materials are easily removed. Work areas can be isolated and identified. Systems, gatherings and orders can be demonstrated on a relative scale with the whole construction or group of facilities. Dynamic data of the building, like sensor measurements and control signals from the building regimes, may also be merged inside BIM to help analyse of building process and preservation.
- iv. BIM is the organization and control of the commercial procedure by using the data in the digital sample to influence the sharing of data over the whole lifecycle of an asset. The advantages contain centralized and visual

communication, initial investigation of choices, sustainability, effective design, integration of specialities, location control, as-built documents, etc., and successfully creating an asset lifecycle procedure and model from beginning to finish (National BIM Standard). BIM includes geometry, spatial relationships, light analysis, geographic information, and quantities and properties of building components (such as manufacturers' details). BIM may be utilized to present the whole building life cycle, as well as the procedures of building and facility operation. Amounts and shared characteristics of materials may be easily obtained. Business areas may be isolated and explained. Systems, gatherings and arrangements can be demonstrated on a relative scale with the whole building or group of facilities. Dynamic data of the facility, like sensor measurements and control signals from the facility regimes, likewise can be merged inside BIM to help analyse facility process and preservation.

2.4.2 BIM and Energy Performance Analysis

Building performance analysis is normally accomplished after the production of architectural and structural design documents. Normally, the building's engineering information is extracted from architectural drawings that show the architect's view of the building. From then on, the building power analyst utilizes this data to explain the thermal vision of the building. This meaning is subjective and is reliant on the information, talent and practice of the power analyst. Many building power analysts will then produce different thermal visions. Accordingly, the most effective decisions regarding sustainable building design can be made only in the design and pre-construction stages. The literature suggests that because there is no continuous analysis of building performance, the traditional approach leads to an inefficient process of retrospective design modification to achieve an agreed-upon set of performance criteria that have been identified as the "single-island of information" problem. They also saw that separating energy-saving technology from building design, as evidenced by the traditional approach, presents real problems for energy performance analyses.

Recent progress in building informatics is now addressing the complex problem of integrating structure power performance analysis and building design. To

do this, it is necessary to have access to the full range of information that defines the building, such as shape, materialization and technical systems. Building Information Modelling (BIM) is one of the rapidly developing technologies that have been envisioned and demonstrated to support Building Information Modelling (BIM), as presented in Figure 2-3. Building Information Modelling has the potential to serve as an independent, multidisciplinary data warehouse, providing new opportunities and avenues for incorporating performance analysis into potential designs (Samuel et al., 2016).

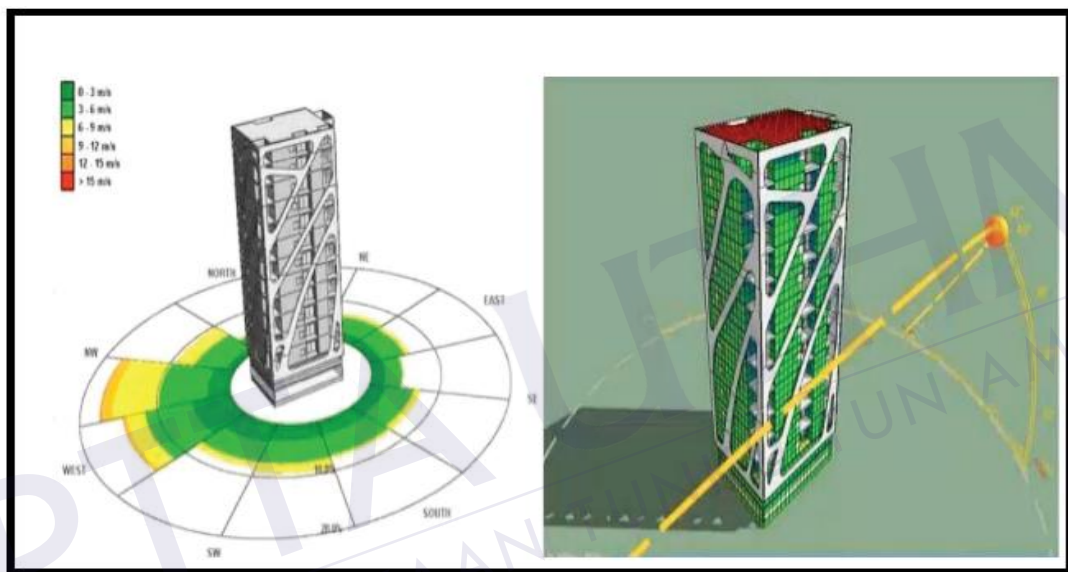


Figure 2.3: BIM based energy analysis showing the windrose and solar path on the BIM model (Samuel et al., 2016)

2.5 Solar Energy

Solar power is known as the heat effect provided by the sun, which is employed by the sun effect, for instance, solar thermal energy, solar architecture, solar heating, photovoltaic (PV), artificial photosynthesis, and molten salt power plants. It is an important renewable power resource. Its techniques are largely described as active solar or passive solar relying on the way they arrest and dispense the solar energy or change it into solar power. The techniques of active solar comprised of the employment of PV regimes focused on solar energy and solar water heating for harnessing the power.

The passive solar techniques comprised the orientation of the building towards the sun, the selection of materials with preferred thermal mass or light scattering properties, and design spaces that typically maintain air circulation. The enormous amount of existing solar power produces an extremely attractive electricity source. The United National Progress program, in its World Power Assessment in 2000, anticipated that the annual forecast for solar power was 1,575–49,837 exajoules (EJ). The orders are bigger than the consumption of power of the whole world, which was 559.8 EJ in 2012. In 2011, the International Energy Agency stated that the development of clean, inexhaustible and inexhaustible solar power technologies would have huge advantages in the long run.

Solar energy will provide a safe power resource due to countries' rising, unlimited, and highly import-independent sources. It also improves sustainability, decreases pollution, reduces global warming mitigation expenses, and keeps fossil fuel prices low.

2.6 Application of Solar Energy

Solar energy is a source of renewable power because it is always an available source of energy. Solar power could be exploited in electricity making to decrease electrical energy consumption, particularly for countries that suffer from a lack of electrical energy processing.

In areas where electricity is not available, the best source to produce electrical power is solar energy. Solar regimes do not require much maintenance effort. Most companies design solar panels that offer a 20–25 years warranty which will lead to an extended lifetime of work and lead to reduced cost. Also, solar energy is employed in various applications, such as processing electricity, heating water, agriculture and horticulture, fuel production, energy storage method, cooking, progress, and economy (Mekhilef, Saidur, & Safari, 2011).

2.7 Types of Solar Collectors

Solar collectors are a particular heat type exchanger that translates solar power into electrical power with heat transfer. It is an apparatus for solar radiation absorbance

that falls upon it, changes it to heat, and conveys such heat to the liquid that flows through it (normally oil, air, and water). The gathered solar energy is removed from the flowing liquid either straight in warm water form or conveyed to an air-conditioner or to a storage depot of thermal energy, which is used for heating at night or on cloudy days. Two basic kinds of solar collectors are available: Non-condensing or Fixed and Condensing. The non-condensing collectors have an area to receive solar radiation which is equal to their absorption area. In contrast, rotating condenser collectors with the sun usually have concave reflective surfaces to receive solar radiation and concentrate on a smaller field, thus growing the flux of radiation.

Condensate collectors are appropriate for elevated temperature uses. Different solar collectors can be discriminated according to the kind of fluids used for heat transfer (air, antifreeze, water, or heat transfer oils), whether they're enclosed or exposed. A large number of them exist in the marketplace (Suman et al., 2015), as shown in Figure 2.4 below.

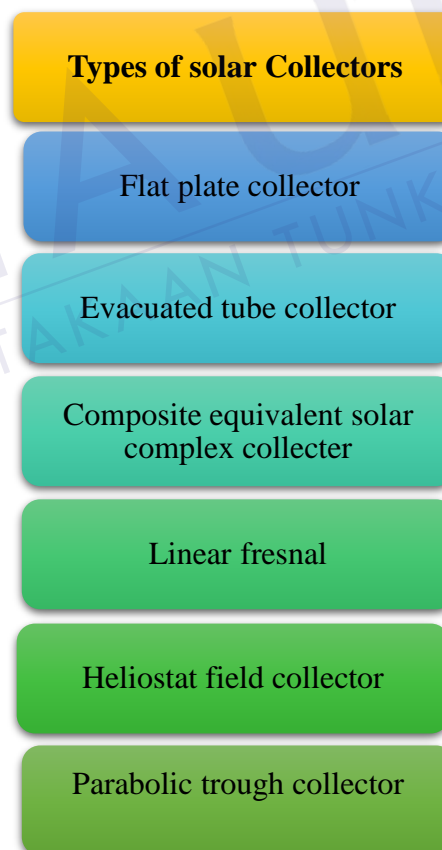


Figure 2.4: Types of solar collectors

2.7.1 Flat Plate Collector

One of the basic solar collector types used to transfer solar energy is for heating water. It is an extension of the basic idea of pointing the glass collector towards the sun. The majority of the flat panel assemblies possess two horizontal pipes at the bottom and the top, as well as several small pipes that connect them. The types of glasses used in the flat panel assemblies are always low iron and tempered glass. Glass can withstand great cold without breaking, which is why flat panel collectors are one of the most durable collectors (Saleh et al., 2014).

Flat panel complexes consist of a black absorber plate, in which the pipes and ducts are installed in the lower part. They are fitted in a closed frame with a transparent cover that can penetrate solar radiation at the top and provide heat insulation from the bottom. Solar energy is absorbed from the black surface, and liquid is supplied through pipes or channels, as presented in Figure 2.5.

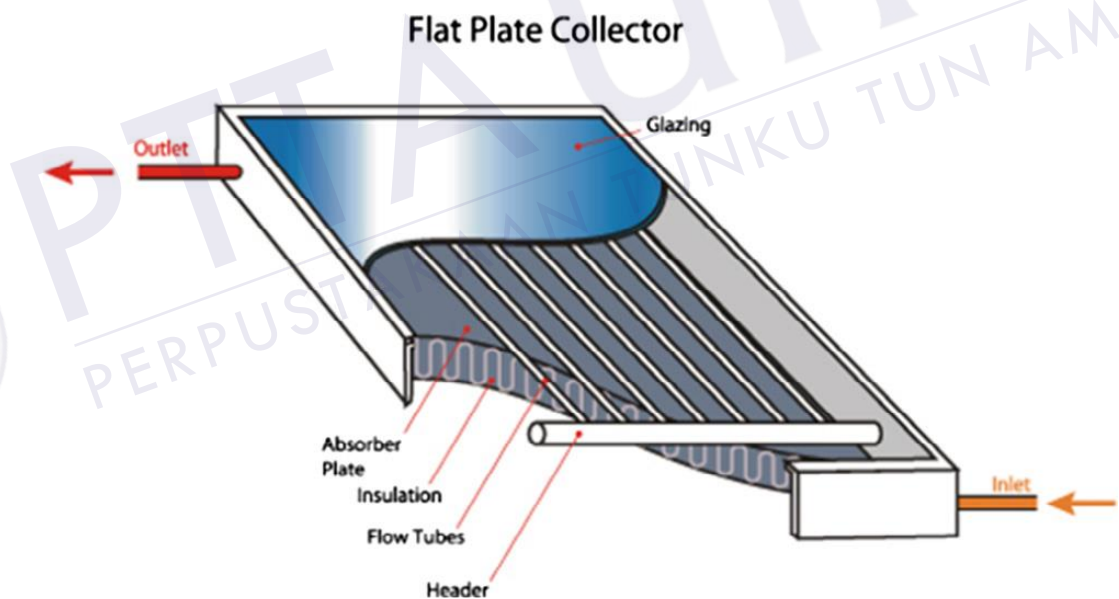


Figure 2.5: Flat plate collectors (Shirazi et al.2018)

Figure 2.5 show the flat plate collectors. The flat-plate collectors could be categorized into three sets in accordance with their principal uses as follows (Suman et al., 2015).

- i. Used with a too small increase in temperature, like in swimming pools where the solar collector requires no shelter or insulation at the sides or rear. A high flow rate is maintained to restrict the increase of temperature (to $\leq 2^{\circ}\text{C}$).

- ii. Domestic heating and other uses where the ultimate temperature needed is not greater than 60°C. The insulation at the rear and at least one transparent shield are essential.
- iii. Uses for heating process or small-scale power provision, in which temperatures significantly higher than 60°C are essential. Highly sophisticated design methods are required to reduce the losses of heat from the collector to the environment.

2.7.2 Evacuated Tube Collectors

Solar collectors with thermal pipes (vacuum tubes) are widely available in the market, and they work differently from other solar collectors. Such solar collectors comprise heat pipes in the vacuum tubes and are tightly closed and connected from the top to a heat exchanger, as depicted in Figure 2.6.



Figure 2.6: Evacuated tube collectors (Suman et al., 2015)

These heat pipes are made of copper material and are connected by copper fins painted in black. Above the upper of every thermal tube, there is a metallic tip that acts as a condenser. The vacuum that exists between the thermal pipes, in addition to the effect

of heat transfer by pregnancy, makes these solar collectors operate at high temperatures because there is little loss of heat. In addition, these solar collectors operate using materials that change phase from liquid to gaseous state, which gives it an advantage as the efficiency of these solar collectors is high compared to other solar collectors (Shirazi et al., 2018).

Due to high cost, many designs have been introduced in the market to reduce manufacturing costs and prolong life. This is done via the reduction in the number of vacuum tubes and utilizing reflectors designed for focusing the solar radiation on the pipes (Hang et al., 2011).

2.7.3 Parabolic Trough Collectors

In recent years, parabolic trough collectors have been the most advanced and matured among the solar energy technologies through the growth of industries based on the production and marketing of these systems, in addition to their installation with different systems.

These solar collectors can be manufactured by bending a sheet of reflective material in the form of a parabola and covered with glass tubes to reduce thermal leaks, as shown in Figure 2.7.

When these ponds are in the direction of the sun, sun rays fall on the surface, and the fluid flowing through its heating and solar power is changed to useful thermal power.

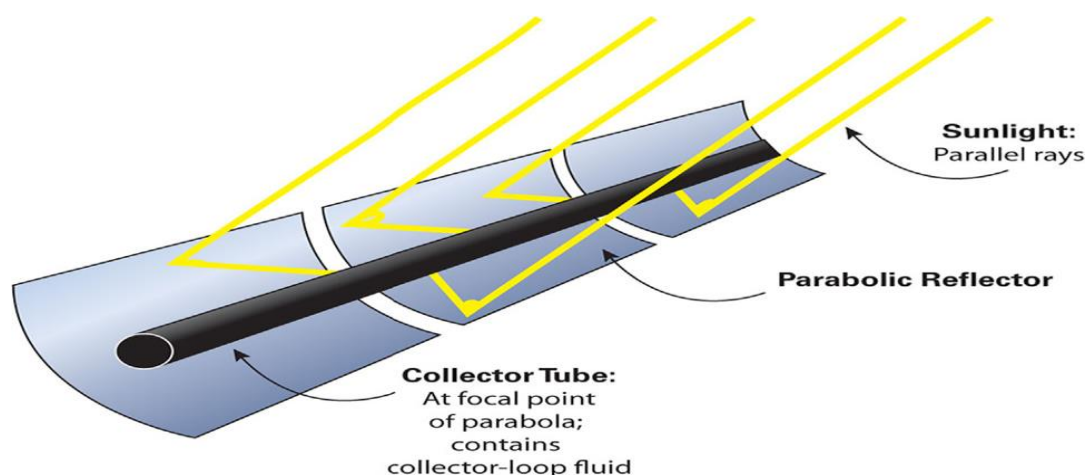


Figure 2.7: Parabolic trough collectors (Shirazi et al., 2018)

These technologies have been used in more than one application: they have been used in a Southern California power plant known as the solar power system and have been used in a project in southern Spain called Platform Solar de Almeria. New developments in the parabolic trough collectors are aimed to reduce the costs of the companies that manufacture many of these technologies, which are capable of heating the fluid flowing between 50°C and 300°C (Shirazi et al., 2018).

2.7.4 Fresnel Solar Collectors

Fresnel solar collectors are of two types: Fresnel lenticular collectors and Fresnel linear reflectors. The first type is made of plastic material, while the second type consists of linear strips of glass that focus the sunlight on the receiving line. They can also be installed on flat ground, making the cost of these complexes low compared to other solar collectors, as presented in Figure 2.8.



Figure 2.8: Fresnel Solar collectors (Facão et al., 2011)

The biggest benefit of this system is employing flat reflectors or curved reflectors. These types of reflectors are cheaper than glass reflectors in the form of equivalent pieces.

Giorgio Francia, a pioneer in the domain of solar power, was the first to work with these systems and developed them in the city of Genoa in Italy in 1968. It has been proven that these systems can reach a high temperature.

Misleading the reflectors on each other is one of the greatest significant difficulties encountered by linear Fresnel reflector techniques, which leads to increased distances between the reflectors. In recent years, Fresnel linear techniques have been developed at the University of Sydney in Australia by placing adjacent linear reflectors in an overlapping form to avoid misinformation (Facão et al., 2011).

2.7.5 Composite Equivalent Solar Complex Collectors

Composite parabolic solar collectors have a great ability to reflect sunlight and direct them to their absorption elements. Using multiple reflective interior surfaces, radiation enters the absorption elements at the bottom of the solar collector. The absorption element can take a large number of different shapes, such as flat, double-sided, cylindrical, or wedge-shaped.

These solar collectors are designed in two types: symmetric and asymmetric. Composite parabolic solar collectors have a gap between the absorption element of the solar radiation and its reflection element in order to prevent the reflection element from conducting heat away from the absorption element, as shown in Figure 2-9.

These solar collectors can be manufactured in the form of a single unit with a single hole, and one absorption element or are installed in the form of a panel; they look like solar collectors with a flat panel (Bellos et al., 2016).



Figure 2.9: Composite equivalent solar complex collectors (Bellos et al., 2016)

2.7.6 Heliostat Field Collectors

This system has several advantages as it collects solar energy and transports it to the receiving surface. This reduces the need for thermal energy transmission. The condensation ratio in this system ranges from 300 to 1500. This indicates that the system is highly efficient. In addition, the electric power generated by this system is large, exceeding 10 MW.

There are solar stabilizers on the surface of the system that absorb sunlight and transport it to the liquid flowing through the system. The heat transfer systems, which consist mainly of pumps, pipes, and electricity generation systems, are shown in Figure 2.10. Heat storage systems store thermal energy and deliver it to electricity generation systems. They also separate the collection of solar energy from the conversion system into electricity.

These solar collectors are found in three forms. In the first form, the solar stabilizers are entirely surrounded by the receiving tower. The receiving surfaces are in cylindrical forms, and the outer surfaces transmit heat to the liquid streaming throughout them. The second form is the installation of solar stabilizers north of the receiving tower and receiving surfaces that transfer heat to liquids. The third form

installs the solar stabilizers north of the reception tower; the receiving surface is flat and vertical towards the north (Marc et al., 2010).



Figure 2.10: Heliostat field collectors (Marc et al., 2010)

Figure 2.10 show the heliostat field collector. Meanwhile, Table 2-1 explains the conditions in which solar collectors operate. The flat plate collector is a constant, the condensation ratio is one, and the temperature level is “30 to 80 °C”. The evacuated tube collector is a constant, the condensation ratio is one, and the temperature level is “50 to 200 °C”. The composite equivalent solar complex is constant and mobile, the condensational ratio is one to fifteen, and the temperature level is “60 to 300 °C”. The linear Fresnel is mobile, the condensation ratio is 10:40, and the temperature level is 60 to 250°C. The Heliostat field collector is mobile, the condensation ratio is 300:1500, and the temperature level is 150 to 2000°C. The Parabolic trough collector is mobile, the condensation ratio is 10:85, and the temperature level is 60 to 400°C.

Table 2.1: Conditions under which solar collectors operate (Real et al., 2014)

No	Type of Solar Collector	Movement Type	Heat Absorption Surface Type	Condensation Ratio	Temperature Level (°C)
1	Flat plate collector	Constant	Flat	1	30 – 80
2	Evacuated tube collector	Constant	Flat	1	50 – 200
3	Parabolic trough collector	Tracking	Amopic	10 - 85	60 – 400

4	Composite equivalent solar complex collector	Constant	Amopic	1 - 15	60 – 300
5	Linear frenal	Tracking	Amopic	10 - 40	60 - 250
6	Heliostat field collector	Tracking	Dots	300 - 1500	150 – 2000

Table 2.2: Absorption chiller: solar thermal collector matching (Shirazi et al.,2018)

Chiller Type	Nominal Operating Temperature (°C)	Collector Type
Single –Effect	80–100	Flat plate collector Evacuated tube collector
Double – Effect	180–200	Linear Fresnel reflector
Triple - Effect	210–240	Parabolic trough collector Parabolic trough collector

In summary, Table 2.2 lists the types of solar thermal collectors that could be potentially used to drive single, double, and triple-effect LiBr-H₂O-based absorption chillers.

2.8 Types of Solar Cooling Technologies

The succeeding Figure displays the kinds of solar cooling technology. As an outcome of population growth and economic growing, energy requests will rise by 35% from 2010 to 2035. Increased energy requirements will increase greenhouse gases. The warm climate and economic growth will cause the use of highly adaptive air conditioning. Figure 2.11 below shows the types of solar cooling technologies.

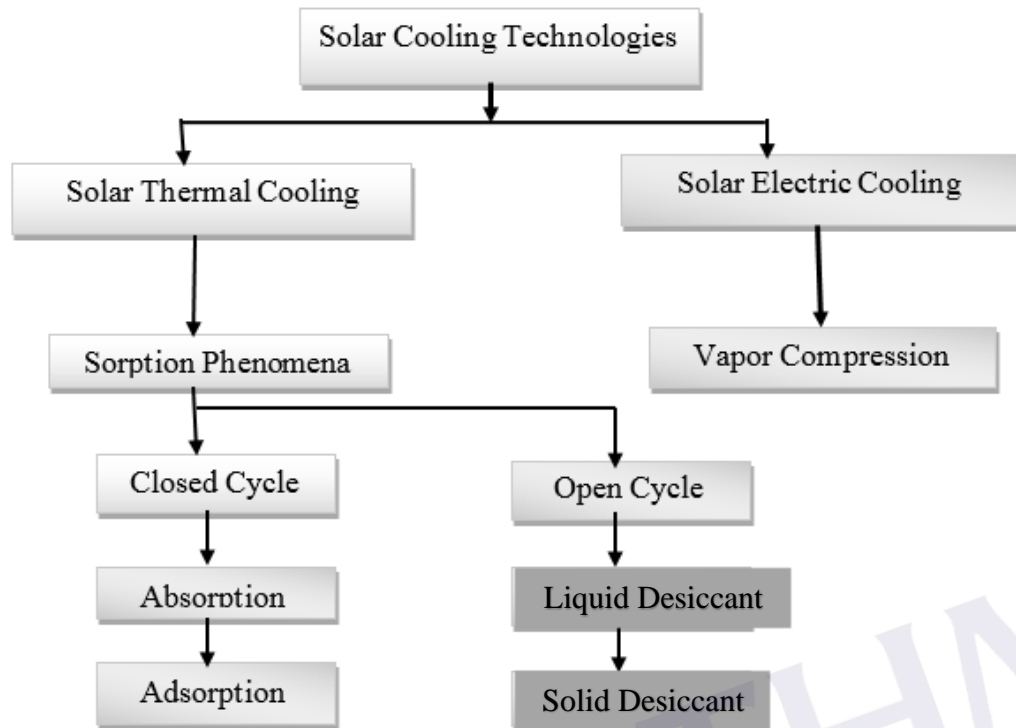


Figure 2.11: Types of solar cooling technologies

One of the solutions that can be utilized to decrease power consumption is renewable energy (especially solar) to provide cooling, which makes solar cooling an important technology to reduce electricity consumption and reduce emissions of toxic gases (Ali Al-Alili, Hwang, & Radermacher, 2014). Solar cooling techniques are divided into two groups in the form of solar electrical cooling and solar thermal cooling. As shown in Figure 2.11, there is a major cycle in solar electrical cooling (Photovoltaic Vapour Compression System). There are also three chief courses in solar thermal cooling: open cycle, closed cycle and thermo-mechanical cycle (Allouhi et al., 2015).

Recent studies of all solar cooling cycles have shown that the efficiency and performance of the cycles have significantly improved since the beginning of the use of solar cooling techniques. Studies have also shown that solar imbibition cooling is one of the best techniques of solar thermal cooling because it achieves higher energy savings than other thermal cooling and can work at night, thus increasing energy savings. Solar absorption cooling efficiency is also good compared to other solar thermal cooling (Soto, Domínguez-Inzunza, & Rivera, 2018). In addition, the photovoltaic vapour compression system is very similar to solar absorption cooling in terms of achieving electrical energy savings, but it is preferable to use a solar

absorption cooling system because it is economically better than a photovoltaic vapour compression system because the cost of solar imbibition cooling system is lower than the photovoltaic vapour compression regime. The payback period of the absorptive absorbers is fewer than the photovoltaic vapour compression regime (Al-Ugla, El-Shaarawi, Said, & Al-Qutub, 2016). Finally, the solar absorption cooling technology achieves high energy savings at a low installed cost, which is attractive to engineers. Solar absorption technology will be discussed in the next section.

2.9 Solar Powered Absorption Cooling System

Obtaining the necessary power for cooling equipment requires energy from solar sources, heat dissipation from manufacturing processes, and direct heat from heating equipment. If electricity is not an option, is expensive, or is not required, as well as when compressors are inconvenient, absorption cooling is the most popular method (Herold et al., 2016).

A low boiling point is required for both absorption and compression cooling systems. To provide a feeling of cooling, both types release a small amount of heat when the cooling fluid evaporates. Obviously, the two methods are not the same in which the cooling fluid in an absorption system alternates between a gaseous and liquid state. Cooling fluid alters from a liquid to gaseous in a compression cooling system. Besides, there is a difference in the cooling fluid type. Water or ammonia are used for absorption cooling systems, while chlorofluorocarbons are used for compression cooling systems (Hang et al., 2011).

Three stages can be explained by the absorption-cooling circuit:

- i. Evaporation: fluid that transports heat from the "evaporator" environment is calculated at low pressure (low partial pressure).
- ii. Absorption: Many fluids are evaporated in the evaporator as absorbed refrigerants degrade and "mix" with another fluid to reduce their pressure.
- iii. Renewing the cooling cycle: the cooling fluid is heated and evaporated and then condensates in a heat exchanger; Evaporator pressure is applied to bring inside a quantity of fluid to evaporate, and then the cooling cycle has been renewed.

Table 2.3: The principal operational used parameters of the solar-powered single-effect absorption cooling systems (Zhai et al., 2011)

No.	Fluid	Operating Temperature (°C)	COP	Solar Collecting Efficiency
1	Hot Water	65-100	0.33-0.70	35% -50%
2	Chilled Water	7-15		
3	Cooling Water	26-32		

The key functioning limits of the solar-powered single-effect imbibition cooling system are explained in Table 2.3, where hot water working temperature varieties from 65°C to 100°C, cooled water varieties from 7°C to 15°C, and chilling water varieties from 26°C to 32°C. The same table also explains the system performance coefficient from 0.33 to 0.7 and the effective ranges for collection.

2.10 Theoretical Analysis and Simulation of Absorption System

Schmid et al. (2019) offered a diffusion absorption cooler directly heated by a solar collector with improved efficiency. The generator, working as the bubble pump of the diffusion absorption procedure, is combined through a double-glazed flat plate gatherer. The design and build-up of the solar-driven diffusion imbibition cooler are offered. Measurement outcomes of the solar-driven diffusion absorption cooler noted in a solar simulator and outside tests are revealed. Most cooling capacities of 226 W and 228 W are reached. The most efficiency of the entire procedure and the ratio of the insolation incident on the solar gatherer converted through cooling capacity is 11.4%. Therefore, the effectiveness is more than in comparable ideas. Lastly, an outlook is given on additional enhancements by means of a bubble pump unit with a plate heat exchanger (PHX) generator to raise the cooling capacity.

Bellos & Tzivanidis (2017) investigated the price and solar cooling ventilator performance for a 100m² structure in ten diverse towns around the world, involving Athens, Cairo, Phoenix, Thessaloniki, Madrid, Abu Dhabi, Rome, Almeria, Istanbul, and Tehran. TRANSIS was used for the analysis. The solar refrigeration unit included an evacuated tube, a storage tank, and LiBr/H₂O. Outcomes revealed that for the work of refrigeration units' solar absorbers, Phoenix and Abu Dhabi were the best cities, with minimum costs of 0.0590 and 0.0575, respectively. Thessaloniki, Madrid, Rome and were fewer suitable and costed, 0.2125, 0.1792, and 0.1771 correspondingly.

Additionally, it has been found that the best sites for the work of solar refrigeration units are those with a great deal of solar energy.

Asim et al. (2016) studied the work of a solar absorption chilling regime for a structure under climatic circumstances in Pakistan. TRNSYS program was employed to design the suction radiator with the empty tube gatherer and the hot water packing tank. The space of the solar complex was 12m^2 . Simulated outcomes verified that solar thermal chilling could be employed in Pakistan in the summer as the sun was available for 10 to 13 hours every day. The energy supply of the compost was around 14% of the chilling load. Great power savings of up to 40% have been reached compared to traditional cooling

Based on the climatic conditions of Athens in Greece, Evangelis et al. (2017) designed a 100 kW solar cooling regime. The regime had a LiBr/H₂O absorption cooler with a single-stage, evacuated-tube collector and storage tank. Many sets of solar panel zones were chosen from 150m^2 to 600m^2 . Likewise, diverse sets of storage tanks were examined from 6m^3 to 16m^3 . The finest circumstances were measured financially.

The outcomes presented that the 450m^2 evacuated tube gatherers by 14m^3 the storage tank was the perfect answer with a monetary retrieval time period of 15 years. The conduct of a solar absorption chilling regime for a structure under the climatic circumstances of Seville in Spain and Chennai in India was studied. The leaching area was 450m^2 and included evacuated tube collectors, storage tank, and ammonia water. The efficiencies in Seville and Chennai were recorded as 6 to 8% and 5 to 7%, respectively, although the annual solar contribution in Chennai was higher than in Seville, which was 23 to 30% and 24 to 28%, respectively (Muye, Ayoub, Saravanan, & Coronas, 2016).

Agrouaz et al. (2017) examined the performance of solar thermal cooling factories in some cities in Morocco. Simulation outcomes presented that the finest performance of the chilling regime of solar absorption was obtained where the performance coefficient value was 0.33 and the solar friction was 30%.

Al-Ugla et al. (2016) compared three kinds of air conditioning regimes. They are the "traditional vapour-compression regime", the solar (LiBr/H₂O) absorption regime and the "solar photovoltaic (PV) vapour-compression regime". The work was conducted in Khoper city, Saudi Arabia, on a huge structure by means of techno-analysis. The work pursued the chance of decreasing the energy supply to get fixed

cooling during the day. Furthermore, it aimed to detect the solution's economic benefits. A greater benefit was derived from the solar absorption regime over the vapour compression regime, according to the conclusion presented. Solar absorption had a payback time of 18.5 years compared to 23.9 years for (PV) vapour compression. COP was also enhanced by lowering the condenser's running temperature and raising the evaporator's running temperature, which impacted economically the solar absorption regime in a positive way.

Allouhi et al. (2015) conducted a study under weather conditions in Morocco depending on the characteristics of the Moroccan present houses to assess solar absorption chilling procedures. Using TRANSOL as a simulation tool, meteorological data were collected for six regions from several climates. The conclusion depended on the outcomes of the simulations, which showed important power saving and CO₂ decrease with the application of solar-powered cooling regimes in modern homes in Morocco. Concerning the economic feasibility, the work showed that the prices of the primary placing determined a wide period of payback. Therefore, in the Moroccan condition, the employment of such regimes was not practical. So as to implement solar-powered cooling regimes, it was essential to decrease the cost of many components. The work similarly showed other problems of such implementation, specifically technical, financial, institutional, and even behavioural parameters.

The study by Fasfous et al. (2013) examined the potential of enhancing the excellence of interior air by employing a solar-powered cooling regime. The examined area was a research laboratory at the Jordan University, in Amman, at Mango Centre for Scientific Investigation. The area limits are a space of 41 m² and an elevation of 3.65 m. The measurements involved the hourly ambient temperature and the once-a-month amount of radiation. The conclusion of the work showed that the 40m² the solar collector was not enough to initiate the air conditioning (8 kW), hot water (up to 100%), and heating (15–25% solar) regimes. The predetermined payback duration of 24 years for the solar-powered cooling system was greater than the project period. The work found out that the application of the project was not desirable under existing investment circumstances. Baniyounes, Rasul, & Khan, (2013) move toward the subtropical environment in Queensland in three places (Rock Hampton, Gladstone, and Emerald). The category of structure examined was a workplace building prepared with a solar absorption regime. The simulation was done utilizing TRNSYS16 and covered the summer season from September to April. The extreme radiation and

temperature per site were 400W/m^2 and 35°C . For the regime in Emerald, 50m^2 zone of collector and 0.3m^3 storage water volume saved reached 73% of power; once utilizing a 1.8m^3 , the power saving increased to 88%, as shown in Figure 2-12.

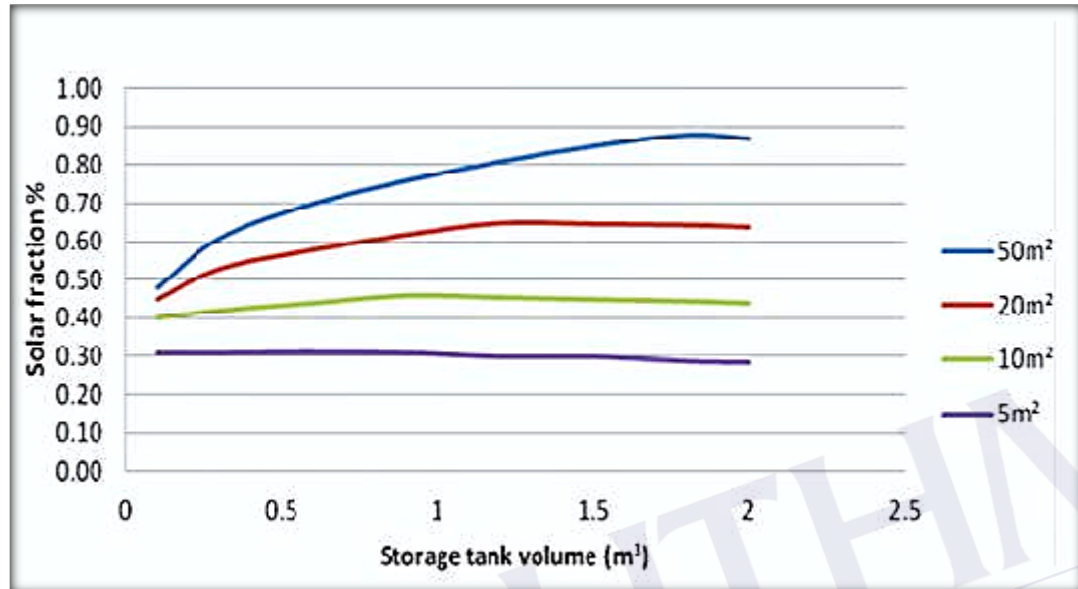


Figure 2.12 Emerald's impact on the annual solar fraction caused by hot water tanks (Baniyounes, Rasul, & Khan, 2013)

For regimes in Gladstone, a 50m^2 solar collector and 0.3m^3 water storage save 69% energy; this can be raised up to 82% once utilizing a 1.8m^3 tank for hot water, as presented in Figure 2.13. As shown in Figure 2.14, a 50m^2 solar collector and a 0.3m^3 water storage yielded 62% electricity savings for the Rock Hampton regime. These savings may be increased to 80% by using a 1.8m^3 hot water tank.

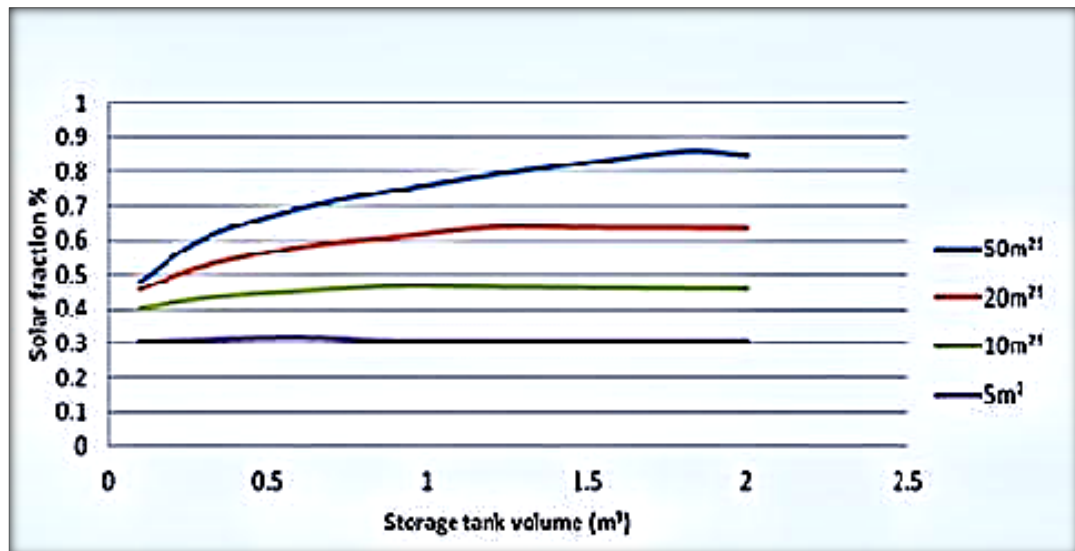


Figure 2.13: Annual solar fraction Gladstone as a function of hot water tank (Baniyounes, Rasul, & Khan, 2013)

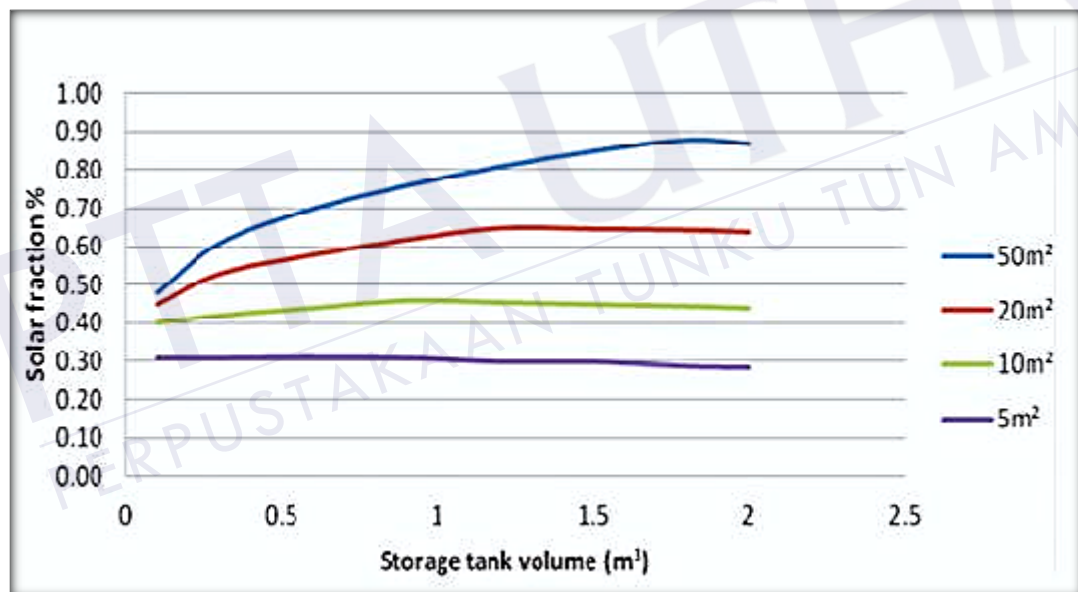


Figure 2.14: Annual solar fraction Rock Hampton as a function of hot water tank (Baniyounes, Rasul, & Khan, 2013)

The study by Ullah et al. (2013) reviewed different regimes of solar thermal refrigeration, zeroing on regimes of solar absorption cooling by utilizing a variety of fluids. There was a wide range of combinations based on their operating temperature limits, capabilities of cooling power, and performance levels.

Garousi Farshi et al. (2013) studied the dual influence absorption cooling regimes. The exergoeconomic analysis made presented that great evaporator and generator temperatures, small condenser temperatures, and small efficiency of the heat

exchanger produced decent outcomes at a good price. The techno-economic analysis specified that solar electric photovoltaic cooling regimes were fewer suggested than solar absorption regimes. Some issues were shown for its influence on solar absorption regimes; these are position, weather situations, components values, cooling load, design of the regime, and execution. This work was the initial analysis prepared on a commercial structure located in Khoper city, eastern Saudi-Arabia, on the probability of applying solar air conditioning systems in such cases.

Jelinek et al. (2012) elucidated that the replacement of jet ejectors with mixers and mechanical compressors led to more effective cooling vapour compression by mixing absorbent with compressed cooling vapours. They concluded that the new compressor mixer decreased the generator temperature, increased the COP, reduced the turnover ratio, and reduced the heat exchanger volume by matching the investigational design with the original design. The proposal had the disadvantage of increasing power consumption.

In Abu Dhabi, Al-Alili et al. (2012) conducted an experiment using a 10 kW $\text{NH}_3/\text{H}_2\text{O}$ absorption cooler with a 6 m² zone and 0.1 m³ volume tank. In addition to analyzing the performance of the regime, the investigation also examined its economic and environmental benefits. The outcomes specified 47% lesser energy consumption, matched to the gas compression cycle solutions for similar circumstances. The early investment was dropped by aiming at the collector surface, as it was a very significant feature in decreasing the payback time.

Eicker et al. (2012) employed dynamic simulation models of a single-effect solar absorption system to analyse the diverse replacements for heat expulsion. Solar absorption coolers of 15 kW were used for the cooling limits. Geothermal heat expulsion regimes and dry and wet cooling towers were examined as probable expulsion approaches. Controlling the frequencies of all elements resulted in 30% lower energy consumption than the top situation for wet cooling towers for geothermal heat expulsion regimes.

Praene et al. (2011) developed a single influence $\text{LiBr}/\text{H}_2\text{O}$ cooling scheme of 30 kW. The regime was fixed and inspected in a classroom at the University Institute of Technology from Saint-Pierre. Findings revealed that with water tanks for cold and hot water storage, temperature comfort could be achieved at 20 kW. A solar loop improvement was needed in order to generate 30 kW of power. Using a 4.5 kW $\text{LiBr}/\text{H}_2\text{O}$ single influence rotary absorption cooling system with 37.5 m² flat plate

collectors and a cooling tower, Monne et al. (2011) analyzed a solar cooling regime. The data was collected in the years 2007 and 2008. A COP of 0.6 kW was recorded for cooling energy in 2007, while in 2008, the COP ranged from 0.46 kW to 0.56 kW. Likewise, the values for the chiller were 4–5.6 kW in 2007 and 3.6–5.3 kW in 2008.

Hang et al. (2011) inspected an average office building size in California. There was also an evacuated tube solar collector and storage tank for hot fluid (water) in the cooling system analysed. 4.5kW single influence absorption chiller, gas powered secondary heater, and storage tank for hot fluid (water) were part of the cooling system analysed. The findings showed that the system's economic, environmental, and energy performances were all balanced. None of the configurations resulted in any appreciable power savings. Even so, the use of solar collector resulted in an 80% reduction in CO₂ emissions. The system's execution was impacted by the water storage tank's volume. Volume to area ratios of 0.02–0.04 was found to provide the best results. This system had an optimal collector area of 280 m² and a tank volume of 11 m³ (0.04 volume to area ratio). The optimum CO₂ emission outcomes were achieved under these circumstances, with a solar contribution of 83% and a cost of \$0.75/kg to minimize the carbon sign. Sarabia et al. (2011) developed a configuration that had the solar collector linked to the single effect absorption cycle in a direct way. The analytical model employed was used to identify the influence of this design. The device's size and solar collector's surface had a direct effect on the temperature of the regeneration. The cycle of LiBr/H₂O absorption was analyzed with basic parameters, which were presented in the study. The study also included an example of fast estimation using these parameters for an application in Spanish weather conditions.

Xu et al. (2011) simulated a solar-powered absorption cycle so as to analyse the performance of the advanced power storage solution. The numerical simulation was based on dynamic models. The solar energy was stored as the chemical potential of the working liquid using the technology of Variable Mass Energy Transformation, and the proposal presented in the paper was based on using a solar collector as a regenerator. The refrigerant was stored afterwards condensation, and the weak fluid solution was stored after regeneration, becoming available for future use according to load necessities.

Shekarchian et al. (2011) conducted their research based on a year's worth of weather conditions in Iran. This study concentrated on the power needed per unit area and overall energy cost. Absorption coolers' COP and their relation to cost reduction

were also analyzed. In absorption coolers, energy utilized per unit area was higher, but energy costs were lower. Absorption cooler COP and costs were directly related to a 0.1 ascend in the COP resulting in a \$50/m² cost reduction.

Tsoutsos et al. (2010) conducted a simulation for the whole system of cooling. The simulation involved a storage tank, a secondary source of heat, a 50 kW additional compression cooler (the absorption cooler was unable to provide the necessary energy), a 70 kW LiBr/H₂O absorption cooler, a water cooling tower, a 500m² solar collector and additional 87 kW preheater. A 40% funding option would reduce the payback period from 11.5 years to 6.9 years, bringing the initial investment down to \$104,395.00, knowing that the initial price was \$173,992.00.

Gomri (2010) analyzed three different absorption cycle types (single influence, double influence, and triple influence) at cooling water while maintaining a constant 300 kW power output. Simulations were conducted based on the outcomes of the coefficient of performance, the percentage mass flow rate, and the exergetic efficiency of the refrigerant produced. Several conclusions on the three suggested systems were drawn from the investigation. First, it was determined that a higher condenser temperature resulted in a lower cycle COP when compared to greater generator and evaporator temperatures. The second conclusion revealed that, for every given condenser and evaporator temperature, there exists an optimal generator temperature at which maximum COP and energy efficiency can be achieved. Maximum COPs were found to be between 0.73 and 0.79 for a single effect system, 1.22 and 1.42 for a double effect system, and 1.62 and 1.90 for a triple effect system while operating at 33-39 °C with evaporation temperatures of 4-10 °C. Energy efficiency rating ranges: for the single effect system as 12.2-23.2%, for the double effect system as 14.1-25.1%, and for the triple effect system as 17.7-25.2%. The study found out that the COP for the double effect solution was double that of the single influence solution, but the exergetic efficiency findings were only a little higher for the double influence regime.

Fong et al. (2010) performed their study by comparing five distinct regimes of cooling. The methods analysed include numerous solutions: solar absorption refrigeration, solar electric compression refrigeration, solar adsorption refrigeration, solar solid desiccant cooling, and solar mechanical compression refrigeration. The simulations performed indicated that for the weather conditions in Hong Kong (subtropical climate), the furthestmost appropriate solutions to be employed were "solar

absorption refrigeration and solar electric compression refrigeration with flat plate and evacuate tubes collectors".

Koroneos et al. (2010) conducted a cost-benefit study of installing a solar absorption cooler with 70 kW LiBr/H₂O. The analysis found that the initial cost of around €138,000 would be recouped in 24 years, whereas the cost of a conventional cooling system is €107,640.

In their research, Desideri et al. (2009) showed how solar absorption devices may be used in two distinct procedures. The authors chose two distinct configurations to estimate the regimes utilization (air conditioning and industrial refrigeration). The refrigeration system was developed with a meat processing company's specific refrigeration needs in mind, either as a replacement for existing equipment or as an extra solution. The study combined solar flat plates with absorption chillers for this application. The air conditioning system was installed in an Italian hotel. The proposal for this use case included increased operating flexibility and heating and cooling needs. Benefits and downsides were evaluated, and the best solution for each application was determined by combining the technical and economic analysis with the experimental analysis.

Kim et al. (2009) did computations on various solar cooling absorption cycles. The authors asserted that a half-effect (LiBr/H₂O) cycle was a highly good option for solar-powered cooling systems in terms of primary investment. This was deduced from the features of the working liquid (better thermodynamic properties) and the requirement for a low driving temperature for the half-effect absorption cycle. The investigation also simulated the suggested system in a very high-temperature environment. The functioning of the system was confirmed to be effective and had low crystallization risk. Both modes of operation have the capability to lessen temperature (indirect cooling and direct). Moreover, for every cooling mode, the cooler was able to drop the water temperature from 90 C to 5.7 C and 7.8 C at a 35 C ambient temperature. The values of COP measured for direct and indirect cooling modes were 0.38 and COP 0.36, correspondingly. The direct air cooling solution's COP dropped to 81.6% and 37.5% when the surrounding temperature reached 50°C, compared to its peak performance (i.e. 35°C). A COP of 75% and 35.6% were achieved by the indirect cooling system.

Thomas & André (2009) included all the necessary components needed to assess the power usage of an air conditioning regime. The elements inspected involved

heating-cooling networks, the solar panels' area, emission circuit, storage components, pumps, rejection system, a heater, and the absorption cooler. In certain instances, the simulation was able to reduce energy usage. Using three distinct methods, it is noticed to gain 34.9 of energy use (when compared to conventional air conditioning solutions).

Balghouthi et al. (2008) utilized TRNSYS and EES software to simulate the weather in Tunisia in order to evaluate the possibility of implementing solar-powered absorption cooling. Data for the analysis included a full year's supply of Tunisian weather conditions. For a building of 150 m², the following components were incorporated into the suggested system, which yielded the best results: a solar collector area of 30 m², 11 kW of cooling capacity from a LiBr/H₂O absorption chiller; a hot water tank with volume 0.8 m³, an angle of oblique as 35°.

2.11 Experimental Investigation of Absorption System

Soto et al. (2018) investigated a solar absorption cooling regime of 5kW of cooling volume with an ammonia-lithium nitrate mixture developed in the Universidad National Autonomy de Mexico. The cooler water created from the absorption regime was used to offer air conditioning. The simulation outcome presented the temperature of the evaporator as low as 7°C and the C.O.P varying from 0.28 to 0.48.

Martínez et al. (2016) manipulated the procedure of solar cooling at the University of Hernandez mogul under the climatic conditions of some towns in Spain (Barcelona, Madrid, Bilbao, and Seville). The outcomes demonstrated that the installation was suitable for an appropriate temperature incubator among 60.8% in Seville and 78.3% in Madrid. The outcomes similarly displayed that the solar cooling regime controlled 75.3% of the entire cooling in Madrid and 52% of the entire cooling in the town of Bilbao. Finally, the high price of solar air conditioning and the absence of preservation have made this technology less common in Spain than traditional air conditioning.

Xu et al. (2015) investigated the work of solar absorption cooling systems for the high-efficient use of solar energy with temperature flexibility. A usual running situation of the cooler from the beginning to the stable operating form was stated to display the dynamic performance. The cooler limits continued stable after the warming-up procedure. A collection of information on the stable form parameters was

given to display the stable state performance. The cooler gain increased COPs from 0.69 to 1.08 under generation temperature from 95°C to 120°C, and the corresponding general COP diverse from 0.67 to 1.05. The effects of cooling water temperature, chilling water temperature, generation pump frequency, HA valve opening, and hot water pump frequency were examined. The cooler work was greater under high cooling water temperature, low chilling water temperature, a suitable frequency of generation pump, enhanced HA valve opening and high frequency of hot water pump. These tendencies fitted to the qualitative analysis of the cooler.

Yin et al. (2013) investigated the work of a minor solar absorption cooling regime of 8 kW. It composed of 96m² of solar panels, a storage tank of 3m³ and LiBr-H₂O. The usually predictable evaluation (PPD) and the predicted rate (PMV) were 0.22 and 5.89, correspondingly. Energy consumption was decreased by 43% compared to traditional chilling, and COP was 0.31. The outcomes likewise displayed that the greater the intensity of the sun, the greater the performance of the regime.

Lizarte et al. (2012) examined a new steady temperature flat fan sheet absorber in a single influence H₂O/LiBr absorption chiller. Palacios as well examined the usage of the formation of a flat fan sheet and found out that it had a greater coefficient of mass transmission than absorbers of other kinds (falling film or spray). A 1.5 m³ hot water storage tank and a 1 m³ absorption unit were components of the cooling system. The test lasted 10 days and covered 40 m², conducted in the summer climate conditions of Madrid. Collector efficiency was typically at 0.27 %, COP at 0.53, and solar COP at 0.062.

Bujedo et al. (2011) additionally used their analyses in Spanish weather circumstances for an office building. These are the conditions under which the experiment was conducted: 200 m² office area, 77.5 m² collector area, 35 kW cooler, one 1 m³ cold water storage tank, and two 2 m³ hot water storage tanks. A variety of control procedures were applied to the experiment: On/off regulator for full load operation (traditional approach); using the on/off controller to optimize temperatures of the condenser to the load and generator temperature, as well as managing the heat source liquid flow rate into the generator to control condensers and loads. It was found that the solar field yield improved between 7 and 12% and that overall system efficiency increased between 44 and 48% based on the results. The two new control strategies proposed demonstrated better results than the traditional strategy, according to the findings.

Al-Dadah et al. (2011) used propane as a refrigeration fluid. The vapours were combined with a variety of lubricants, including the alkylated benzene oils AB150 and AB300 and the naphthenic mineral oils 32 and 64. Propane-alkylated benzene AB300 is the most effective combination happened. An absorption cycle of 1.3 kW was conducted with this mixture. The energy contained heat tubes that recovered the heat of absorption, reducing the amount of heat needed by the generator. There were tubes affirmed among the pre-generator and the absorber. A COP of 1 was obtained within the regime.

Qu et al. (2010) suggested placing their system at Pittsburgh's Carnegie Mellon University. This solar-powered cooling system had a 16 kW double-influence absorption chiller. The design involved a natural vapour supplementary heater, a heat exchanger with control valves and pumps, a 52 m² parabolic trough solar collector, an absorption cooler for Li Br/H₂O combined with a cooling tower. At temperatures of 150–160 °C for the heat transfer fluid, the system achieved 33–40% efficiency over the period of more than a year of successful operation within the summer months. The solar COP varied from 0.33 to 0.44, whereas the absorption cooler's COP was between 1.0 and 1.1. Due to the very humid weather and relatively low solar radiation (600–850 W/m²), the output capacity was limited to a maximum of 12 kW, which was less than the 16 kW capability.

Ortiz et al. (2010) conducted their experiment on a 7000 m² educational building and concentrated on high-desert weather conditions. The Yazaki single-effect LiBr/H₂O water cooler used in the study was a solar cooling system with two types of solar collectors: the 108 m² vacuum tubular collectors and the 124 m² flat plate collectors. The collectors and heat exchanger connected to the thermally stratified 34 m³ hot water storage tank utilizing a water and glycol combination as their cooling liquid. The temperature of the hot water scope is 70-95 °C. To store the cold water, seven tanks with a total capacity of 50,000 m³ were employed, each of which was thermally stratified. In the event that the system's own heating and cooling output was inadequate, the campus's cold water and steam systems were called to support the system. A total of 18% of the required chilling load was found to be produced by the examined regime, with an ascend to 36% possible via air handler operating tweaks and improved storage tank insulation.

Rosiek & Batlles (2009) performed an experimental study at Spain's Solar Energy Research Centre. Depending on the season, the location's heating and cooling

were provided by a solar-powered single-influence absorption cooling regime. The annual heating and cooling power demands were 8124 kWh and 13255 kWh, respectively. Flat-plate solar collectors with 160 m² of surface area were used. A 70 kW single effect absorption chiller was used for cooling. A complete year of operation was covered by the data gathered under the control and data-acquisition regime. The authors came to the conclusion that the solar collectors were adequate for supplying the required energy for cooling during the summer months and for heating during the winter months. The average chilling capacity was 40 kW, while the average COP computed for the summertime was 0.6.

Hidalgo et al. (2008) examined a cooling single-effect LiBr/H₂O system in a 90 m² area in Spain during the summer. The 50 m² area covered by the flat plate solar collectors generated 6-10 kW of cooling power. All of the solar collectors were flat plates, with a total surface of 160 m². A single-effect absorption chiller with a capacity of 70 kW was employed for cooling. A full year of data was collected in a control and data acquisition regime. The study's authors determined that solar collectors provided sufficient energy for air conditioning in the summer and heating in the winter. For the summertime, an average COP of 0.6 and 40 kW of chilling capacity were determined.

Jelinek et al. (2008) analysed a triple compression level single phase absorption cycle. The authors implemented several different mixes of refrigerant and absorbent were employed in their experiment. The pressure was recovered, and the absorbent-refrigerant mixture was enhanced by a customized jet thrower installed at the absorber input. The absorbent di methyl ethylene urea (DMEU) was combined with numerous refrigerants: hydro chlorofluorocarbon (HCFC) (R22 and R124) and hydro fluorocarbon (HFC) (R32, R125, R134a, and R152a). According to the effect on the COP, the generator circulation ratio, condenser, and evaporator temperatures, the authors revealed that R124-DMEU (from the HCFCs) and R125-DMEU (from the HFCs) were the most effective mixtures. In order to boost COP and lower generator temperature needs, the R125-DMEU experiment was repeated.

Ali et al. (2008) Evaluated the performance of a combined system comprised of a free cooling system and a solar-powered H₂O/LiBr absorption chiller. The system was located in Oberhausen, Germany. Since August of 2002, the system has been in use, providing for the cooling of a 270m² space. The next components were involved within the system: 134 kW cooling tower, 6.8m³ hot water storage tank, 108m²

vacuum tube collectors, 1.5m³ cold water storage tanks and 10-TR absorption chiller.

They obtained the next conclusions:

- i. In addition to providing 25% of the total chilling need throughout a 5-year operating span, the system offered 70% free cooling during specific months. The regime's general design was to promote an eco-efficient system. The demand for multifunctional equipment like cooling towers might be greatly reduced as a result.
- ii. There was a monthly enlargement in the average solar heat fraction, from 31.1% to 100%, with an average of 34% to 60% during the 5 years of operation.
- iii. As a yearly average, the area of the collector had an efficiency of 41.8%, and over the period of 5 years, it had an efficiency of 28.3%.
- iv. It was found that the COP ranged between 0.37 and 0.81 on sunny days with no clouds and no solar radiation, while the solar heat fraction ranged between 0.33 and 0.41. Also, the solar collectors' efficiency was between 0.352 and 0.492.
- v. For maximum solar energy collection and absorption cooler power, the collector area must be 4.23 m²/kW.
- vi. From August 2002 to November 2007 the solar cooling system furnished 8125 kWh of cooling power.

2.12 Solar Powered Absorption Cooling New Design Opportunities

Bellos et al. (2017) studied the climatic circumstances in Athens, Greece, by developing a 100 kW solar absorption cooler. The regime has a single-phase absorption chiller with LiBr/H₂O, a storage tank, and a vacated tube collector. Many sets of solar panel zones were chosen from 150m² to 600m². Likewise, diverse sets of storage tanks were examined from 6m³ to 16m³. The greatest cases were assessed financially. The outcomes presented that the 450m² of evacuated pipe collector with 14m³ the storage tank was the perfect solution with a financial recovery time of 15 years.

Bellos et al. (2016) planned a solar absorption chilling plant of 100 kW in the climatic conditions of Athens in Greece. Four sorts of collectors, combination

parabolic gatherers, parabolic in collectors, flat plate gatherers, and vacated tube collectors, were examined to conclude the most appropriate one for this mixture. The outcomes presented that evacuated pipe collectors were the most suitable technology for the procedure, but the financial price of this technology was greater than its three natures. This was a no-cost solution.

Said et al. (2012) offered new plans of solar-powered absorption regimes for a day process. The writers offered two plans, one with a continuous process and one with a discontinuous process. The continuous process regime involved storage for cold water, refrigerant, and for heat, whereas the discontinuous process regime included a storage tank for cold water. During the day and at night, these were needed to provide continuous cooling. The heat storage regime was found to have the highest COP, although it required adequate insulation. The regime with refrigerant storage for the continuous process was seen as the preferred option for the climatic conditions in Dhahran, Saudi Arabia. Most chilling regimes employed water chilling towers, which though had problems connected to water consumption, generating greater prices, which were inspected carefully.

Marc et al. (2010) exhibited the problems of determining an optimum capacity of refrigeration. For thermal comfort in a building, a large chiller operating at less than normal conditions was found to be optimal, whereas an undersized chiller operating at nominal conditions was shown to be inadequate. Agyenim et al. (2010) suggested a 4.5 kW LiBr/H₂O solar thermal absorption cooling system with cold storage. In Cardiff, UK, the system was installed and tested. A liquid based on ethylene glycol was collected in vacuum tube collectors with 12 m² of area. The minimum temperature for chiller activation was 80 °C. The cold water temperature produced was 7–16 °C. Every day, the average electrical COP was 3.6, whereas the average thermal COP was 0.58. The authors suggest coupling heating and hot water systems with a solar-power chilling regime within the winter.

The chiller was the biggest energy consumption even when it wasn't cooling. Prasartkaew & Kumar (2010) presented a solar-biomass mixed absorption cooling regime. The components of this type of residential installation system were as follows: a hot water boiler employing biomass gas, a water heater utilizing solar power accompanied by a storage tank, and a single influence absorption chiller, and between the absorption cooler and the storage tank there was an insulated hot water boiler. During times of low solar output, the insulated boiler provided supplemental heat, and

in the absence of sunlight, it served as the primary heat generator. The continuous 24-hour operation resulted in a charcoal usage of 24.44 kg/day and a registered chiller COP of 0.7, while the whole system COP was 0.55. Bangkok is the location where the system was constructed. The suggested system has a number of advantages in the aspects of lowering greenhouse gas emissions and improving comfort.

Helm et al. (2009) analyzed a system that combined dry air chillers with low-temperature latent heat storage utilizing solar power. A cooling tower-based traditional system was compared with the regime's execution. Low-temperature periods saw the stored heat from the absorption chiller's exhaust be released into the surrounding. The absorption technique was simpler to adopt in applications without cooling towers, particularly those with smaller capacities. As opposed to conventional designs with wet cooling towers, storing the latent heat reduced the size of the system. Cooling dry air caused the difference. The authors employed a calcium chloride hex hydrate phase transitioning between 27 and 29 ° C. in their experiment. In stage-change material (PCM), transforming from liquidus and solidus states may happen. Thus, better volumetric storage was achieved, that anticipated to be about 10 times larger than in the case of water heat storage. Additionally, with just a very little increase in power consumption during low demand and peak hours, the latent heat storage allowed for the switching to the additional power source. The chiller rejection loop has included latent heat storage. Operating costs were reduced due to the lower power price throughout the night. It also reduced costs and improved overall system efficiency since there were fewer peaks and fixed loads during the day. Using a 72 m² evacuated tube solar collector, Pongtornkulpanich et al. (2008) proposed a LiBr/H₂O single-influence absorption chilling regime. An LPG-fired auxiliary heating unit supplemented the remaining 19%, according to the results, with 81% of the cooling power coming from solar sources.

Mazloumi et al. (2008) demonstrated that solar power could provide a chilling load peak of 17.5 kW by using single-influence absorption chilling. A typical Ahwaz house's chilling requirements were provided by the application. An isolated heat storage tank was proposed as part of the design of the N-S parabolic small tank collector. In order to provide the cooling load required, the collector area was at least 57.6 m². Solar collectors with flat plates or exiled pipes require a large installation surface, making them unsuitable for large cooling loads. Solar thermal power collection from parabolic trough collectors was more efficient in zones with

convenient displays. As opposed to stationary collectors, which must be exposed to direct sunlight for operation, the cooling system can start earlier and continue to operate even when there is no direct sunlight.

Ali et al. (2008) gathered the data of a solar-powered, single-effect Li Br/H₂O absorption chiller in operation in Oberhausen, Germany, from August 2002. It was integrated with a free cooling system to provide cooling for 270 m² of space. The studied design was constructed from the following components: 108 m² vacuum tube collector, 134 kW tower of cooling, 35.17 kW cooling absorption chiller, 6.8 m³ hot water storage tank and 1.5 m³ cold water storage tank. A total of 70% of cooling requirements were met through free cooling over 5 years, with an average of 25%. On sunny days, the chiller's COP was between 0.37 and 0.81, while the collectors' COP was between 0.352 and 0.492.

2.13 System Optimization of Absorption System

Jing et al. (2018) conducted an exergoeconomic optimizing solar-powered single-influence absorption cooler in low-height structures to attain price effective and power-efficient design of chilling capacity in sub-absorption regimes. The writers stated that the collector zone must be determined by the ideal chilling capacity of the absorption cooler, not the opposite. The writers also concluded that the optimum chilling capacity of the absorption subsystem powerfully relied on solar irradiance and chilling requirements. Furthermore, it concluded that the optimum size of the cooler must be designed according to the lowest product price flow rates or the minimum relative price diversity, with the last being delicate to the local mean solar irradiance.

Calise et al. (2011) concluded a single-aim optimization procedure on solar assisted single-influence and double-influence absorption coolers to know their optimum economic work. The system overall price or simple payback time was chosen as an objective function which was reduced. The writers employed the TRNOPT optimization software, a TRNSYS component that linked the TRNSYS simulation with an optimization algorithm named GenOpt, able to make single-objective optimization difficulties. In these researches, the writers employed a simple economic model, where the price of tools fitting, integration, and tubing and the expense escalation rate and fuel cost were not taken into account.

Hang et al. (2013) designed and optimized dual effect Solar LiBr/H₂O absorption cooler for small and medium-sized office structures. The writers used a linear regression analysis to a series of information points gained from the parametric work of the factory, yielding three equations signifying the current worth price, life cycle power, and life cycle carbon dioxide releases of the factory as functions of the regime's main parameters. Putting diverse weights to these equations and merging them into one equation, a single-objective optimization problem was done to find the optimum design of the factory. Meanwhile, the purposes were formulated through a usual parametric work; this optimization model likewise is weak to being stuck in local optimum regions.

Iranmanesh & Mehrabian (2014) conducted a multi-objective optimization Work on a double-influence absorption cooler coupled with exiled pipe collectors. The secondary power consumption and the clear revenue gained from the solar-derived power were considered objectives for system optimization, although the environmental aspect of the system was not taken into account. It was concluded that optimal mass flow rates had a significant part in decreasing the secondary power. Since ETCs were not suggested for high-temperature applications, as an outcome of high heat losses, they would have had a negative influence on the size of the solar field and, therefore, on the economics of the suggested regime.

Gebreslassie et al. (2012) established an optimization model joined with life cycle evaluation values to enhance the work of a single-influence H₂O-NH₃ absorption cooler regime from economic and environmental features in Barcelona. No structure model was considered in their work, supposing that the end operators required a constant chilling load throughout the year. The entire price of the regime and the quantity of CO₂ emissions released into the air were processed as two objective functions and were reduced. The outcomes proposed that considering government subsidies on solar technologies, the modelled regime is economically attractive under the power price in Spain. The writers, though, did not examine how the optimum design of the modelled regime would compare contrary to solar multi-influence absorption coolers.

Shirazi et al. (2017) established a simulation model of these three patterns in the TRNSYS 17 environment. A joined power, economic, and climatic analysis of the modelled regime was conducted to determine the main power use in addition to the levelled entire yearly price of every factory, which was considered as two differing

objective purposes. The work of the offered regime was compared to that of the traditional regime chosen as a reference. The writers likewise conducted a sensitivity analysis to measure the effect of fuel price, capital price of advanced components, and the yearly interest percentage on the Pareto front of optimum solutions. Generally, the optimization results revealed that the proposed configuration, the SHC double-influence cooler, had the greatest trade-off among the power, economic, and environmental performances of the regime, having a total price of ~0.7–0.9 M\$ per year and decreasing the yearly main power use and CO₂ releases by 44.5–53.8% and 49.1–58.2%, correspondingly (relative to the reference traditional regime). The writers concluded that with the high capital price related to these regimes, government subsidies and incentives were still wanted in order for this technology to attain acceptable payback times and become price-competitive with traditional HVAC regimes.

2.14 Summary of previous research of the Solar Absorption System

The detailed summary based on reviewed literature is summarized in Table 2-4. Table 2.4 depicts the findings of different past research work done in the area subjected area.

Table 2.4: Summary of previous research of the absorption system

No	Author	Title	Summary of Finding
1	Schmid et al. (2019)	Development of a solar-driven diffusion absorption chiller.	Presented a diffusion absorption chiller directly heated by a solar collector with enhanced efficiency. The generator, acting as the bubble pump of the diffusion absorption process, was integrated into a double-glazed flat plate collector. Maximum cooling capacities of 226 W and 228 W were reached. The maximum efficiency of the whole process was achieved, and therefore the percentage of the insolation incident on the solar collector converted into cooling capacity was 11.4%.
2	Jing et al. (2018)	Exergoeconomic-optimized design of a solar absorption-Subcooled compression hybrid cooling system for use in low-rise buildings.	Carried out an exergoeconomic optimization of a solar-driven, single-effect absorption chiller in low-rise buildings to achieve a cost-effective and energy efficient design of the cooling capacity in absorption sub-systems. The authors reported that the collector area should be determined by the optimal cooling capacity of the 3absorption

Table 2.4 (Continued)

No	Author	Title	Summary of Finding
			chiller, not vice versa. The authors also found that the optimal cooling capacity of the absorption subsystem strongly depended on solar irradiance and cooling demands.
3	Soto et al. (2018)	Preliminary assessment of a solar absorption air conditioning pilot plant.	Analyzed an ammonia-lithium nitrate mixture solar absorption cooling system developed at Universidad Nacional Autonoma de Mexico with a cooling capacity of 5 kW. The absorption system provided air conditioning by producing cooler water. As an outcome of the simulation, the evaporator's temperature dropped to 7°C, and the C.O.P. raised from 0.28 to 0.48.
4	Bellos et al. (2017)	Energy, exergetic, and financial evaluations of a solar driven absorption chiller A dynamic approach.	The cost and performance of solar cooling fan have been investigated for a 100m ² building in ten different cities around the world. The analysis was conducted via TRNSYS. The simulation result showed Abu Dhabi and the city of Phoenix were the most suitable for the work of refrigeration unit's solar absorber, and the minimum cost was 0.0575 and 0.0590, respectively. Rome, Madrid, and Thessaloniki were less appropriate and cost 0.1771 and 0.1792 and 0.2125, respectively.
5	Bellos et al. (2017)	Energy and financial analysis of solar cooling systems with single-effect absorption chiller in various climates.	A solar cooling system of 100 kW was designed under the climatic conditions of Athens in Greece. The best cases were assessed financially. Outcomes showed that with a financial recovery period of 15 years, the 450m ² evacuated tube collectors with a 14 m ³ storage tank proved to be the optimum solution.
6	Shirazi et al. (2017)	A comprehensive, multi-objective Optimization of solar-powered absorption chiller systems for air-conditioning applications.	A simulation model of these three configurations was developed in the TRNSYS 17 environment. A combined energy, economic, and environmental analysis of the modelled systems was carried out to calculate the primary energy use as well as the levelled total annual cost of each plant, which were considered two conflicting objective functions. The performance of the proposed optimal systems was compared with a conventional system as a reference. The optimization results revealed that of the proposed configurations, the SHC double-effect chiller had the best trade-off between the energy, economic, and environmental performances of the system, having a total cost of ~0.7–0.9 M\$ per year and reducing the annual primary energy use and CO ₂ emissions by 44.5–53.8% and 49.1–58.2%, respectively.

Table 2.4 (Continued)

No	Author	Title	Summary of Finding
7	Bellos et al. (2016)	Comparaison de performances de systèmes solaires autonome et assisté à absorption en Espagne.	Under the Athens climatic conditions, a 100 kW solar absorption cooling plant was designed. Tests were conducted on four different collector kinds to determine which was most suitable for this mixture: evacuated tube collectors, flat plate collectors, parabolic trough collectors, and compound parabolic collectors. After analyzing the data, it was found that evacuated tube collectors were the optimal technology for the procedure; nevertheless, the expense of this technology much outweighed its other three aspects. This solution was financially useless.
8	Al-Ugla et al. (2016)	Techno-economic analysis of solar-assisted air-conditioning systems for commercial buildings in Saudi Arabia.	PV cooling system was more beneficial than solar absorption cooling. The P.V system payback period was 23.9 years, versus 18.5 years for the solar absorption system.
9	Evangelos and Christos (2018)	Energy and financial analysis of solar cooling systems with single effect absorption chiller in various climates.	Showed the city of Abu Dhabi and the city of Phoenix were the most suitable cities for the work of refrigeration solar absorption system, and the minimum cost was 0.0575 and 0.0590, respectively.
10	James et al. (2016)	Performance study of a solar absorption power-cooling system.	The efficiency of the system in the city of Seville was better than the efficiency of the city of Chennai in India.
11	Amine Allouhi et al. (2015)	Economic and environmental assessment of solar air-conditioning systems in Morocco.	High energy saving and CO ₂ reduction. Regarding the economic feasibility, the study indicated that the cost of initial investment required an extensive payback period.
12	Fasfous et al. (2013)	Potential of utilizing solar cooling in the University	The estimated payback period of 24 years for the solar-powered cooling system was longer than the duration of the project. The study concluded that the implementation of the project was not advisable under current investment conditions.
13	BANI Younes et al. (2013)	Assessment of solar assisted air conditioning in Central Queensland's subtropical climate, Australia.	The highest saving energy was in Emerald with 88%, followed by energy saving of 82% in Gladstone and 80% for Rock Hampton. The energy saving increased when the storage tank increased.
14	Farshi et al. (2013)	Exergoeconomic analysis of double-effect absorption refrigeration systems.	High-temperature generator, high-temperature evaporator, low-temperature condenser, and low-effectiveness of heat exchanger had good results cost-wise.
15	Jalinec et al. (2012)	Performance of a triple-pressure level absorption/compression cycle.	As a result of the new compressor-mixer, the necessary generator temperature was reduced, the COP was increased, the circulation ratio was

Table 2.4 (Continued)

No	Author	Title	Summary of Finding
			reduced, and the heat exchanger volume was reduced.
16	Al-Alili (2012)	Modelling of a solar-powered absorption cycle for Abu Dhabi.	Comparatively, 47% less power is consumed for the same conditions when using a vapour compression cycle solution.
17	Eicker et al. (2012)	Heat rejection and primary energy efficiency of solar-driven absorption cooling systems.	The lowest power consumption for the geothermal heat rejection system is 30% lower than the best scenario for wet cooling towers.
18	Praene et al. (2011)	Simulation and experimental investigation of solar absorption cooling system in Reunion.	The temperature comfort was achieved at 20 kW for the system.
19	Pongtornkulpanich et al. (2008)	Experience with fully operational solar-driven 10-ton Li Br/H ₂ O single-effect absorption cooling system in Thailand.	Solar power produced 81% of the required power for the system.
20	Hang et al. (2008)	Energy and carbon emission savings in Spanish housing air-conditioning using solar-driven absorption system.	The CO ₂ emission was reduced by 80% with the implementation of the solar collector, the solar fraction was 83%, and the cost of reducing the carbon footprint was \$0.75/kg.
21	Said et al. (2011)	Alternative designs for a 24-h operating solar-powered absorption refrigeration technology.	The necessity of balancing the regenerator temperature in the sub-system.
22	Xu et al. (2011)	An investigation of the solar-powered absorption refrigeration system with advanced energy storage technology.	The refrigerant was stored after condensation, and the weak fluid solution was stored after regeneration.
23	Shekar Chiana et al. (2011)	Energy savings and cost-benefit analysis of using compression and absorption chillies for air conditioners in Iran.	A direct relationship between COP and costs, 0.1 increased the COP produced a \$ 50/m ² reduction.
24	Ozgoren et al. (2012)	Modelling of a solar-assisted HVAC system with thermal storage.	The atmospheric temperature affected the value of COP. The value of COP changed during the day from 0.243 to 0.454, while COP changed from 1.454 to 1.243.
25	Tsoutsos et al. (2010)	Design of a solar absorption cooling system in a Greek hospital.	The payback period of the initial cost (\$173.992 without funding subsidies) was 11.5 years but was reduced to 6.9 years with funding subsidies which brought the initial cost to \$104.395.
26	Xu et al. (2015)	Experimental evaluation of variable effect Li Br-water absorption chiller designed for high-efficient solar cooling system.	The chiller parameter appeared steady when making the system net change.

Table 2.4 (Continued)

No	Author	Title	Summary of Finding
27	Monk et al. (2010)	Experimental investigation of a solar cooling absorption system operating without any backup system under tropical climate. <i>Energy and Building</i> .	It was possible to achieve thermal comfort inside a building by installing an oversized chiller working below nominal conditions, while an undersized chiller working in nominal conditions cannot provide thermal comfort.
28	Lizaret et al. (2012)	An innovative solar-driven directly air-cooled Li Br-H ₂ O absorption chiller prototype for residential use.	They found the average collector efficiency was 0.37, the COP was 0.53, and the solar COP was 0.062.
29	Bujedo et al. (2011)	Experimental results of different control strategies in a solar air-conditioning system at part load.	They found an improved solar field yield (between 7 and 12%) and higher overall system efficiency (between 44 and 48%).
30	Al-Dadah et al. (2011)	Solar powered vapour absorption system using propane and alkylated benzene AB300 oil.	They found the best mixture resulted from the combination of propane-benzene AB300.
31	Rosick and Batles (2009)	Integration of the solar thermal energy in the construction: Analysis of the solar-assisted air-conditioning system installed in CIESOL building.	The average COP for the summer period was 0–6, and the average cooling capacity was 40 kW.
32	Hidalgo et al. (2008)	Energy and carbon emission savings in Spanish housing air-conditioning using solar driven absorption system.	The energy costs were 62%, and the CO ₂ emission was also 36% lower with the solar-powered system.
33	Rodrigo Hidalgo et al. (2008)	Energy and carbon emission savings in Spanish housing air-conditioning using solar driven absorption system.	They found the value of seasonal COP was 0.33.
34	Qu et al. (2010)	A solar thermal cooling and heating system for a building: Experimental and model-based performance analysis and design.	The system recorded 33–40% efficiency at 150–160°C, heat transfer fluid temperatures, the absorption cooler COP between 1.0 and 1.1 and a solar COP between 0.33 and 0.44.
35	Ortiz et al. (2010) and Mamoli et al. (2010)	Modelling of a solar-assisted HVAC system with thermal storage.	They found that the system produces 18% of the required cooling load, with the possibility to increase the percentage up to 36% by insulation of storage tanks.
36	Martinez et al. (2016)	Comparison de performances de systems solarise autonomic et assist à absorption en Espane.	Solar cooling contributes 75% of the Madrid cooling and 52 of the Bilbao cooling from the total cooling.
37	Jelinek et al. (2008)	The performance of a triple pressure level absorption cycle (TPLAC) with working fluids based on the absorbent DMEU	They found that the best combinations were R124-DMEU (from the tFCs).

Table 2.4 (Continued)

No	Author	Title	Summary of Finding
		and the refrigerants R22, R32, R124, R125, R134a, and R152a.	
38	Ali et al. (2008)	Performance assessment of an integrated free cooling and solar-powered single-effect lithium bromide-water absorption chiller.	The free cooling rate during certain months was up to 70%. Additionally, the system was able to provide 25% of the total cooling necessity over a 5-year operation time.
39	Evangelos et al. (2017).	Energy, exergetic and financial evaluation of a solar driven absorption chiller — A dynamic approach.	They found that 450m ² of evacuated tube collectors with a 14 m ³ storage tank was the ideal solution with a financial recovery period of 15 years.
40	Evangelos et al. (2016)	Exergetic, energy and financial evaluation of a solar driven absorption cooling system with various collector types.	A vacuum tube collector was found to be the most suitable technology for the process.
41	Said et al. (2012)	Alternative designs for a 24-h operating solar-powered absorption refrigeration technology.	They found that the most suitable solution was considered the system with refrigerant storage for continuous operation.
42	Agyeum et al. (2010)	Design and experimental testing of the performance of an outdoor LiBr/H ₂ O solar thermal absorption cooling system with a cold store.	For the cold season, the authors recommended integrating the solar-powered cooling system with the heating and hot water systems.
43	Prasartkaew and Kumar (2010)	A low carbon cooling system using renewable energy resources and technologies.	The chiller COP was 0.7 and 0.55 for the entire system, and the charcoal consumption of 24.44 kg/day.
44	Maz Loumi et al. (2008)	Simulation of solar lithium bromide-water absorption cooling system with parabolic trough collector.	They found that the parabolic trough collector was more efficient in terms of solar thermal energy collection in areas with convenient displays and the cooling system was able to start earlier operation and to even continue to operate in the absence of direct sunlight.

2.15 Summary

This chapter comprehensively assessed the literature on solar energy and its applications, air-conditioning system, and type of solar cooling technology.

It also provided a detailed review of previous studies conducted on solar absorption cooling (theoretical analysis, experiments, and new designs) in various world countries and knowledge of the ways and conditions during which this system worked and how to implement it in the conditions of Iraq..

CHAPTER 3

METHODOLOGY

3.1 Introduction

The procedure in this chapter is developed to calculate the cooling energy of the residential building. This building is located in Baghdad city in Iraq, and this building is chosen as a case study to investigate the energy consumption of a typical building's operating costs. This method represents an essential priority for used energy and demands the availability of detailed information. For that, the first step in developing the air conditioning system is the heat gain calculations. This process involves the outdoor conditions, indoor conditions and the heat resources such as occupants, equipment and lightning. The calculation method applies ASHRAE procedures and data tables to study this case using the Microsoft Excel program to apply calculations. The next step after calculating the cooling load of the structure is to calculate the cooling systems using the Engineering Equation Solver (EES) program. This software is employed to determine the cooling equipment consumption energy. The research methodology of the present work is shown in Figure 3.1, and the technical calculation of the energy consumption is shown through the proposed steps in this chapter.

3.2 Research Flow Chart

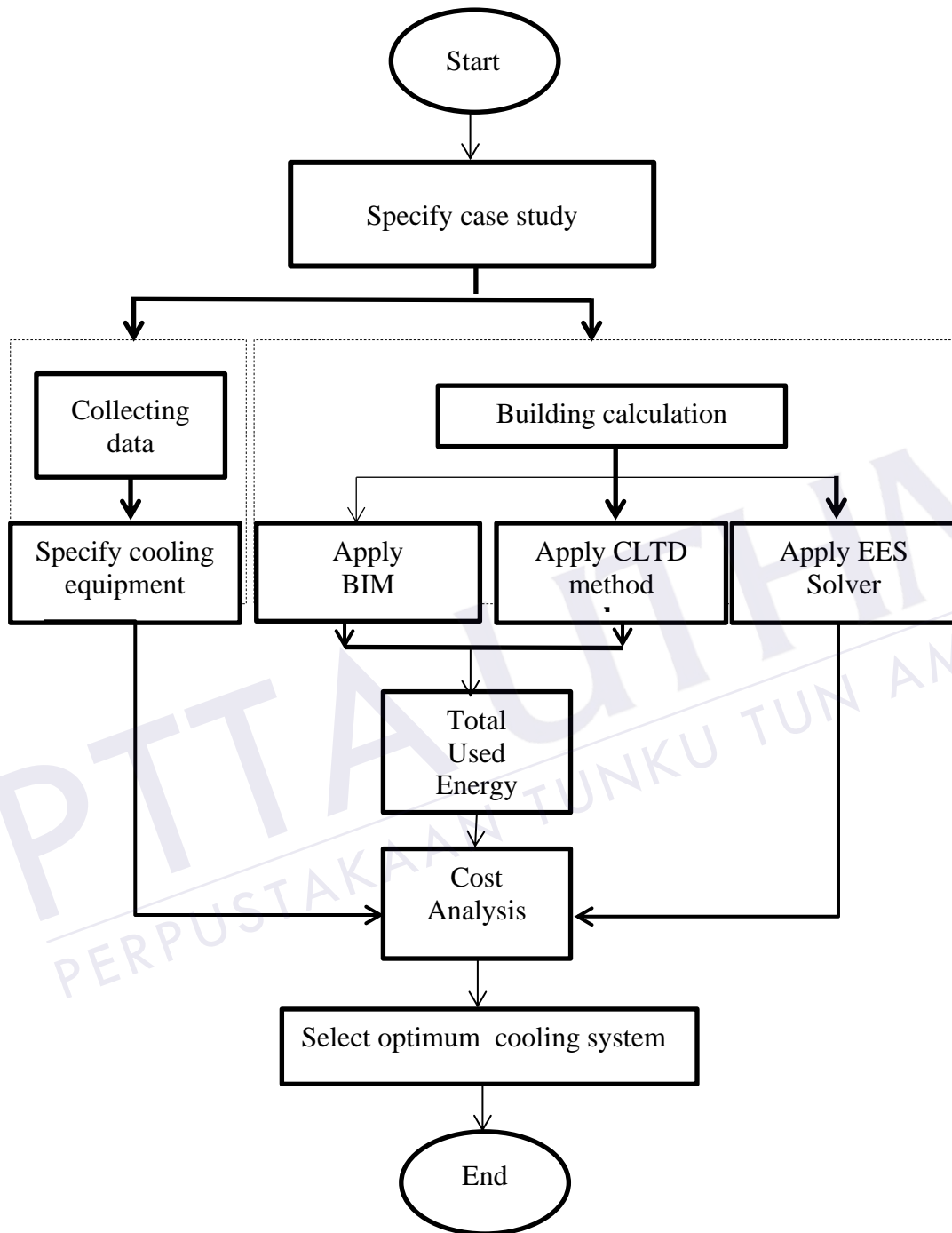


Figure 3.1: Flow chart of Research Study

This approach begins by identifying possible energy-efficient measures, which represent specific actions that could improve building energy efficiency if applied. Opportunities to aid in decreasing the structure's energy consumption, energy-efficient measures were categorized into the sections outlined below: (1) occupants and

operations; (2) building envelope and features; (3) lighting systems and process equipment; (4) HVAC systems with related to indoor, outdoor air quality.

3.3 Case Study Location

The structure considered in this study is located in Baghdad city, Iraq. This case is chosen because of the high temperature with a long time of summer in the year and major electrical problems in this country.

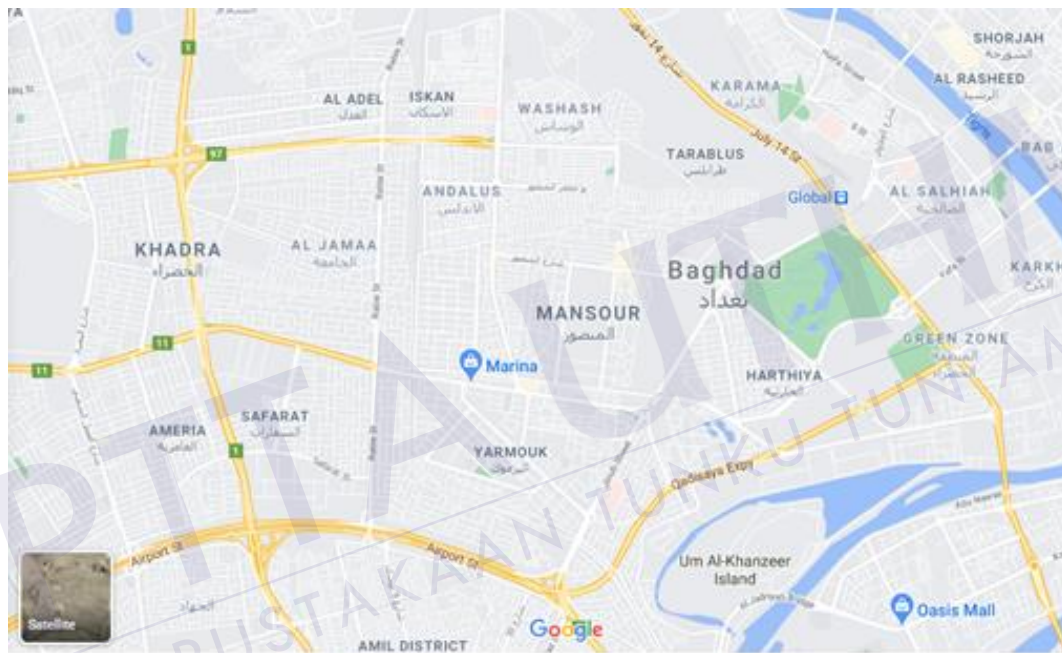


Figure 3.2: Location of the residential building (Kithara city, Baghdad, Iraq)

The building is located at (44.361488°) longitude and (33.312806°) latitude at the height of around (39) meters above mean sea level. The case study design involves three building levels, as shown in Figures 3-3, Figure 3.4 and Figure 3.5 below.

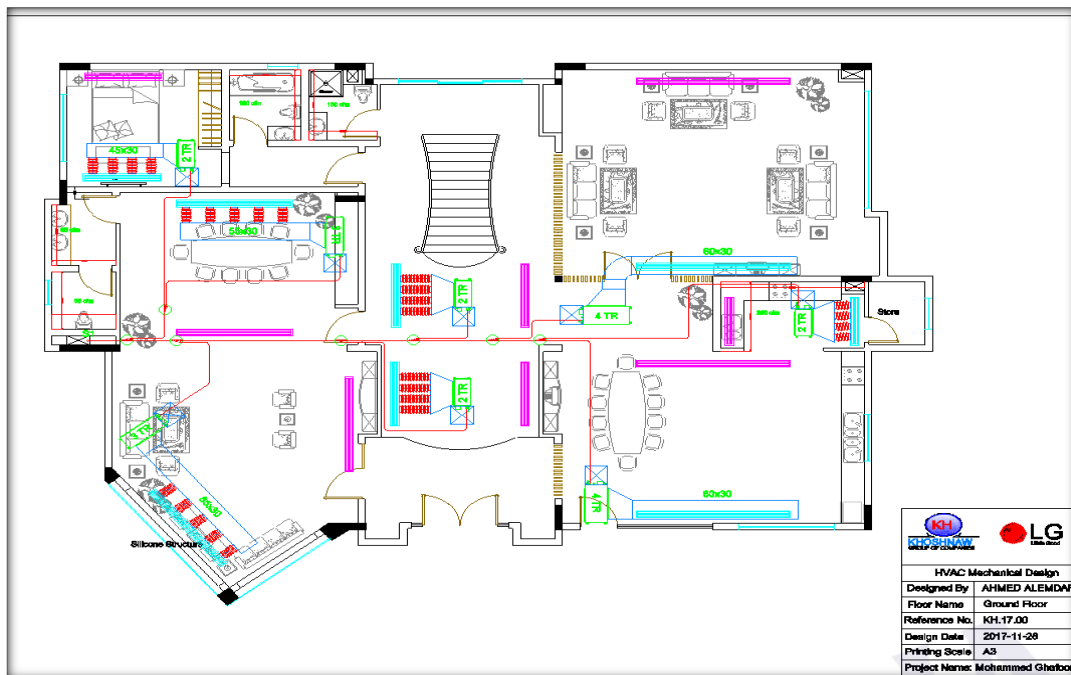


Figure 3.3: Ground Floor of the residential building

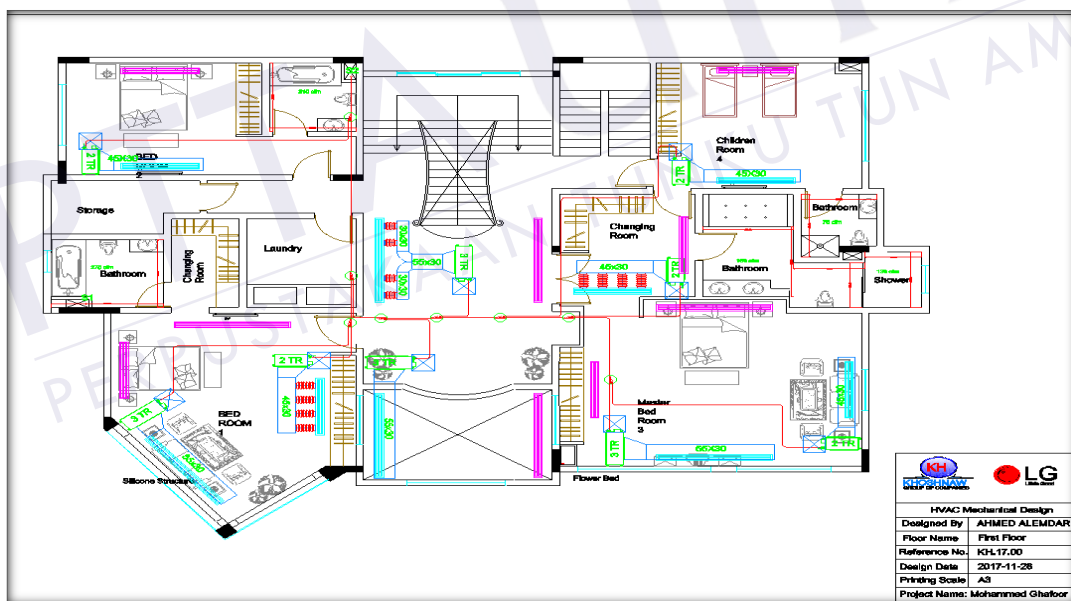


Figure 3.4: First floor of the residential building

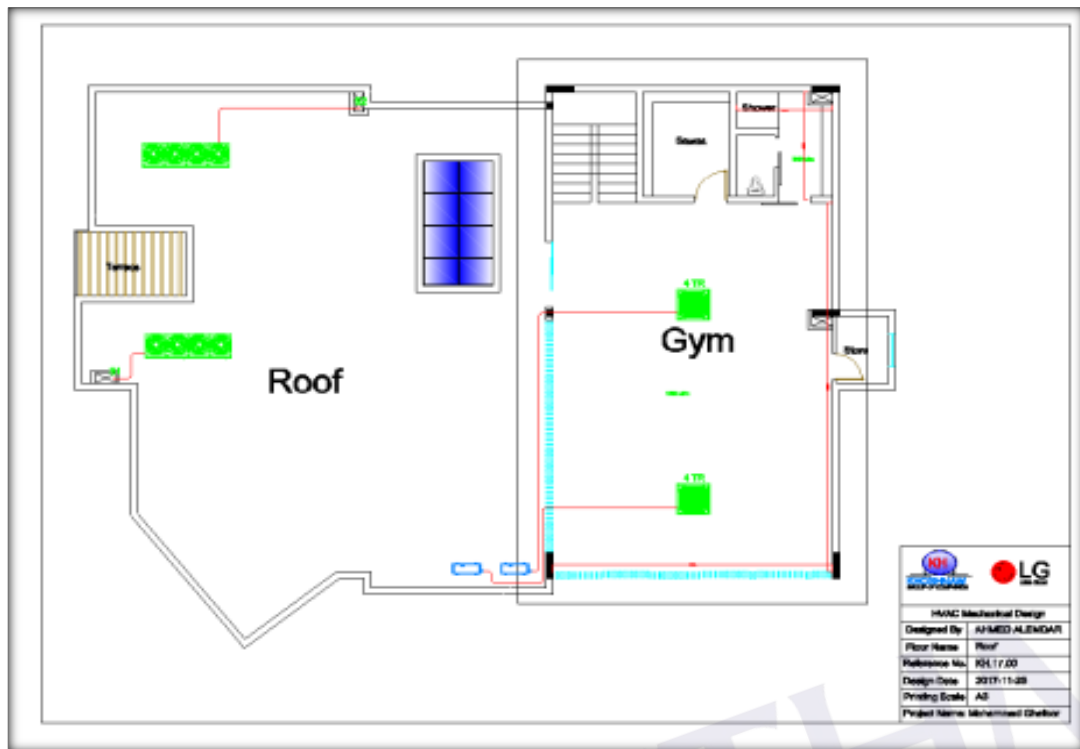


Figure 3.5: Second floor of the residential building

3.4 Climate Condition

The lack of ocean has a significant influence on the weather in this area. The winters are frigid, while the summers are scorching. In the winter, temperatures drop due to the short daylight duration and the tendency of the sun's rays to fall at a low angle, as well as the area's vulnerability to the domination of cold continental polar air masses, which produce a considerable drop in temperatures. The clearness of the sky and the lack of clouds throughout the day cause the air temperature to rise significantly in the summer. Climate conditions have an impact on human comfort and mental output. Solar radiation, temperature, relative humidity, and wind are examples of these elements. When using the equation of real temperature in Baghdad to determine the extent to which people are comfortable. The official resources, such as (www.worlddata.info) present the climate as shown in Figure 3.6.

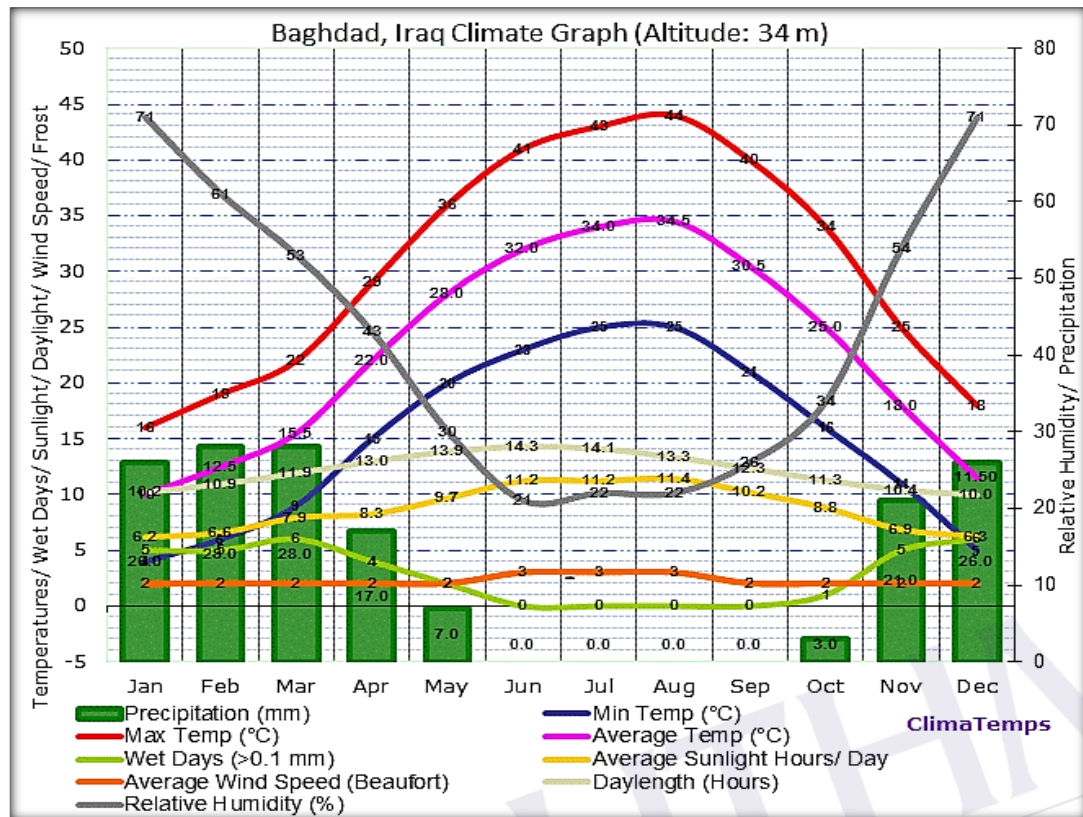


Figure 3.6: Climate Annual Condition (ASTM E2877)

The effective temperature averages for December, January, and February were 11.50, 10.00, and 12.50, respectively, as shown in Table 3.1 below.

Table 3.1: Average temperature guide (°C) for the city of Baghdad

Month	Average Max Temperature °C	Average Temperature °C	Average Min Temperature °C
January	16.00	10.00	4.00
February	19.00	12.50	6.00
Marc	22.00	15.50	9.00
April	29.00	22.00	15.00
May	35.00	28.00	20.00
June	40.00	32.00	23.00
July	45.00	34.00	25.00
August	50.00	34.80	25.00
September	40.00	30.50	21.00
October	34.00	25.00	16.00
November	25.00	18.00	11.00
December	18.00	11.50	5.00

In December, January, and February, the effective day-to-month temperatures were 15.7, 14.7, and 16.1, respectively. Table 3.2 depicts these months based on weather comfort and climatic transitions produced by low temperatures and high

relative humidity levels, or not. The weather is ideal in March (18.5), with effective temperatures of 21.6 and 24.9 in April and May, respectively.

Table 3.2: Effective temperature day manual (°C) to the city of Baghdad

Month	Effective Temperature (°C)
January	14.70
February	16.10
Marc	18.50
April	21.60
May	24.90
June	27.30
July	28.50
August	28.30
September	26.60
October	23.30
November	18.50
December	15.70

The effective temperature degree (ET) was discovered using wet and dry bulb temperatures, as well as wind velocity, in prior experiments. The effectiveness of human heat has an impact on whether or not one feels calm. When the bio-meteorological temperature hits 1°C, the climate is frigid; nevertheless, when it reaches this class between 6 and 12 °C, the weather will be pleasant. Even yet, if the temperature is between 8 and 24 degrees Celsius, man feels the heat. In this study, the offered principles are used to create the computations and supply the beginning circumstances.

3.5 Comfort Condition

For comfort conditions, structures are designed for humans, and those humans are trying to achieve a task, whether it is raising a family, running an office, or making goods. The structure wants to preserve humans comfortably. Making comfortable circumstances is one of the major uses of power in structures, and it is likewise critical to the happiness and productivity of its operators. Frequently factors, for example, airflow and radiant temperature, are ignored in a design, causing higher power use and tenancy dissatisfaction. For all structures other than villas, all Heating, Ventilation, and Air Conditioning (HVAC) regimes should be delivered with controls to make sure the achievement of power efficiency during utilization in accordance with the American Society of Heating, Refrigerating, and Air-Conditioning Engineers

(ASHRAE) 90.1-2007, Section 6.4.3. in case of design tactics like high or clerestory windows, light shelves, well-located skylights and other elements aid in reducing energy use by using effective features natural and artificial lighting, good control and automatically thermal balance and others. Figure 3-7 shows the human comfort condition obtained from the website www.pinstopin.com.

For lighting Power, ASHRAE 90.1-2007, Table 9.5.1 refer to densities of lighting for a building. For a green building, the synthetic lighting in spaces inside six (6) meters in depth from exterior windows must be fitted with lighting controls incorporating photocell sensors able to modify the level of electric lighting to add natural daylight only when necessary. The mixed synthetic and daylight should offer a lighting level at the functioning plane between four hundred (400) and five hundred (500) lux.

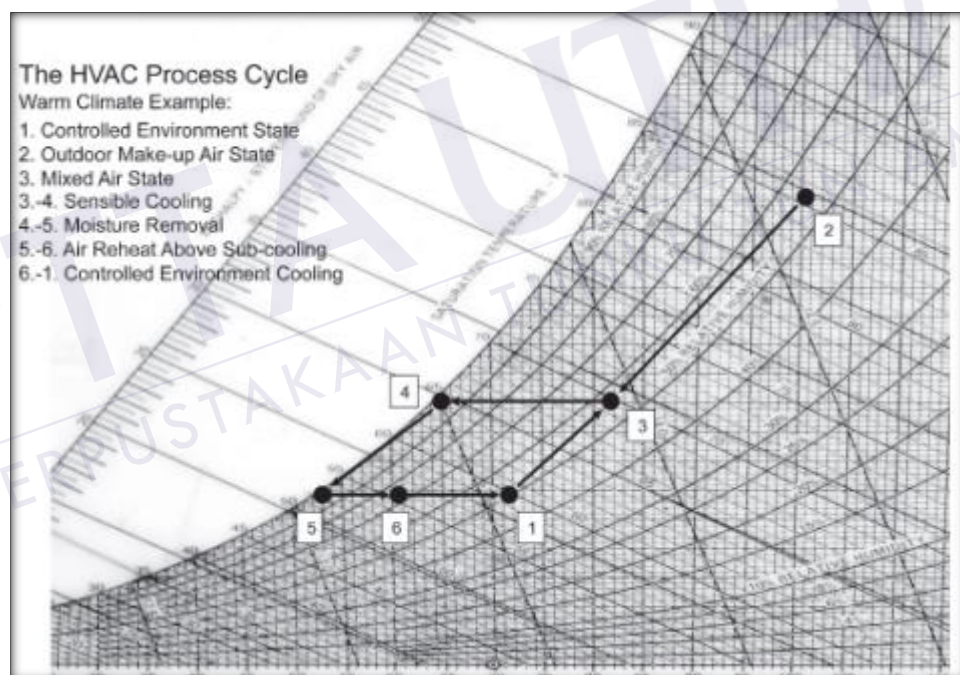


Figure 3.7: Comfort Condition Based on Psychrometric Chart (Paoli., 2012)

3.6 Building Characteristic

The construction sector in most countries is a main consumer of power. There are two main tactics for enhancing power efficiency in structures: the first is active cooling systems, and the second is building design. Active mostly concentrates on the employ

of power efficient structure service regimes. To decrease power dissipation through the building's operation stage, the environmental circumstances in the house use building design elements, for example, layout and shape, rather than mechanical regimes. In this study, the case study design provides a consistent baseline for comparison; Table 3.3 displays the data for the chosen housing building under analysis. This housing structure is positioned in Baghdad city, Iraq.

Table 3.3: Building Characteristic

No.	Characteristics	Description
1	Type	Three floors
2	Ground floor area	336.00 meter square
3	First floor area	336.00 meter square
4	Second floor area	100.00 meter square
5	Total height	11.00 meter square
6	Gross wall area	650.00 meter square
7	Window area	105.00 meter square
8	Window to wall ratio	16.15%

Building envelope design affects 20–60% of the building energy input, making it crucial for high-performance, sustainable buildings. Efficient designs generally require fewer life cycles cost and present more significant energy-saving effects as well as longer lifespans.

3.7 Cooling Load Calculation

Calculation of heat loads for summer chilling buildings requires operating requirements, proper distribution of air in thermal comfort, and suitable design and selection of air conditioning equipment and air handling units. Earlier to assessing the chilling load of any structure, there are some basic data required to design exact HVAC regimes, such as building orientation, weather conditions, building spacing, building materials etc. The more exact the data, the more exact load expected.

3.8 Load Component

Cooling load calculations depend on the structure interior design situations, position, orientation, and structure construction design. The transferred heating power from the external hot average to the interior of the room provides exterior heat gains.

Conduction via external walls, top roof, and bottom ground, solar radiation through windows and doors, ventilation, and infiltration all contribute to heat transfer. Interior heat gain from humans, electric equipment, and light are some of the other sources. The principal source of sensible thermal load is heat gain from building structures such as walls, floors, roofs, doors, and windows. Thermodynamic transfer occurs when the temperature of impervious surfaces changes. Convection transports the heat from the outside air to the exterior surface. The heat is subsequently transferred to the internal surface of the building via conduction. The rate of heat transmission from outdoor air to inside air is calculated by the formula 3.1.

$$Q = UA(CLTD) \quad (3.1)$$

Where:

U = overall heat transfer coefficient (W/m²·°C)

CLTD = cooling load temperature difference (C)

A = surface area (m²).

When the wall, floor, or ceiling is made up of a layer of different materials, then the overall heat transfer coefficient 'U' was calculated by the equation using formula 3.2 below.

$$U = \frac{1}{\frac{1}{h_v} + \frac{x_1}{k_1} + \frac{1}{k_u} + \frac{x_2}{k_2} + \frac{1}{h_l}} \quad (3.2)$$

Usually, the structure walls may involve non-homogeneous materials such as hollow bricks, air gap and plaster. Thermal transmission through these kinds of the wall is quite complex as it includes simultaneous thermal transmission by conduction, convection and radiation. In the next section, the systematic mathematical model for cooling load calculation will present in detail.

3.9 Cooling Load Temperature Difference (CLTD)

Choosing a fit air conditioning zone for any building needs a cost approximation of the cooling load. The CLTD technique employs factors like CLTD, SCL and CLF for approximating thermal gains due to exterior loads, windows and interior loads correspondingly. The thermal gain caused by interior loads is directly transformed to a chilling load in TETD technique, while in CLTD technique, the interior loads are partially added to the chilling load. CLTD is the effective temperature change across a wall or roof, which accounts for the influence of radiant thermal in addition to the temperature change.

The ASHRAE has established the CLTD values for external walls and ceilings founded on solar radiation differences with certain outdoor and inside air temperature situations. The cooling load components are based on sensible and latent thermal loads in addition to the space and internal loads. Space load is utilized to calculate the lowest air supplies to preserve inside psychometric conditions. The addition of space load is utilized for sizing the air conditioning equipment. Table 3.4 presents the components of the cooling load

Table 3.4: Components of Cooling Load

No	Cooling Load Components	Sensible Load	Latent Load	Space Load	Coil Load
1	Conduction through roofs, walls, windows and skylights	✓		✓	✓
2	Solar radiation through windows and skylight	✓		✓	✓
3	Conduction through the ceiling, interior partition walls and floor	✓		✓	✓
4	People	✓	✓		
5	Lights	✓		✓	✓
6	Equipment/Appliances	✓	✓	✓	✓
7	Infiltration	✓	✓	✓	✓
8	Ventilation	✓	✓	✓	✓
9	System Heat Gain	✓			✓

In this research, an entire equivalent temperature change (TETD) and chilling load temperature change (CLTD) approaches are developed in the excel spread sheets Software design for computing the chilling load for a structure. The chilling load and

CLTD are utilized to approximate the chilling load on an hourly basis. The main page of the Excel sheet involves the main initial input data, as shown in Figure 3.8.

project:	Heating & Cooling Load Calculation		
method:	CLTD		
reference:	ASHRAE Handbook of Fundamentals		
Design Firm:	UTHM		
Project Engineer:	ali alqaisi		
Project Name:	master project		
Project Location:	Baghdad, Iraq		
initial conditios		results	
Site:			cooling load
	Latitude:	44.23 E	ground floor load
	Longitude:	33.23 N	8 rooms
	Elevation (feet)	112	336m ²
Inside Design Conditions:			first floor load
	cooling (F)	73	7 rooms
	Air Velocity (fpm)	<50	336m ²
Max. Mean			
	cooling (F)	362	second floor load
	heating (F)	377	gym
Internal Loads			100m ²
	People:	15	
	Lighting (W)	7200	
	Equip.(W)	12000	Total Cooling load (KW)
			225

Figure 3.8: Excel Sheet for result observation

The results data in the main sheet are calculated based on the sequence of the formula below.

3.9.1 Solar Heat Gain through Glass

The heat gain over glass regions accounts for the majority of the load on the cooling system. This might be direct radiation, such as sunrays, or indirect radiation, such as reflections from other objects outside. The wavelength of radiation and the physical and chemical properties of glass were used to determine how much heat was passed through a glass. A portion of the radiation is absorbed, while the remainder is reflected and dispersed. Glass transmits heat in two ways: through transfer thermal gain and through solar heat gain. The formulae below are used to calculate heat gain from glass zones. Heat gain is transferred across the glass in the following way. Figure 3.9 shows the excel sheet of this project. The space of glass window cooling load Q is calculated as

$$Q = A_{\text{unshaded}} * \text{SHGF} * \text{CLF} * \text{SC}. \quad (3.3)$$

Where:

A_{unshaded} = Area of the glass windows in m^2

SHGF = solar heat gain w/m^2 (ASHRAE 1985 fundamental handbook chapter-26 table 11)

CLF= Cooling load factor (CLF For Glass ASHRAE 1985 fundamental Handbook chapter 26 table 14)

SC=Shading Coefficient

Windows data calculations							
Solar	Shade Coeff.	SCL (am)	SCL (pm)	Area (sf)	qc (am)	qc(pm)	
North	0.86	140	22	23	2769.2	435.16	
NE	0.9	95	24		0	0	
East	0.93	43	30		0	0	
SE	0.93	25	25	12	279	279	
South	0.92	23	97		0	0	
SW	0.9	21	140	11	207.9	1386	
West	0.92	22	141	14	283.36	1816.08	
NW	0.92	22	21	15	303.6	289.8	
sum					3843.06	4206.04	
Conduction	U (Btu/hr-ft ² -F)	CLTD(am)	CLTD(pm)	ΔT	Area (ft ²)	qc (am)	qc(pm)
North	0.55	8	15	18	12	0.0396	0.0858
NE	0.55	8	15	18		0	0
East	0.55	8	15	18	11	0.0363	0.07865
SE	0.55	8	15	18	16	0.0528	0.1144
South	0.55	8	15	18	20	0.066	0.143
SW	0.55	8	15	18		0	0
West	0.55	8	15	18		0	0
NW	0.55	8	15	18		0	0
sum						0.1947	0.42185

Figure 3.9: Heat gain through glass sheet

3.9.2 Heat Gain from Occupants

In a chilly setting, the human body generates a cooling load of functional and latent heat. The temperature difference between the body and the room air causes the sensible heat load to be assumed out in an air-conditioned environment. The average number of individuals likely to be present in a conditioned environment is used to calculate the thermal gain from inhabitants. Each human's thermal burden is determined by his or her actions. The value of thermal gain increases as the number of individuals moves. The following formulae are used to calculate the thermal gain from human occupancy

of individuals' moves. The following formulae are used to calculate the thermal gain from human occupancy. Sensible heat gain from occupants

$$Q_{\text{sensible}} = N * (QS)(CLF) \quad (3.4)$$

$$Q_{\text{latent}} = N * (QL) \quad (3.5)$$

N = number of people in space.

QS, QL = Sensible and Latent heat gain from occupancy is given in 1997 ASHRAE Fundamentals Chapter 28, Table 3. CLF = Cooling Load Factor, by an hour of occupancy. See 1997 ASHRAE Fundamentals, Chapter 28, table 37. CLF = 1.0 if the operation is 24 hours or cooling is off at night or during weekends.

People:	Btu/person	CLF(am)	CLF(pm)	People	qc (am)	qc(pm)
Sensible	225	0.78	0.94	15	2632.5	3172.5
Latent	105	1	1	15	1575	1575
SUM					4207.5	4747.5

Figure 3.10: Occupant Heat Gain Sheet

3.9.3 Heat Gain from Lighting and Electric Equipment

Lighting and overall electric equipment and uses like typewriters, computers, printers, fax machines, TV, refrigerator, washing machines, kitchen equipment, and any other equipment of this sort likewise add heat to the air conditioning space, and it is handled in a comparable means as lighting. The thermal gain by the equipment is found by the wattage of the equipment and is calculated by:

For the lights result in sensible heat gain.

$$Q = 3.41 * W * FUT * FBF (CLF) \quad (3.6)$$

Where:

W = Installed lamp watts input from electrical lighting plan or lighting load data

FUT = Lighting use factor, as appropriate

FBF = Blast factor allowance, as appropriate

CLF = Cooling Load Factor, by an hour of occupancy. See 1997 ASHRAE Fundamentals, Chapter 28, Table 38. Note: CLF = 1.0 if the operation is 24 hours or if cooling is off at night or during weekends. For Power Loads & Motors

Three diverse equations are employed under diverse situations. Thermal gain of energy-driven equipment and motor when both are positioned inside the space to be conditioned

$$Q = 2545 * (P / \text{Eff}) * \text{FUM} * \text{FLM} \quad (3.7)$$

Where

P = Horsepower rating from electrical power plans or manufacturer's data

Eff = Equipment motor efficiency, as decimal fraction FUM = Motor use factor (normally = 1.0). FLM = Motor load factor (normally = 1.0), Note: FUM = 1.0, if operation is 24 hours

Thermal gain of when driven equipment is positioned inside the space to be conditioned space, and the motor is outside the space or air stream.

$$Q = 2545 * P * \text{FUM} * \text{FLM} \quad (3.8)$$

Where:

P = Horsepower rating from electrical power plans or manufacturer's data, Eff = Equipment motor efficiency, as a decimal fraction,

FUM = Motor use factor

FLM = Motor load factor, Note: FUM = 1.0, if operation is 24 hours.

Thermal gain of when driven equipment is positioned outdoor the space to be conditioned space and the motor is inside the space or air stream

$$Q = 2545 * P * [(1.0 - \text{Eff}) / \text{Eff}] * \text{FUM} * \text{FLM} \quad (3.9)$$

Where:

P = Horsepower rating from electrical power plans or manufacturer's data,

Eff = Equipment motor efficiency, as a decimal fraction,

FUM = Motor use factor

FLM = Motor load factor, FUM = 1.0, if operation is 24 hours

The value of the wattage of light is given in Figure 3.11.

q Lighting	TLW	UF	SAF	CLF(am)	CLF(pm)	qc(pm)	qc (am)
	7200	1	1.3	0.88	0.92		
SUM						8611.2	8236.8

Figure 3.11: Lightning Heat Gain Sheet

3.9.4 Infiltration Heat Gain

Untreated outside air is allowed to enter the conditioned environment without being filtered. The interaction of wind and a chimney causes air to escape from both inside and outside. Infiltration was reduced by using gates, air curtains, and locking windows and doors. Estimate the entrance rate, which is affected by the building's type and age, internal and outdoor conditions, wind velocity and direction, and exterior temperature and humidity.

The rate of sensible heat transfer owing to infiltration is calculated as follows:

$$Q_S = m_o C_{pm} (t_o - t_i) \quad (3.10)$$

Latent heat transfer rate due to infiltration is given by:

$$Q_L = m_o h_{fg} (W_o - W_i) \quad (3.11)$$

Infiltration is induced by a pressure difference between the two sides of windows and doors, and it is dependent on wind speed and direction, as well as changes in densities caused by temperature differences between the inside and outside air.

Table 3.5: Number of Air Variations per Hour (Shubbar et al., 2017)

No	Kind of room or building	Number of air changes per hour(AC)
1	Room with no windows or outside doors	0.5 to 0.75
2	Room, one wall exposed	1
3	Room, two walls exposed	1.5
4	Room, three walls exposed	2
5	Room, four walls exposed	2
6	Entrance halls	2 to 3
7	Reception halls	2
8	Room with no windows or outside doors	0.5 to 0.75

Table 3.5 shows the air fluctuations value per hour and its value. Because infiltration occurs on the building's windward side, the complete room entrance air for

a full structure is half of the estimated Figure. The pile effect causes entrance and exfiltration in fully air-conditioned multi-story structures. Exfiltration at lower floors and ingress at higher floors may occur in the summer due to the chilly air column within. The phenomenon is inverted in the winter.

3.9.4.1 Heat Transfer through Opaque Surface

This is a practical thermal transmission procedure. The heat transmission rate through opaque surfaces like walls, roof, floor, doors etc. is given by:

$$Q_{\text{opaque}} = A \cdot U \cdot \text{CLTD} \quad (3.12)$$

Solar transmission gain from a wall relies on the mass of the wall and direction Mass of the wall per unit area, Adjustments to Values:

$$\text{CLTD}_{\text{corre}} = [(\text{CLTD} + \text{LM}) \cdot K + (25.5 - T_i) + (T_{\text{av}} - 29.4)] \quad (3.13)$$

(Chapter 26 of the ASHRAE Fundamental Handbook, table 7) CLTD adjustment for latitude and month applied to LM = latitude – month correction North Latitude (Ref-AHRAE 1989 Fundamental handbook chapter 26 table-9 K = color adjustment factor, k= 1 for dark colored walls and ceilings) in walls and ceilings 3.3.2 Gain in solar transmission from roofs:

$$Q_{\text{roof}} = A \cdot U \cdot \text{CLTD} \quad (3.14)$$

(CLTD from ASHRAE fundamental handbook 1985 chapter 26 table 5)

Calculation of heat gain through doors:

$$Q_{\text{doors}} = A \cdot U \cdot \text{CLTD} \quad (3.15)$$

The value of CLTD =16.5

Roof/Ceiling							
Conduction	U (Btu/hr-ft ² -F)	CLTD(am)	CLTD(pm)	ΔT	Area (ft ²)	qc (am)	qc(pm)
type 1	0.33	15	84	20	3616.67	15515.51	97867.09
Walls							
Conduction	U (Btu/hr-ft ² -F)	CLTD(am)	CLTD(pm)	ΔT	Area (ft ²)	qc (am)	qc(pm)
North	0.58	6	15	19	6996.54	16.2319728	52.7539116
NE	0.58	27	35	19		0	0
East	0.58	39	49	19		0	0
SE	0.58	28	45	19		0	0
South	0.58	7	24	19		0	0
SW	0.58	6	13	19		0	0
West	0.58	6	12	19		0	0
NW	0.58	6	11	19		0	0
sum						16.2319728	52.7539116

Figure 3.12: Opaque surfaces heat gain sheet

3.10 Assumptions

Based on ASHRAE Handbook- 1997 Fundamentals, The following assumptions were made during the calculation: People's occupying hours. The time is 24 hours. The residence has a total of 15 occupants. From 0900 to 1700 hours, the light is turned on. Lights in rooms range from 400 to 800 watts, depending on how they are used. Per room, 200 watts for the PC. Roof heat coefficient values range from 0.1337 and 2.31 Watt/ m².°C, depending on location. As shown in Tables 32 to 33C, the wall number is 13, and the U value is 5.485 Watt/ m².°C. Table 11 shows that the window is uncoated single glazed with a U value of 0.55. Table 32 and Table 34 shows the values of Cooling Load Temperature Difference (CLTD) for wall and glass. Table 11 shows the values of the Shading Coefficient (SC). Values of Solar Cooling Load (SCL) are taken from Table 36, and Values of Cooling Load Factor (CLF) for lighting are taken from Table 38 based on lights on for 14 hours. Values of Cooling Load Factor (CLF) for people are taken from Table 37 based on 14 hours. Rates of Sensible Heat Gain (SHG) and Latent Heat Gain (LHG) from people are taken from Table 3.

3.11 BIM Model

The BIM models were provided by the designer, and other project-associated data was gained and prepared through the selected case study. The procedure utilized basically

had a case-study model examination. Initially, a literature review was done, mostly considering the methods of project period and price control and CAD and BIM applications. Basic ideas and existing approaches to project period and price control were reviewed and offered. Present problems that lead to period and price overruns in AEC manufacturing were defined. The procedure and model were analysed. Information analysis founded on the 3D models was made to demonstrate how this new project delivery technique help enhance a project's period and price control.

3.11.1 As-built 3D BIM Model

Modelling an as-built model is a process of creating BIM objects that represent structure components, with both geometric and non-geometric properties and connections taken into account. If BIM is built on previously acquired building data, the preceding information gathering, processing, and recognition techniques have an impact on the information value and the amount of detail provided. To compare different methodologies and their modelling capabilities, created models might be evaluated based on modelling accuracy or amount of detail, for example (Tang, et al., 2010). The standard BIM assessment approach for comparing model characteristics has been devised. In reality, "as-built" BIM modelling is typically done interactively, which takes time and is prone to errors (Eastman et al., 2011; Arayici. 2011; Remond et al., 2012). In this research, the case study has been modelled by Rivet software, as shown in Figure 3.13 and Figure 3.14.



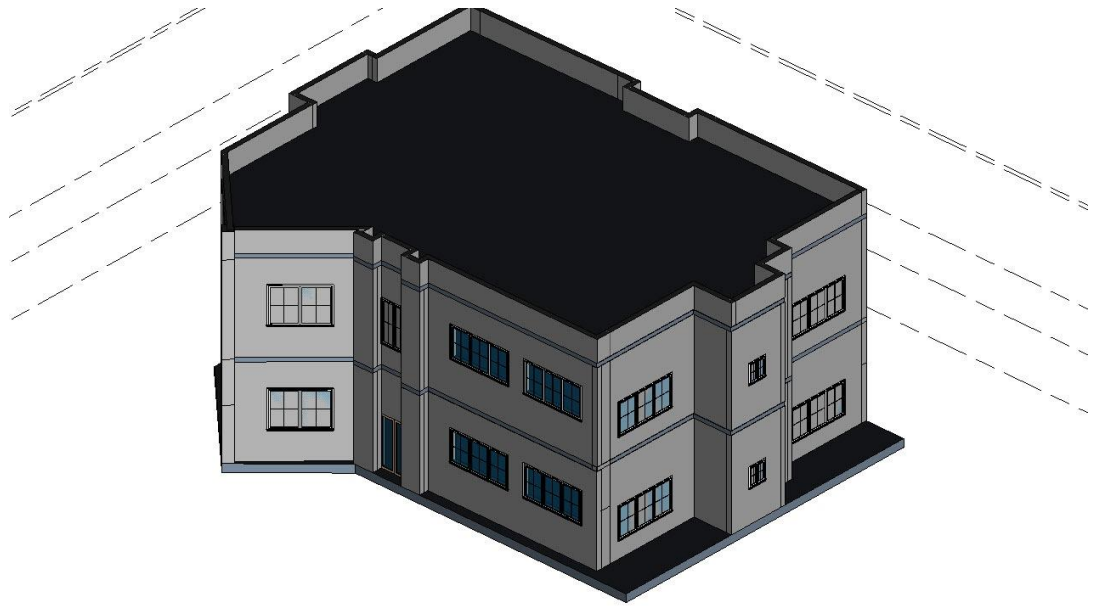


Figure 3.13: BIM- Rivet drawing geometry result

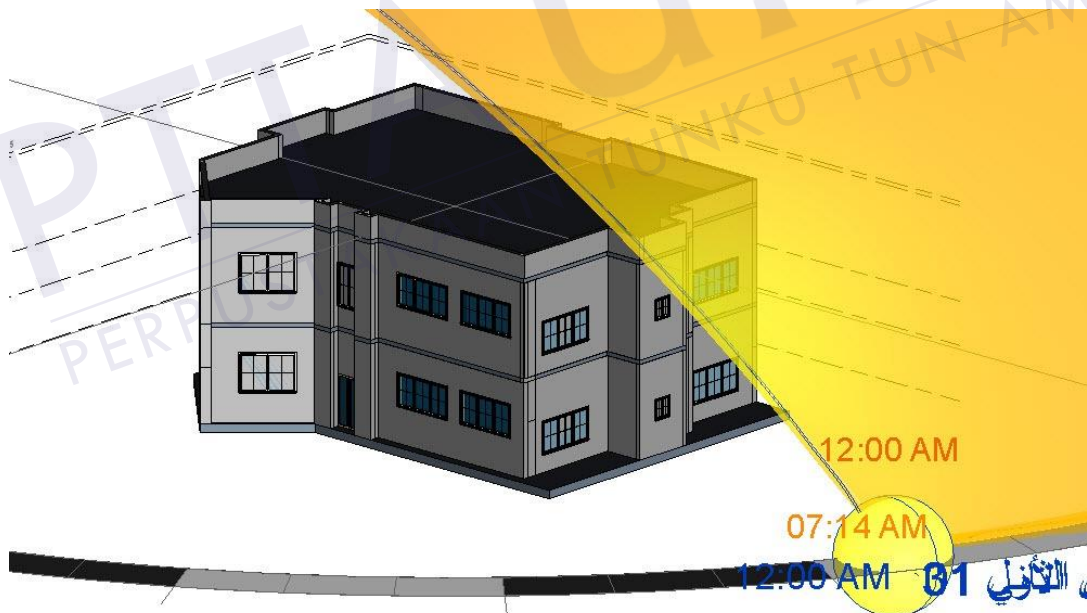


Figure 3.14: BIM- Rivet drawing sun rise result

3.12 Cooling System

The HVAC system has diverse power demands when applied to the same building's heating and cooling requirements. Oppositely, structure heating and chilling require to rely on many limits such as structure fabrics, glazing ratio, structure form, occupancy pattern, and numerous others. HVAC regime power demands and building power requirements were calculated by mathematical modeling.

3.12.1 System Design

This study was conducted on a residential building in Baghdad. The air conditioning system in this building is conventional. The study's objective is to convert from traditional air conditioning to an absorption system that runs on solar power in order to reduce the consumption of electricity and make better use of the solar throughout the day, about 13 hours of running (from 6 a.m. to 7 p.m.), as seen in Figure 3.15.

The economic evaluation of the two systems is based on their main components (vapour compression chiller machine, hot water tank, absorption chiller machine and flat plate collector). An absorption chiller machine with a solar radiation average of 7 kWh/m² in Baghdad (Iraqi metrological) is designed based on a presumed efficiency of 50% for flat plate collectors, which have lower costs and simpler designs than evacuated plates. Moreover, an assumed solar absorption chiller machine COP 0.7 based on the solar cooling overview (Al Uгла et al. 2016) and recommendations report developed by the Intelligent Energy Europe IEE program. The hot water Tank for the solar absorption system is used to accommodate the solar energy when the cooling load is less than available solar energy during daytime operation. In order to meet the highest cooling requirements, the solar absorption chiller machine has been designed with a maximum power of 350kW to receive most of the solar energy during noontime.

Because the building-cooling load is constant for both solar absorption and conventional vapour compression systems, the chiller machine size is also the same.

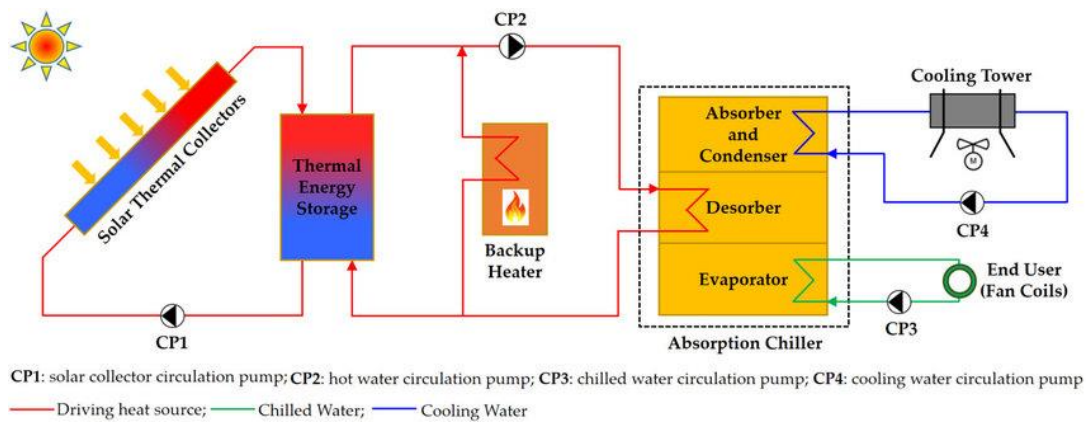


Figure 3.15: Solar absorption cooling process (Ayou & Coronas., 2020)

3.13 Evaluation Method

Various methods have been used to calculate and evaluate the cooling system's performance. This review's economic examination of the two regimes assesses their viability and outlines the economic benefits and drawbacks. The payback period of each system is calculated using the early investment price and the annual operating price of energy for the provided regimes. The payback period (PBP) is the most straightforward method for researching one or more investment prospects. The statistic denotes the time required to recover investment prices; it may be calculated by dividing the investment price by the annual savings:

$$PBP = \frac{IC}{ACF} \quad (3.16)$$

Where IC is the investment price, and ACF is the yearly cash flow. But, this technique has some limitations as it:

- i. Disregards the advantages happening after the PBP, which are suggested for consideration, as the solar air conditioning regime could work dependably for up to 25 years.
- ii. Disregards the varying values of money over time.

Table 3.6: Electricity rates for Rosenthal building in Iraq (Iraqi ministry of electricity)

No	Monthly Consumption Range (kWh)	Rate (ID/kWh)	Rate (\$/kWh)
----	---------------------------------	---------------	---------------

1	0 – 1,500	20	0.016
2	1,501 – 3,000	35	0.029
3	3,001 – 4,000	80	0.066
4	More than 4,000	120	0.1

The electricity rates for the Rosenthal sector in Iraq are shown in Table 3.6. For a monthly consumption range from 0 to 1500 kWh, the rate is 0.016 \$/kWh; for a monthly consumption range from 1501 to 3000 kWh, the rate increases to 0.029 \$/kWh; for monthly consumption range from 3001 to 4000 kWh, the rate increases to 0.066 \$/kWh; and for monthly consumption range more than 4000 kWh, the rate increases to 0.1 \$/kWh. The studied building consumes more than 4000 kWh on a monthly basis, at the rate of \$0.1/kWh.

Table 3.7: Cost Rate of key parameters of economic analysis

No	Parameter	Rate
1	Collectors	\$320/m ²
2	Absorption Chiller, COP = 0.7	\$516/ kW
3	VC Chiller, COP = 3.5	\$400/ kW
4	Hot Water Tank	\$100/ m ³

**The rates are based on the markets in Iraq*

The price rate of the absorption regime is shown in Table 3.7. The collector cost is \$320/ m², the absorption chiller cost is \$516/ kW, and the hot water tank cost is \$100/ m². The VC chiller life cycle is 10 years, and the absorption chiller life cycle is 20 years.

3.14 Technical simulation of absorption system and vapour compression system

The absorption system was investigated using a thermodynamic study. The thermodynamic analysis was carried out to determine the critical intake and outlet thermodynamic conditions of the refrigerant and refrigerant-absorption solutions at each phase of the absorption cycle during steady-state operation. The first law of thermodynamics and the appropriate property relations were used to construct the thermodynamic analysis. The cycle design for the LiBr/H₂O solar absorption method is shown in Figure 3.16. The thermodynamic analysis equations employ the thermodynamic state points 1 to 5, as indicated in Figure 3.16.

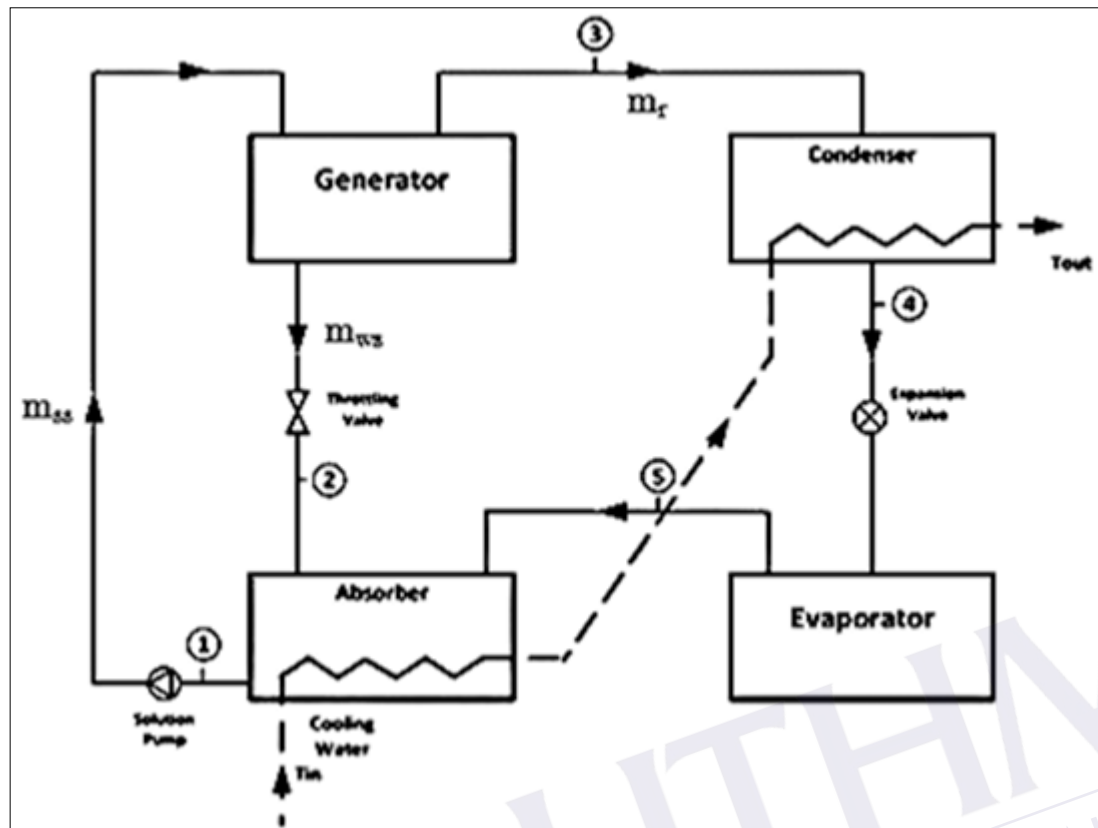


Figure 3.16: LiBr-H₂O absorption system

In the generator, the refrigerant-absorbent solution is heated, and the refrigerant is released as a vapour from the absorbent.

$$Q_G = \dot{m}_r h_3 + \dot{m}_{ws} h_2 - \dot{m}_{ss} h_1 \quad (3.17)$$

The enthalpy h (1–5) is based on the point's thermodynamic condition, as shown in Figure 3.16. The weak refrigerant-absorbent solution goes to the absorber, but the refrigerant vapour goes to the condenser, where it is cooled to the fluid stage and releases heat into the environment.

$$\dot{m}_{ss} = \frac{x_{ws}}{x_{ws} - x_{ss}} \dot{m}_r \quad (3.18)$$

$$\dot{m}_{ws} = \frac{x_{ss}}{x_{ws} - x_{ss}} \dot{m}_r \quad (3.19)$$

The saturated refrigerant undergoes a throttling process in which it expands from a liquid to a liquid-vapour mixture and travels to the evaporator. In the

evaporator, the refrigerant absorbs heat from the cooling space as it vaporizes completely. This low-pressure saturated vapour travels to the absorber, where it is reabsorbed by the weak refrigerant-absorption solution to create a strong refrigerant solution. Q_e is obtained from the cooling load of the building and the designed chillier machine size.

$$\dot{m}_r = \frac{Q_e}{(h_5 - h_4)} \quad (3.20)$$

The heat generated during this action is expelled from the system and discharged into the atmosphere. After that, the powerful refrigerant solution is delivered to the generator.

$$W_p = \dot{m}_{ss} (h_1 - h_1') \quad (3.21)$$

The coefficient of performance (COP) is given by

$$COP = \frac{Q_e}{Q_g + W_p} \quad (3.22)$$

The refrigerant is compressed in the compressor, and the pressure rises from low pressure (1) to high pressure high temperature gas (2). The superheated high-pressure gas travels from the compressor to the condenser, where it is cooled to saturation temperature before condensing to liquid (3). The high-pressure, sub-cooled liquid refrigerant then passes through the expansion valve and expands to a low-pressure, low-temperature liquid (4). The liquid refrigerant then passes through the evaporator, where heat (extracted from the room) is injected into the liquid refrigerant, causing it to evaporate back into (low pressure) gas. The refrigerant is compressed to greater pressure in the compressor. The following tasks are performed in the compressor:

$$W_{compressor} = \dot{m}(h_2 - h_1) \quad (3.23)$$

In the condenser, heat is transferred to the ambient air, cooling down the superheated gas until it condenses to a liquid.

$$Q_{condenser} = m(h_3 - h_2) \quad (3.24)$$

In the expansion valve, the high-pressure sub-cooled liquid is expanded to low-pressure, low-temperature liquid. It is modelled as a throttling process where

$$h_3 = h_4 \quad (3.25)$$

It is assumed that no heat losses occur. In the evaporator, the liquid refrigerant is evaporated by adding energy (from the room) to the refrigerant.

$$Q_{evaporator} = \dot{m}(h_1 - h_4) \quad (3.26)$$

$$COP = \frac{Q_e}{W_p} \quad (3.27)$$

The total energy balance of this system is:

$$Q_{evaporator} + W_{compressor} = Q_{condenser} \quad (3.28)$$

The presented mathematical formulas were solved by using a specific software in order to ensure the numerical results, as shown in the next section.

3.15 Engineering Equation Solver (EES)

This section has explained the methodology applied in this research. The EES program was used to solve mathematical equations and analyse the results shown for both systems (vapour compression system and absorption system). Engineering Equation Solver (EES) is a simple-to-use tool for addressing engineering issues. It is very useful for addressing heat transfer and thermodynamic issues since it has various built-in libraries of thermodynamic and thermos physical characteristics, eliminating the need to hunt them up in tables. Furthermore, there are no algebraic errors to worry about. Therefore, using EES to solve hard engineering issues saves time. EES has a number of advantages, including the ability to solve a system of simultaneous equations, which

is difficult to perform using Excel. The system having a transcendental equation (i.e., one in which the dependent variable cannot be isolated) falls into this category (Ali et al., 2019). The solution of a set of non-linear algebraic equations is the most basic feature given by EES. As illustrated in Figure 3.17, the EES makes no distinction between upper and lower case characters, and the sign (or **) indicates rising to power. The solve command from the Calculate menu must be selected to solve the equations. The progress of the solution was displayed in a dialog box. The button switches from Abort to Continue after the computations are finished, as seen in Figure 3.18 below.

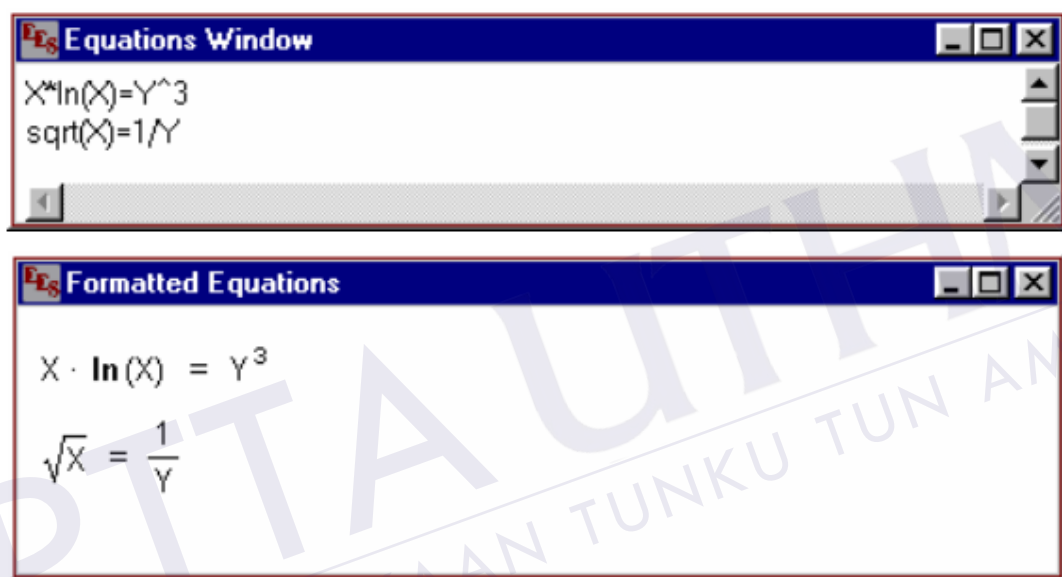


Figure 3.17: Input process in EES software

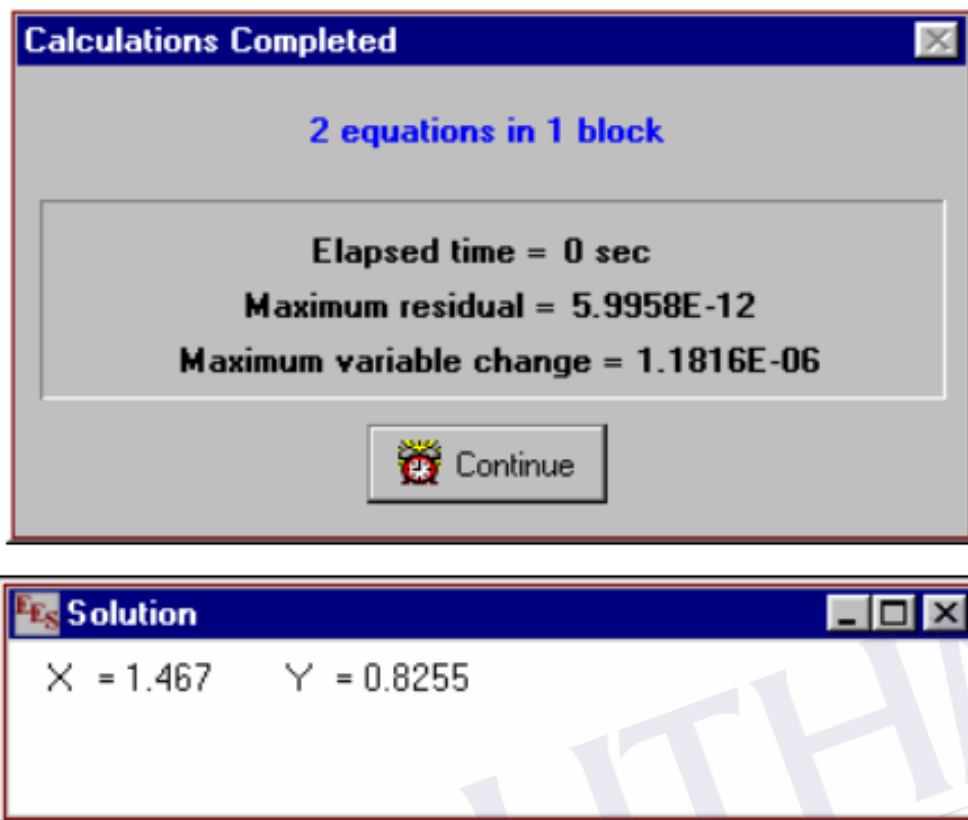


Figure 3.18: Results of EES Software

In a sequence of windows, information about the calculations are given. The equations window is where you enter your equations and comments. The values of the variables are displayed in the Solution and Arrays windows when the equations are solved. The Residuals pane displays the equations' residuals as well as the computation order. The Parametric and Lookup Tables, as well as a schematic and up to 10 plots, have their own windows. A Debug window is also available. This section contains a full overview of the features and information for each window type. At the same time, all of the windows can be open (i.e. visible). The current window is recognizable by its highlighted (black) title bar in the foreground. Three EES windows are overlapping in the diagram below. For different versions of the Windows operating system, the look may alter somewhat.

CHAPTER 4

SIMULATION RESULTS AND DISCUSSION

4.1 Introduction

Energy consumption in residential houses is dependent on the building characteristics. The cooling load evaluation is concerned with the thermal characteristics of the material, local climate and type of building structure. For that, in this chapter, the analysis of the building provides an investigation of the level of energy efficiency and consumption based on the Cooling Load Temperature Difference method (CLTD). The study includes the characteristics and the conditions of temperature, wind, and rain in all seasons of the Iraqi climate. The thermal properties of external walls, top roof, the floor of ground floor, windows and doors have been investigated. The chapter is divided into three parts; the first part presents the CLTD results using the Microsoft Excel software fed by a set of equations presented in chapter three. The second part presents the results of the solar effect on the cooling load using different materials and the BIM program. The last part of this chapter observes a consumption comparison in the air-conditioning systems to find out the economic system that is used in this type of buildings.

4.2 Design Condition

The climate in Iraq is desert in the centre and south, with warm winters and extremely hot summers; semi-desert in the north, with comparatively chilly winters; and mountainous in the north, with cold and rainy (or snowy) winters and bright and sunny summers, but colder evenings due to the high altitude. The average temperature of Baghdad, Iraq's capital, ranges from 9.5 degrees Celsius in January to 35 degrees

Celsius in July, with highs of 44 degrees Celsius. Summer is hot and sunny here as well, with temperatures reaching 50 degrees Celsius and making Baghdad one of the warmest cities in the world. The days are moderate in the winter, but the evenings are typically frigid, with temperatures dropping to a few degrees below freezing. The essentials of the cooling calculations that must be completed to keep buildings pleasant in the summer are the interior design condition and the exterior design condition. The suggested client information for design conditions is obtained from Iraqi climate resources for most of the comfort system calculations, as indicated in Tables 4.1 to 4.3.

Table 4.1: Design Criteria Data of Dry Bulb temperature (Iraqi metrological)

Dry Bulb Temperature (T)	Design value F	Wet Bulb temperature (F)	Humidity ratio (gr/lb)	Wind speed (mph)
Median of Extreme Highs	117	71	42	12.1
0.4% Occurrence	115	71	43	12.3
1.0% Occurrence	111	69	43	13
2.0% Occurrence	109	69	42	13.1
Mean Daily Range	26	----	----	----
97.5% Occurrence	37	34	26	3.6
99% Occurrence	34	32	23	4.2
99.6% Occurrence	30	29	20	3.9
	28	27	18	3.8

Table 4.2: Design Criteria Data of wet Bulb temperature (Iraqi metrological)

Wet Bulb Temperature (Twb)	Design value F	Dry Bulb temperature (F)	Humidity ratio (gr/lb)	Wind speed (mph)
Median of Extreme Highs	76	107	83	9.9
0.4% Occurrence	74	106	72	10.8
1.0% Occurrence	72	104	64	11.3
2.0% Occurrence	71	103	61	11.6

Table 4.3: Design Criteria Data of Humidity ratio (Iraqi metrological)

Humidity ratio	Design Value (gr/lb)	Dry Bulb temperature (F)	Vapour Pressure (in.Hg)	Wind Speed (mph)
Median of Extreme Highs	98	85	0.65	10.4
0.4% Occurrence	87	86	0.58	10.0
1.0% Occurrence	81	83	0.54	10.9
2.0% Occurrence	76	82	0.50	9.6

The above values represent the base of cooling load design data conditions of the load factors and spreadsheet. The results are presented in detail in the next sections.

4.3 Cooling Load Temperature Results

It is necessary to calculate the cooling load before installing HVAC because if HVAC is established without it, it would be difficult to achieve the desired impact. In general, air-conditioning systems are intended to give comfort to humans since human comfort is now a top concern. An estimated cooling load is necessary in order to construct a properly sized HVAC system that is more efficient. The results of calculating the cooling load of climatic conditions using the CLTD technique for the specified building using the design circumstances of Baghdad, Iraq. The MS Excel tool was used to calculate cooling load components such as people's heat gain, illumination heat gain, infiltration, and ventilation heat gain. The program is used to calculate the cooling load due to building components. The calculation in this project is considered in three parts; each part represents a roof of the selected case condition. Each part has been calculated based on the main eight factors, as shown in Figure 4.1.

project: Heating & Cooling Load Calculation		initial conditios		results	
method:	CLTD	Site:			cooling load
reference:	ASHRAE Handbook of Fundamentals	Latitude:	44.23 E	ground floor load	92
Design Firm:	UTHM	Longitude:	33.23 N	8 rooms	
Project Engineer:	ali alqaisi	Elevation (feet)	112	336m ²	
Project Name:	master project	Inside Design Conditions:		first floor load	101.5
Project Location:	Baghdad, Iraq	cooling (F)	73	7 rooms	
		Air Velocity (fpm)	<50	336m ²	
		Max. Mean			
		cooling (F)	362	second floor load	31.5
		heating (F)	377	gym	
		Internal Loads		100m ³	
		People:	15		
		Lighting (W)	7200		
		Equip.(W)	12000	Total Cooling load (KW)	225

main factors for calculate floors heat load

Figure 4.1: The main factors for building heat load calculation

The reason for calculating each floor separately in the case study is due to differences in room size and number, which change the cooling load capacity of the building. The next sub-sections will present the CLTD calculation results for each floor.

4.3.1 Results of First Floor

The output of the computational calculations used in the presented processes provides the total cooling load, total sensible, and total latent cooling loads of each room on each floor. The room dimensions and building direction is shown in Figure 4.2.

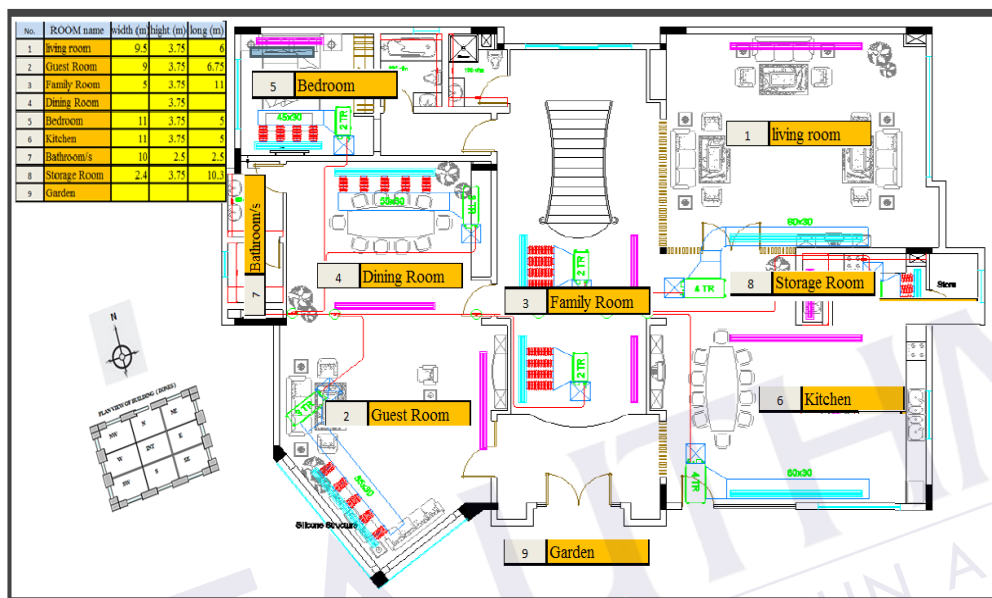


Figure 4.2: First-floor rooms dimensions

In addition, the rooms' functions are based on actual usage. Analysing each component that contributed to the overall cooling load might be utilized to correct the building's design and eliminate any cooling load excess. Table 4-4 shows the findings from the first floor.

Table 4.4: Numerical results of first-floor heat calculation

Location/ Aspect	Living Room	Guest Room	Family Room	Dining Room	Bedroom	Kitchen	Bathroom	Storage Room
Width (m)	9.00	9.00	5.00	8.00	6.00	9.00	10.00	2.40
Height (m)	3.75	3.75	3.75	3.75	3.75	3.75	2.50	3.75
long (m)	5.00	6.75	11.00	5.00	4.00	5.00	2.50	6.30
q (roof)	0.60	0.80	0.70	0.50	0.30	0.60	0.30	0.20
Q(walls)x100	0.32	0.36	0.37	0.00	0.23	0.32	0.19	0.20
q (windows)	0.40	0.40	0.90	0.40	0.40	0.40	0.00	0.10
q (doors)	0.20	0.20	0.60	0.20	0.20	0.20	0.20	0.20
q (vent)	6.50	6.90	8.30	7.50	5.90	6.30	3.70	3.80
q (light)	0.30	0.30	0.40	0.30	0.30	0.40	0.10	0.10
q (people)	2.60	2.60	2.60	2.60	2.60	2.60	2.60	2.60
q (equip)	0.70	0.80	0.90	0.60	0.40	4.70	0.00	0.00
q (Total)	11.62	12.36	14.77	12.1	10.33	15.52	7.9	7.2
Total Cooling Load					92.00 kW			

As seen from the table, low heat gains from the roof are noticed because of the shadow by the second-floor. It is noted that there is high infiltration heat load due to dynamic open doors and windows. Also, the higher equipment heat load occurs in the kitchen due to heat resources such as ovens, coffee makers and other devices. The total cooling load needed for this floor is 92 kW.

4.3.2 Results of Second Floor

The second-floor calculations output provides the total cooling load, total sensible, and total latent cooling loads of each room on each floor. Also, room dimensions and building direction are shown in Figure 4.3. Each room is labelled and specified to determine the cooling load.

As seen that the heat gain from the roof is divided into two responses, the first response of high heat gain due to the sunshine effect, and the other part presents low heat gain because of the shadow of the third floor. It is noted that there is a low infiltration heat load due to little use outdoors. The total cooling load needed for this floor is 101.5 kW; this high heat gains because of the roof effect.

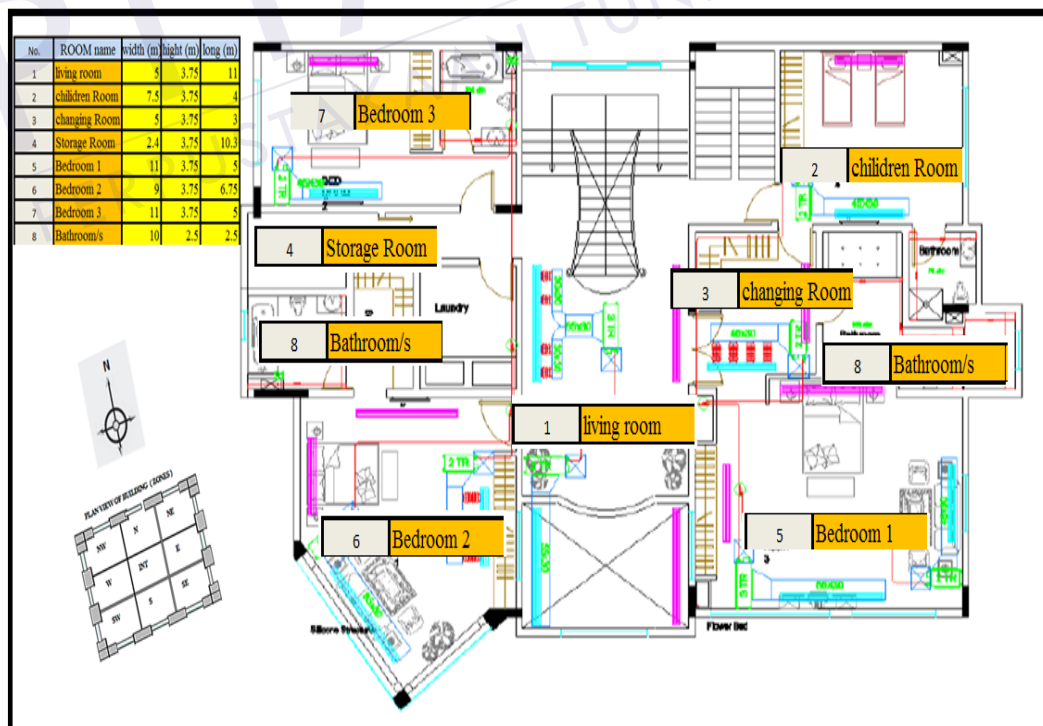


Figure 4.3: Second-floor rooms dimensions

Analysing each of the components that contributed to the total cooling load presents in Table 4.5.

Table 4.5: Numerical results of second-floor heat calculation

Location/ Aspect	Living Room	Children room	Changing room	Storage Room	Bedroom	Bedroom	Bedroom	Bathroom
Width (m)	5.00	7.50	5.00	2.40	11.00	9.00	11.00	10.00
Height (m)	3.75	3.75	3.75	3.75	3.75	3.75	3.75	2.50
long (m)	11.00	4.00	3.00	10.30	5.00	6.75	5.00	2.50
q (roof)	11.50	0.68	3.04	4.18	0.93	12.22	11.53	5.00
Q(walls)x100	0.44	0.26	0.22	0.31	0.44	0.41	0.44	0.23
q (windows)	0.44	0.44	0.87	0.40	0.40	0.40	0.04	0.13
q (doors)	0.22	0.22	0.61	0.22	0.22	0.22	0.22	0.22
q (vent)	5.47	3.32	3.32	3.32	4.47	3.32	3.75	3.21
q (light)	0.34	0.34	0.41	0.30	0.27	0.41	0.14	0.14
q (people)	2.61	0.70	0.35	0.00	0.70	0.70	0.70	0.35
q (equip)	0.70	0.40	0.00	2.00	0.20	0.20	0.20	2.00
q (Total)	21.72	6.36	8.82	10.73	7.63	17.88	17.02	11.28
Total Cooling Load					101.50 kW			

4.3.3 Results of Third Floor

The third-floor calculations provide the total cooling load for the gym room, total sensible, and total latent cooling loads of this room. The room dimensions and building direction is shown in Figure 4.4. The use of this room is for physical training using different types of equipment. For that, there is a high cooling load in this room.

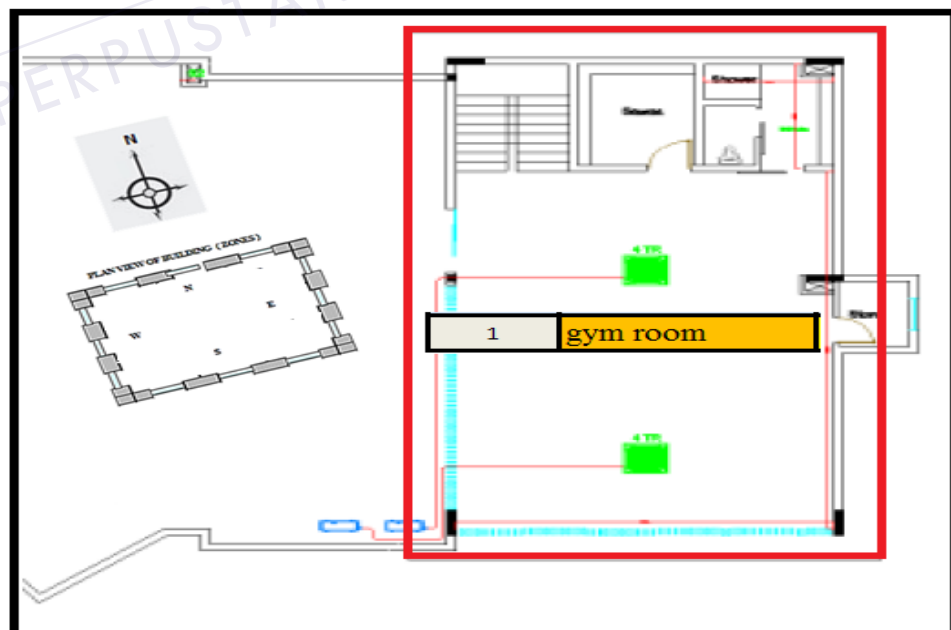


Figure 4.4: Third Floor Room Dimensions

Analysing the room components provides a total cooling load which presents in Table 4.6

Table 4.6: Numerical results of third-floor heat calculation

Location/Aspect	Gym Room
Width (m)	8.00
Height (m)	3.50
long (m)	12.50
q (roof)	19.70
Q(walls)x100	0.20
q (windows)	1.10
q (doors)	0.90
q (vent)	5.00
q (light)	0.30
q (people)	2.60
q (equip)	1.90
q (Total)	31.50

The heat gain from the roof is high due to the sunshine effect, and it is noted that there is high infiltration heat load due to the recirculation of air needed in this room. The total cooling load needed for this floor is only 31.5 kW.

4.3.4 Load Summation

The summation of the total cooling load based on the details above combined the entire load from the various sections. The data on the Microsoft Excel program provides the results, as shown in Table 4.7.

Table 4.7: Summary of the CLTD results

initial conditions			Results	
Site:				cooling load
	Latitude:	44.23 E	ground floor load	92
	Longitude:	33.23 N	8 rooms	
	Elevation (feet)	112	336m ²	
Inside Design Cond.			first-floor load	101.5
	cooling (F)	117	8rooms	
	Air Velocity (fpm)	<50	336m ²	
Humidity ratio		40	second-floor load	31.5
Internal Loads				
	People:	15	Gym	
	Lighting (W)		100m ²	
	Equip.(W)		Total Cooling load (KW)	225

4.4 Results of BIM Model

Interviews with important building owners in the research subject are employed in the case study. Furthermore, such interview data may be used alongside a review of any documentation. A concept sketch was used to start the design process. The drawing was designed to be readable enough to convey a partial connection. After the drawing was completed, it was saved as an image file and put into the Vector Architect program. The picture file was then traced over, extruded to the proper height, then refined with the push/pull tool to create a massing model. The Vector Architect software was chosen because it shines as a tool for BIM design and writing while also facilitating interoperability and cooperation among team members and project contributors. This interoperability was only achievable because of the usage of IFC, and the team members were free to utilize their best-in-class tools thanks to the open BIM Program.

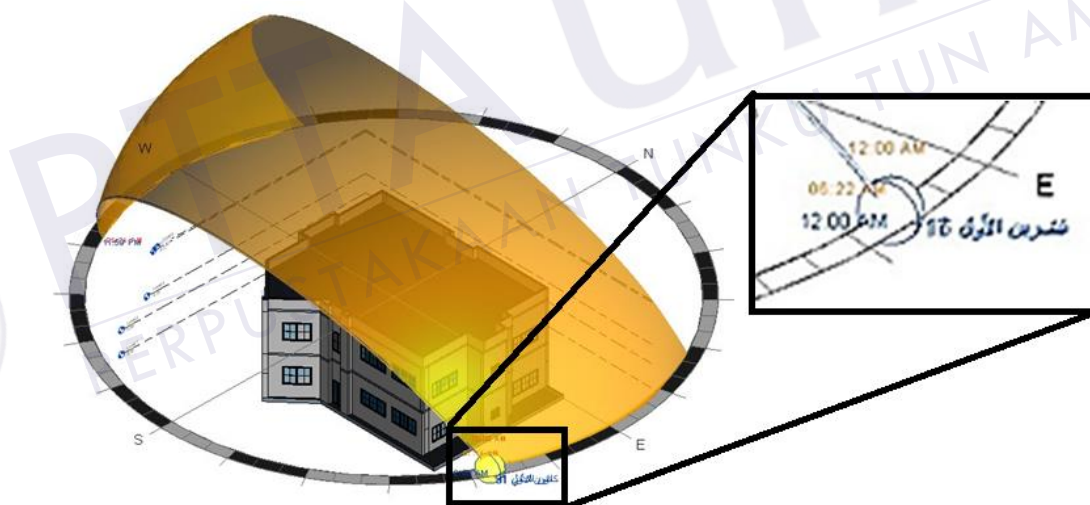


Figure 4.5: Solar angle results

Building Information Modelling, employed on the project, is a time-saving design method. It maximizes resources and, as a result, economic potential. When the building is on-site, it improves coordination between the consultants and reduces risk/unknowns. From Stage D forward, BIM was employed (when the designs were developed and fixed). It served as the source of all architectural and structural designs.

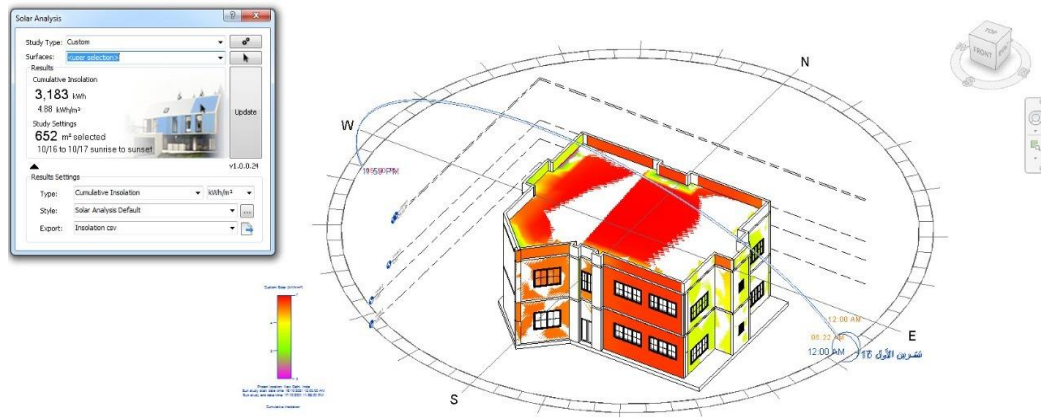
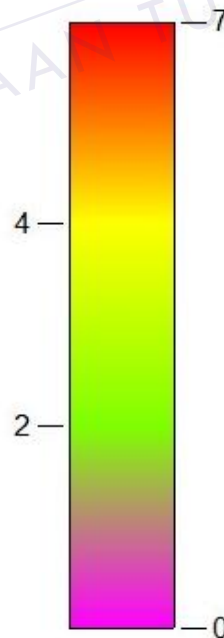


Figure 4.6: Effect of solar angle

The case studies above have shown some long-term benefits of integrating energy analysis tools with a BIM model. During the ideation and design phases of projects, this integration has shown to deliver a quick and accurate examination of the model data. Members of the Design team may construct and simulate a variety of design scenarios, visualize their ramifications, and make well-informed decisions.

Custom Solar (kWh/m²)



Sun study start date time: 16/10/2021 12:00:00 AM
Sun study end date time: 17/10/2021 11:59:00 PM

Figure 4.7: Thermal evaluation by Rivet software

The design team employed Building Information Modelling to analyse and optimize the features of the building form for lower energy consumption in the project at hand. For example, the design team's capacity to review its design assumptions and make well-informed judgments was boosted by the close integration of the BIM model with the energy analysis tools. In addition, the design team was able to use the take-offs created by the BIM model to quantify natural resource use and assist in anticipating the usage of sustainable materials.



Figure 4.8: Solar heat effect (Case 1)

The project team was also able to:

- i. Develop a more accurate cost and budget model as a result of the BIM and energy analysis integration and prepare a more accurate cost and budget model as a result of the BIM and energy analysis integration.
- ii. Maintain track of factors like total recycled content and embodied carbon dioxide level.
- iii. Define carbon objectives for specific project parts.
- iv. Compare and assess design choices.

- v. Get real-time updates on the project's carbon content.
- vi. Create fewer RFIs throughout construction.

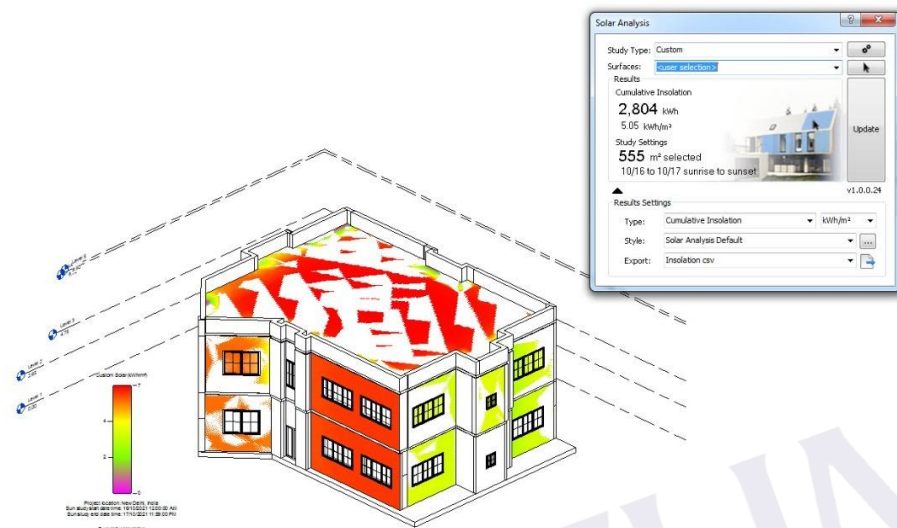


Figure 4.9: Solar heat effect (Case 2)

BIM maximizes project resources due to high reliability in choosing different materials and testing the heat gain from solar energy. This is the major characteristic that was employed in this study. It provides the amount of solar heat to the selected case study building based on two types of materials, the first one is the brick which represents the traditionally used material as shown in Figure 4.8, and the second is the new material which contains the isolation as a part of the material component as shown in Figure 4.9. The results observe a reduction in the heat effect on the building.

4.5 Results of Conventional Vapour Compression System

The data of working parameters and the performance parameters were analysed EES program to find the conventional vapour-compression system performance based on the same design conditions. The standard working condition is shown in Table 4-8:

Table 4.8: The standard condition for the VCRS

No.	Capacity (kW)	Condenser Temp. (°C)	Evaporator Temp. (°C)	Refrigerant Type
1	225	54.4	7.5	R22.

As seen from the input data representation, the cooling load capacity has been taken from the calculations of the previous stage. While the other data specification is taken from the original device operation, which means it represents real working data for this device operation. The EES – Engineering Equation Solver is used to solve the equations presented in chapter three, provide uncertainty analyses, perform linear and non-linear regression, convert units, and check unit consistency. The results from the EES program are shown in Figure 4.10

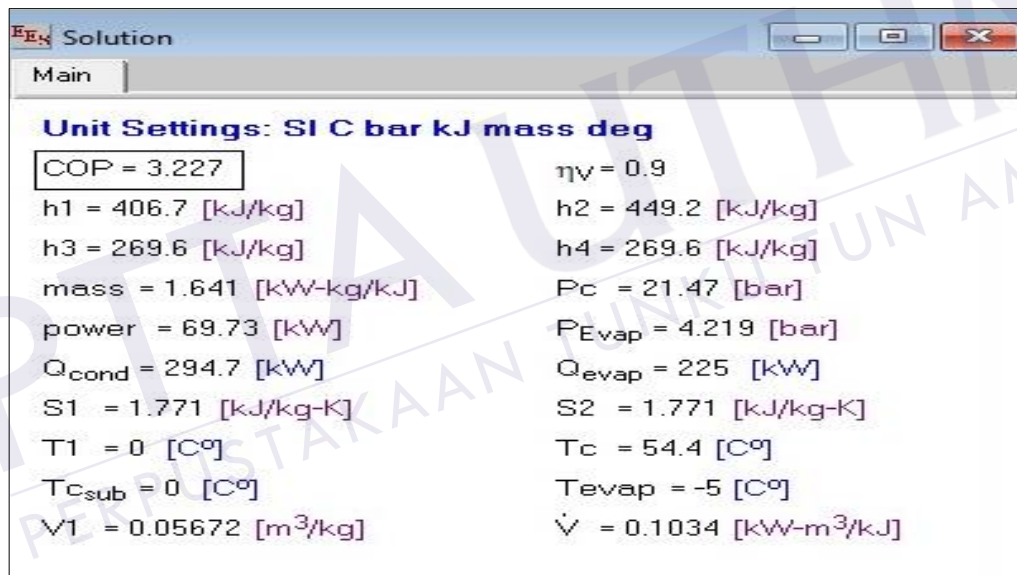


Figure 4.10: The solution window of the EES program for the Vapour Compression system

The results of enthalpies values presented by the program were h_1 , h_2 , h_3 , h_4 and their values were 406.7, 449.2, 269.6, 269.6 kJ/kg, respectively. The pressures of the condenser and evaporator are 21.47 and 4.219 bars, respectively; $Q_{Condenser}$ and $Q_{Evaporator}$ are 294.7 and 225 kW, respectively; $T_{Condenser}$ and $T_{Evaporator}$ are 54.4 and -5 °C, respectively, and the coefficient of performance (COP) is 3.227.

4.6 Result of Solar Absorption System

4.6.1 COP for Absorption System

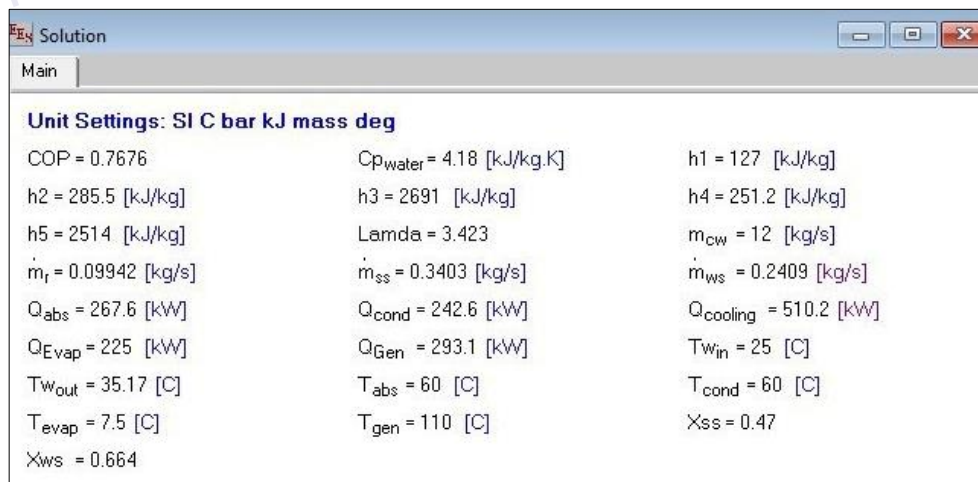
The Engineering Equation Solver (EES) was used to create the engineering codes for this system. The mass and energy balance equations are employed in these engineering algorithms to analyse the system performance when the parameters of the design changed. Because the condenser and absorber must release heat to the environment, their working temperatures must be greater than the ambient temperature; the initially anticipated temperature differential was 10°C larger than the ambient temperature (Allouhi et al., 2015).

The highest temperatures recorded in Baghdad city for the four months of May, June, July, and August were 35, 40, 45, and 50 degrees Celsius, respectively (Iraqi metrological). Based on the summer temperature in Iraq, the researcher may compute the coefficient of performance (COP) in different months. The design values in Table 4-9 are based on the hottest temperature in August.

Table 4.9: Design temperature variables in August

Component	Generator	Condenser	Evaporator	Absorber
Temperature (°C)	110.00	60.00	7.50	60.00

All the enthalpies and other properties are calculated automatically by the program, and the results are shown in Figure 4.11.



The screenshot shows the 'Solution' window of the EES program. The 'Main' tab is active, displaying the following data:

Unit Settings: SI C bar kJ mass deg		
COP = 0.7676	$C_{p_{water}} = 4.18$ [kJ/kg.K]	$h_1 = 127$ [kJ/kg]
$h_2 = 285.5$ [kJ/kg]	$h_3 = 2691$ [kJ/kg]	$h_4 = 251.2$ [kJ/kg]
$h_5 = 2514$ [kJ/kg]	$\lambda = 3.423$	$m_{cw} = 12$ [kg/s]
$\dot{m}_r = 0.09942$ [kg/s]	$\dot{m}_{ss} = 0.3403$ [kg/s]	$\dot{m}_{ws} = 0.2409$ [kg/s]
$Q_{abs} = 267.6$ [kW]	$Q_{cond} = 242.6$ [kW]	$Q_{cooling} = 510.2$ [kW]
$Q_{Evap} = 225$ [kW]	$Q_{Gen} = 293.1$ [kW]	$T_{w_{in}} = 25$ [C]
$T_{w_{out}} = 35.17$ [C]	$T_{abs} = 60$ [C]	$T_{cond} = 60$ [C]
$T_{evap} = 7.5$ [C]	$T_{gen} = 110$ [C]	$X_{ss} = 0.47$
$X_{ws} = 0.664$		

Figure 4.11: The solution window of the EES program for the Absorption system in the condition of August

The Figure shows the solution presented by EES program for the Absorption system in the condition of August. The enthalpies of h_1 , h_2 , h_3 , h_4 , and h_5 were 127, 285.5, 2691, 251.2, and 2514 kJ/ kg, respectively. Also, m_{cw} , m_r , m_{ss} , and m_{ws} are 12, 0.09942, 0.3403, and 0.2409 kg/ s, respectively; Q_{abs} , Q_{cond} , $Q_{cooling}$, Q_{evap} , and Q_{gen} are 267.6, 242.6, 510.2, 225, and 293.1 kW, respectively; T_{abs} , T_{cond} , T_{evap} , and T_{gen} are 60 , 60, 7.5, and 110°C, respectively, and the coefficient of performance is 0.7676. The same procedure is repeated to find out the coefficient of performance (COP) in the hot season, as shown in Table 4.10

Table 4.10: Results of COP Absorption system in the hot season of Baghdad

No.	COP	Month
1	0.8048	May
2	0.7922	June
3	0.7798	July
4	0.7676	August

As seen that the performance coefficient is highest in May and minimum in August. This is because environmental factors influence operation circumstances and, as a result, the system's performance factor. In addition, as the absorber temperature rises, the coefficient of performance augments, and as the temperatures of the generator and condenser lower, the performance coefficient rises. The condenser's temperatures in May, June, July, and August are 45, 50, 55, and 60 °C, respectively, and generator Temperatures are 80, 90, 100, and 110 °C, respectively.

As demonstrated in Figure 4.12, the greatest COP is achieved when the generator temperature is 80°C. In addition, as illustrated in Figure 4.13, the highest COP occurs when the condenser temperature is 45°C. The system's best performance coefficient is achieved in May at temperatures of 80°C for the generator, 45°C for the condenser, 45°C for the absorber, and 7.5°C for the evaporator.

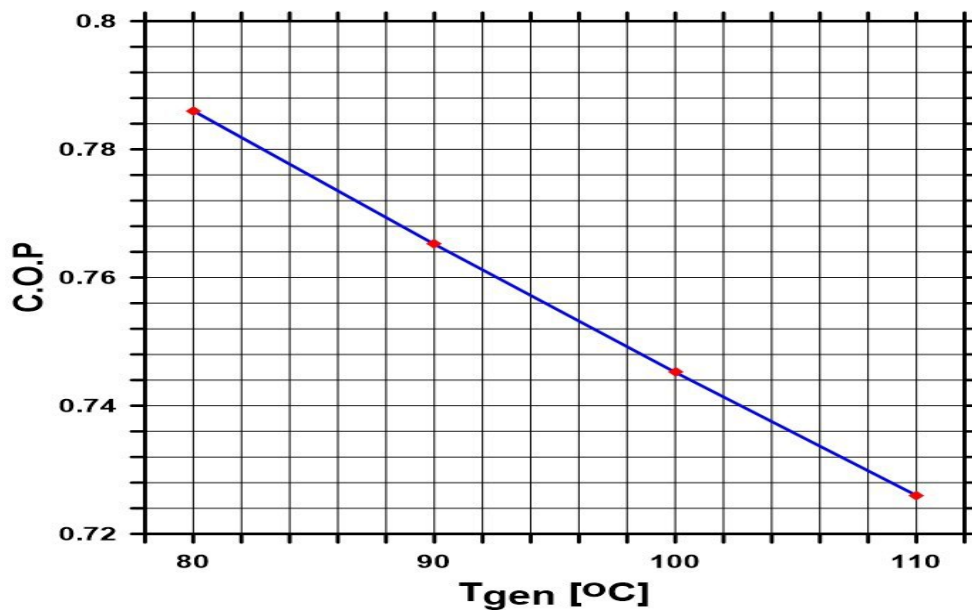


Figure 4.12: The coefficient of performance with temperature of generator

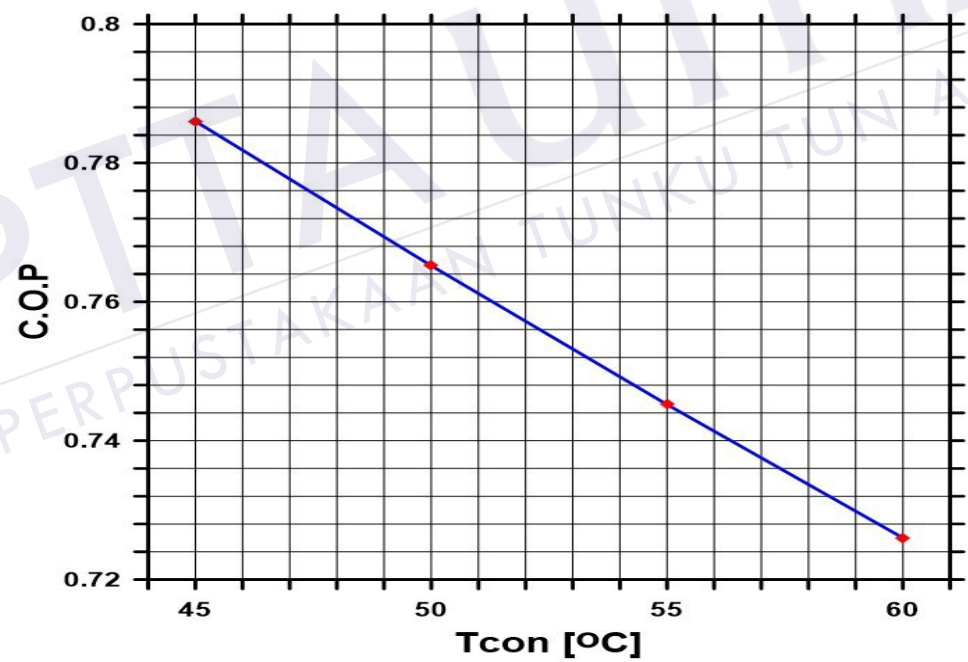


Figure 4.13: The coefficient of performance with temperature of condenser

4.6.2 Temperature Component Effect on Coefficient of Performance of Solar Absorption System

One of the most difficult aspects of absorption refrigeration is the COP, which is quite low when compared to compressor refrigeration. Material balances are used to calculate the mass flow rate using the appropriate concentrations of LiBr in the solution. Because the condenser in the generator is saturated, the temperature in the condenser is fixed, and the pressure in the condenser is fixed (or in the generator). The evaporator temperature and low pressure show the LiBr solution's state points using similar logic. First, the governing equation of the absorption system is coded in this software's equation window (terminology of EES). Then, for the analysis, various parameters such as mass flow rate, generator temperature, heat provided to the generator, and so on are varied, and the system's COP is displayed. Figure 4.14 demonstrates that when the amount of heat given to the generator increases, the system's COP decreases. This demonstrates that the system's COP is inversely proportional to the amount of heat delivered to it.

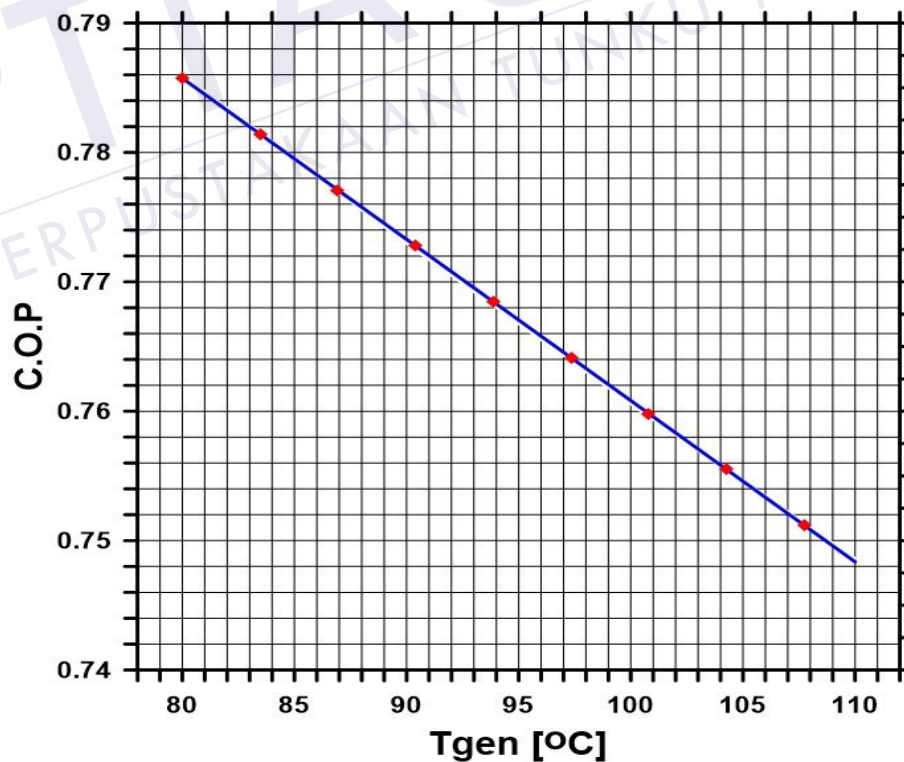


Figure 4.14: The effects of the generator temperature of the solar system on the coefficient of performance

The COP of the system is decreased on increasing generator heat; it is based on the fact that a higher amount of water was separated from the ammonia. Thus, more solutions had to be circulated so refrigerant.

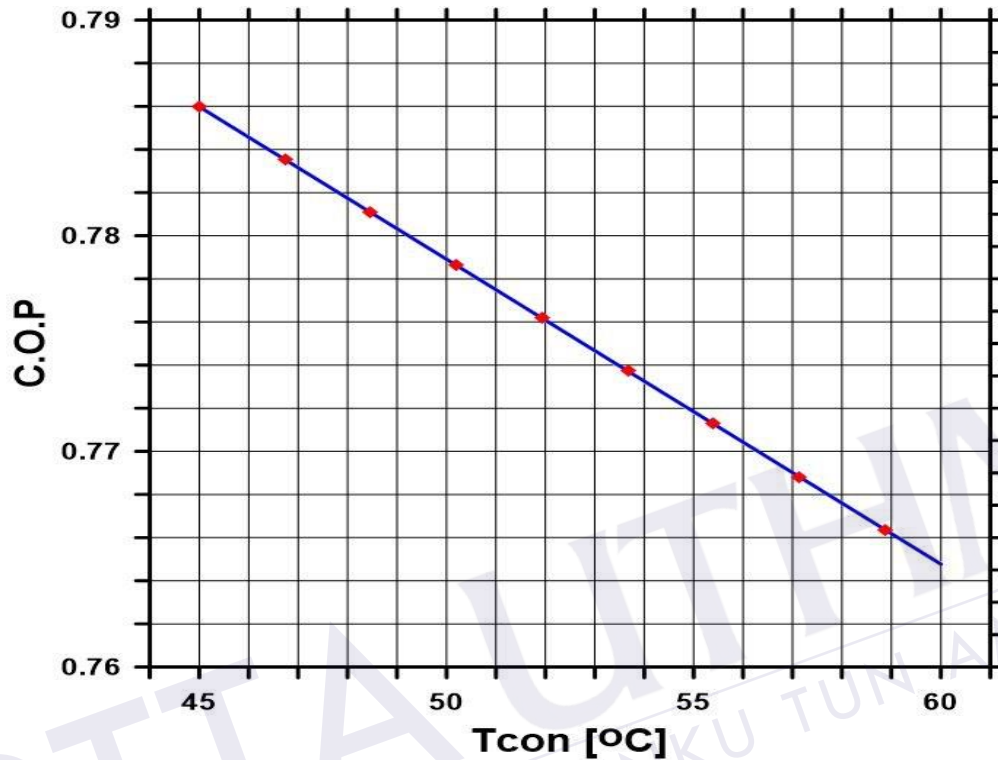


Figure 4.15: The effects of the condenser temperature of the solar Absorption system on the coefficient of performance

The influence of the solar Absorption system's condenser temperature on the coefficient of performance is shown in Figure 4.15. The condensed icing coefficient decreases as the condensate temperature rise. According to the legislation, the cooling capacity (Q_e) will drop, and the coefficient of performance will fall.

$$\text{C.o.p.} \downarrow = \frac{Q_{E \downarrow}}{Q_G} \quad (4.1)$$

The vapour is compressed using a thermally operated 'compressor,' which consists of two major components: an absorber and a generator. The effect of the solar Absorption system's absorber temperature on the coefficient of performance is shown in Figure 4.16.

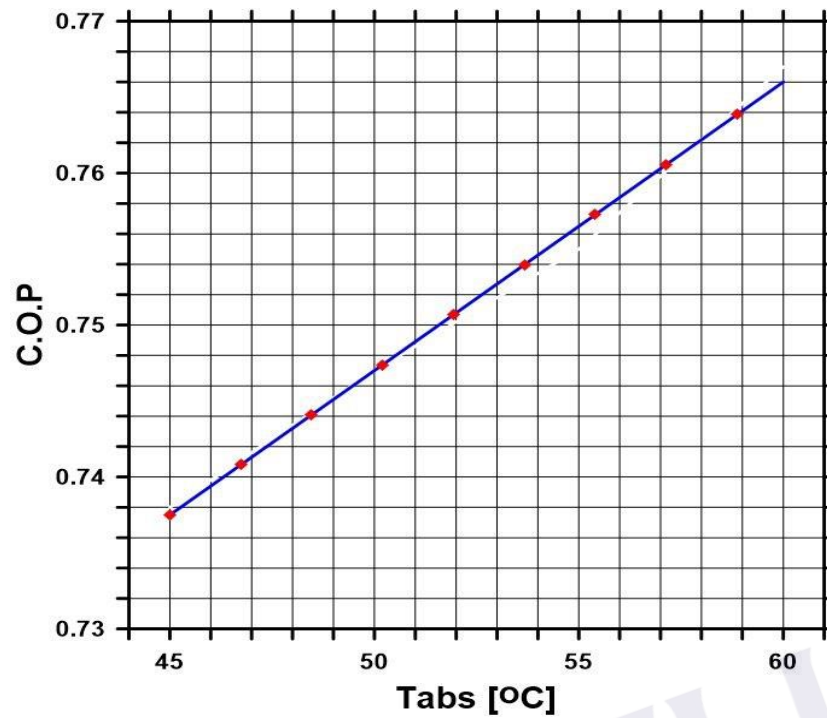


Figure 4.16: The effect of the absorber temperature of the solar Absorption system on the coefficient of performance

Figure 4-16: The influence of the solar Absorption system's absorber temperature on the coefficient of performance. As the temperature of the absorber rises, so does the temperature of the water entering the generator. As a result, lowering the energy consumed in the generator raises the performance factor.

$$\text{C.o.p} \uparrow: T_{\text{absorber}} \uparrow \quad (4.2)$$

4.7 Evaluate Results of Power Consumption

The total cost (T_C) accounts for the capital and operational costs of the integrated system (T_{CC} and T_{OC} , respectively) in the economic assessment of cooling systems, as illustrated in the equation below:

$$T_C = T_{CC} + T_{OC} \dots \quad (4.3)$$

T_{CC} denotes the cost of electricity, whereas T_{OC} denotes the cost of running the gas-fired heater, pump, and solar collectors, as well as the cost of cooling water.

4.8 Investment Cost for Vapour Compression System and Absorption System

Table 4.11: The investment cost for the Vapour Compression system and Absorption system

No	Component	Vapour Compression System (\$)	Absorption System (\$)
1	VC Chiller	140,000	
2	Absorption Chiller		180,600
3	Collector		32,000
4	Storage Tank		400
5	Total Investment Cost	140,000	213,000

Table 4.11 explains that the initial cost of the absorption system is \$213,000, and the initial cost of the vapour compression system is \$140,000. By comparing the initial costs of both types, the cost of the absorption system is \$10,650 per year, while the cost of the vapour compression system is \$14,000 per year. It is, therefore, more economical to use the absorption system instead of the vapour compression system.

4.9 Annual Operation Cost for Vapour Compression System and Absorption System

The annual operation cost is determined by calculating the annual electricity at all rates for the systems and the annual maintenance for the systems. The annual maintenance for the Vapour Compression system is 4% of the investment cost (Al-Ugla et al., 2016), the annual maintenance for the Absorption system is 1% of the investment cost (Allouhi et al., 2015), and the annual electricity for the Absorption system is 10% of the Vapour Compression system, only for pumps.

4.9.1 Annual Operation Cost at Rate 0.10 \$/kWh

Table 4.12: Annual operation cost for VC system and Absorption system at a rate of 0.10\$/kWh

No	Annual operation cost	VC system (\$)	Absorption system (\$)
1	Electricity	35,100	3,510
2	Maintenance	5,600	2,130
3	Total annual operation cost	40,700	5,640

The overall annual operating cost for the VC system is \$40,700, whereas the total annual operating cost for the Absorption system is \$5,640, as indicated in Table 4-12. This indicates that at the rate of 0.10 \$ kWh, the total yearly operating cost of the VC system exceeds that of the Absorption system.

4.9.2 Annual Operation Cost at Rate 0.066 \$/kWh

The overall annual operating cost for the VC system is \$28,766 in Table 4-13, whereas the total annual operating cost for the Absorption system is \$4,446. This indicates that the total yearly operating cost of the VC system is higher than the rate of 0.066\$ kWh for the Absorption system.

The annual operation cost at the rate of 0.066\$/kWh is less than the annual operation cost at the rate of 0.10\$/kWh because the cost of electricity consumption at the rate of 0.06\$/kWh is less than at the rate of 0.10\$/kWh.

Table 4.13: Annual operation cost for VC system and Absorption system at a rate of 0.066\$/kWh

No	Annual operation cost	VC system (\$)	Absorption system (\$)
1	Electricity	23,166	2,316
2	Maintenance	5,600	2,130
3	Total annual operation cost	28,766	4,446

4.9.3 Annual Operation Cost at Rate 0.029 \$/kWh

The entire annual operating cost for the VC system is \$15,779, whereas the total annual operation cost for the Absorption system is \$3,147, as indicated in table 4-14. This suggests that the total yearly operating cost of the VC system is higher than the rate of 0.029\$ kWh for the Absorption system.

Table 4.14: Annual operation cost for VC system and Absorption system at a rate of 0.029\$/kWh

No	Annual operation cost	VC system (\$)	Absorption system (\$)
1	Electricity	10,179	1,107
2	Maintenance	5,600	2,130
3	Total annual operation cost	15,779	3,147

The annual operation cost at the rate of 0.029\$/kWh is less than the annual operation cost at the rates (0.1\$/ kWh and 0.06\$/ kWh) because the cost of electricity consumption at the rate of 0.03\$/ kWh is less than at the rates (0.010\$/ kWh and 0.066\$/kWh).

4.9.4 Annual Operation Cost at Rate 0.016 \$/kWh

As shown in Table 4-15, the overall annual operating costs for the VC system are \$11,216, whereas the total annual operation costs for the Absorption system are \$2,692. This indicates that the VC system's total yearly operation cost is higher than the Absorption system's at a rate of 0.016\$ kWh.

Table 4.15: Annual operation cost for VC system and Absorption system at a rate of 0.016 \$/kWh

No	Annual operation cost	VC system (\$)	Absorption system (\$)
1	Electricity	5,616	562
2	Maintenance	5,600	2,130
3	Total annual operation cost	11,216	2,692

The annual operation cost at the rate of 0.016\$/kWh is less than the annual operation cost at the rates of 0.1\$/kWh, 0.066\$/kWh, and 0.029\$/kWh because the cost of electricity consumption at the rate 0.016\$/kWh is less than at the rates 0.1\$/ kWh, 0.066\$/kWh, and 0.029\$/kWh.

4.9.5 Summary of Analysis Cost

The findings of the comparison between the absorption system and the vapour compression system have shown that the absorption system has a lower initial and yearly cost than the vapour compression system. The absorption system is, therefore, more cost-effective and practicable than the vapour compression method. The next section will compute the payback periods for the absorption system.

4.10 Discussion

As shown in Chapter 3,

$$PBP = \frac{IC}{ACF} \quad (4.4)$$

From Table 4.12, the annual cash flow is \$35,060 from Table 4.13. The annual cash flow is \$24,320 from Table 4.14. The annual cash flow is \$12,632, and from Table 4.15, the annual cash flow is \$8,524.

Payback period at a rate of 0.1\$/kWh is 6 years.

Payback period at a rate of 0.066\$/kWh is 9 years.

Payback period at a rate of 0.029\$/kWh is 17 years.

Payback period at a rate of 0.016\$/kWh is 25 years.

Table 4.16: Payback periods versus electricity rate range

No	Electricity rate (\$/kWh)	Pay back periods (Years)
1	0.016	25
2	0.029	17
3	0.066	9
4	0.100	6

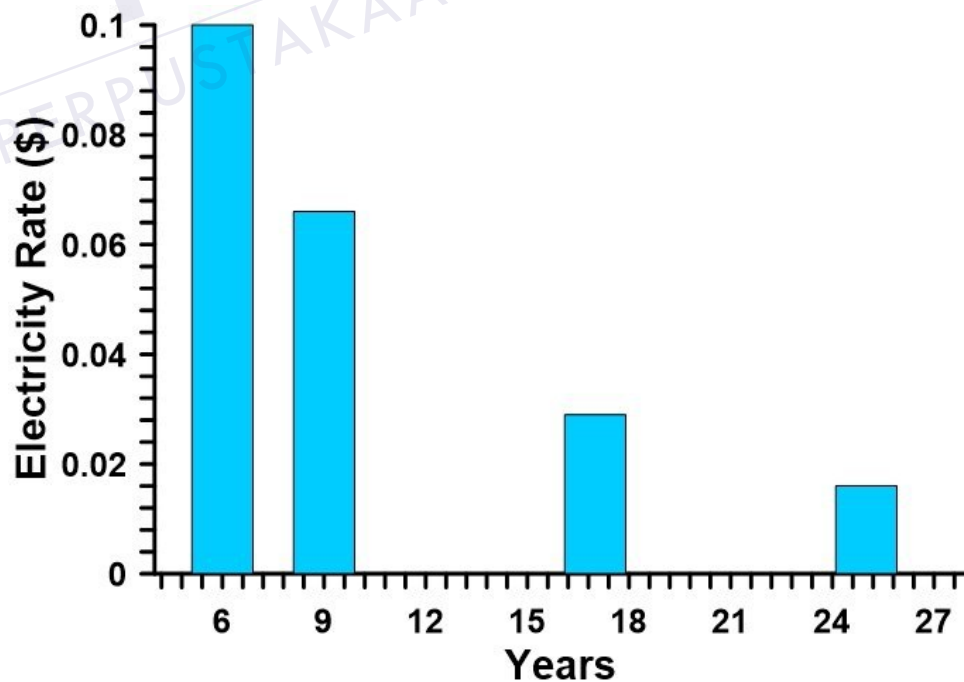


Figure 4.17: Payback periods by electricity rate

Table 4.17: Payback period versus electricity rate range with 50% government subsidy

No	Electricity rate (\$/kWh)	Pay back periods (Years)
1	0.016	12.5
2	0.029	8.5
3	0.066	4.5
4	0.100	3.0

Table 4.16 and Figure 4.17 explain that the payback periods at the rate of 0.016\$/kWh is 25 years, at the rate of 0.029\$/kWh is 17 years, at the rate of 0.066\$/kWh is 9 years, and the rate 0.1\$/kWh is 6 years.

This shows that the payback period decreases as the electricity rate increases. The payback periods become very small at high electricity rate, such as the international electricity range.

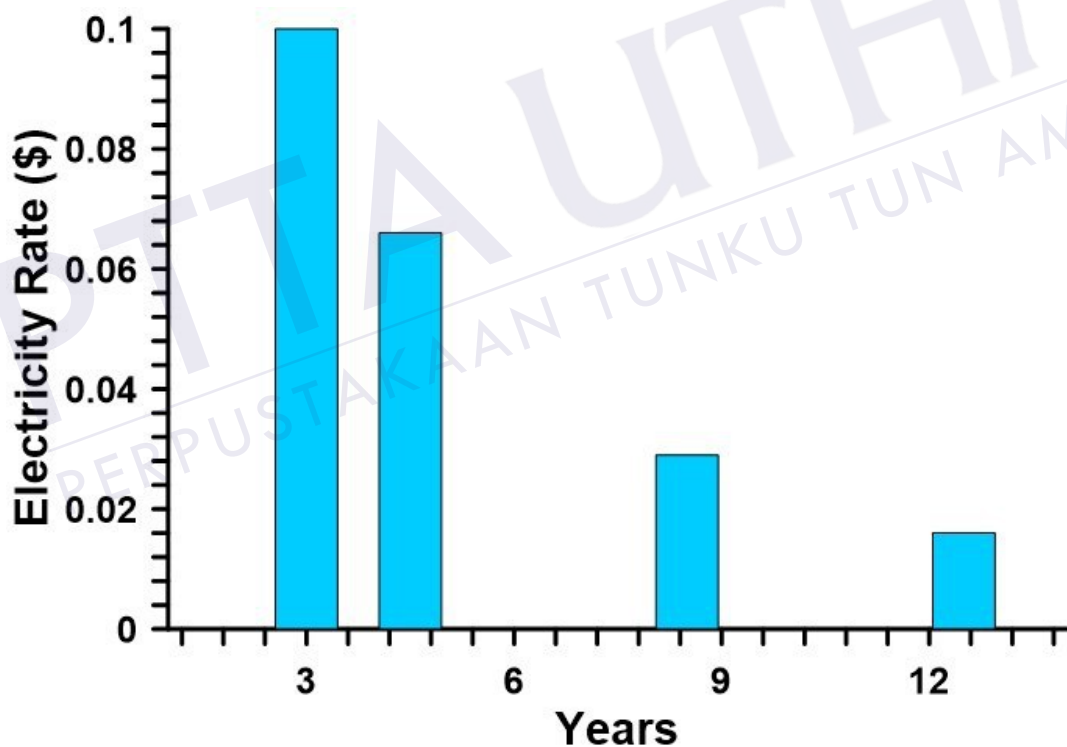


Figure 4.18: Payback periods by electricity rate with 50% government subsidy

In order to improve the economic feasibility of the system, a government subsidy of 50% of the total investment would reduce the PBP for the system, as shown in Table 4.17 and Figure 4.18. The PBP for the solar Absorption system is reduced to 3 years at an electricity rate of \$0.1/kWh, 4.5 years at a rate of \$0.066 /kWh, 8.5 years at a rate of \$0.029/kWh, and 12.5 years at a rate \$0.016/kWh.

4.11 Summary of Simulation Result

To determine the required cooling load of a case study, evaluate the solar effect on the cooling load differences based on different materials and find the cooling system's performance to eliminate the cooling cost. The objectives are achieved by applying CLTD cooling load method for the first objective, applying the BIM software for the second objective and selecting the solar energy system to achieve the third objective. By calculating the cost in each case, the researcher found that elimination in the cost can be achieved, as shown in Table 4.18.

Table 4.18: Summary of the simulation results for the Vapour Compression system and Absorption system

No	Parameters	Vapour Compression system	Absorption system
1	Investment cost (\$).	140,000	213,000
2	Annual Maintenance (\$).	5,600	2,130
3	Annual Electricity (\$).	35,100	3,510
4	Payback periods (Years).	6
5	C.O.P	3.227	0.8048

The simulation results for the Vapour Compression and Absorption systems are summarized in Table 4.18. The Vapour Compression system will set you back \$140,000 over ten years. This indicates that the system's starting cost is \$14,000 per year, and the Absorption system's initial cost is \$213,000 over twenty years. This indicates that the Absorption system's starting cost is \$10,650 per year. According to the chart, the yearly maintenance for the Vapour Compression system is \$5,600, while the annual maintenance for the Absorption system is \$2,130, implying that the Absorption system's annual maintenance is \$3,500 less than the Vapour Compression system's.

The annual electricity cost of the Vapour Compression system is \$35,100. In contrast, the annual electricity cost of the Absorption system is \$3,510, as shown in the table, indicating that the Absorption system's annual electricity cost is substantially cheaper than the Vapour Compression system's.

The chart also reveals that the Absorption system's payback period at a rate of \$0.1 is 6 years. The coefficient of performance of the Vapour Compression system is 3.227, while the maximum coefficient of performance of the Absorption system for May is 0.8048, indicating that the Vapour Compression system's coefficient of

performance is greater than the Absorption system's coefficient of performance. Finally, based on the preceding findings, It is possible to remark that the Vapour Compression system is less cost-effective than the Absorption system.



CHAPTER 5

CONCLUSION AND RECOMMENDATION

5.1 Introduction

This research aims to address the gap between equipment cooling response and non-efficient simulation models to determine the energy consumption that has been achieved in this research. The efforts to solve these tasks start with determining the required cooling load using the Cooling Load Temperature Difference method (CLTD). The calculations depend on the effective factors of residential building characteristics by developing a Microsoft Excel model spreadsheet. This process concerns the boundary conditions of the hot environment, quantities of important baseline parameters such as temperature, air speed, lux capacity and humidity ratio of the internal environment using standard resources. The second objective was the process of evaluating the performance of different materials' effect on the cooling capacity. Two types of materials are applied in building construction to find the differences in solar heat effect. The third objective was to apply two cooling systems that have been used, a conventional vapour-compression system and a solar absorption system. This objective investigates the effect of cooling factors in the residential building, which is necessary to recognize the operation effect of the cooling device and the rate of energy used. The process evaluates the used energy and the cost of selected cooling systems. The result of this study proposed the solar absorption system as a cooling system that can reduce the costs of systems used in cooling buildings. The absorption system was chosen due to its economic results shown in Chapter 4. This chapter presents and describes the overall achievements and the conclusion of this study, which is in line with the study's objectives as stated in Chapter 1. The future

works of the study are presented, and recommendations for future works are also suggested.

5.2 Conclusion

In this research, many of the advanced and specialized methods in the field of air conditioning systems have been addressed. The methodology applied the standard mathematical formula to calculate the heat loss in a residential building and applied two types of air conditioning systems in Kithara city, Baghdad, Iraq country. The scenarios yielded some challenges regarding the air conditioning system operating efficiency, such as the cost of used energy. To achieve the first objective, the amount of cooling load has been calculated based on ASHRAE standard. The assumptions for calculating the cooling load amount considering that the building is used by fifteen persons for twenty-four hours. The light remains not more than seventeen hours, and there is other equipment in the building such as an oven, refrigerator, computer, televisions etc. also, U value for the roof is 0.1337 and 2.31 Watt/ m².°C., depending on the position, U value is 0.55 for windows, while U value for the wall is 5.485 Watt/ m².°C. For the second objective, the study's goal was to determine the long-term benefit of Building Information Modelling (BIM), which involves attaching a BIM model to an energy analysis software/tool to speed up the energy analysis process while providing more complete and accurate data. The researcher also illustrated through a real-world project that Building Information Modelling aids the evaluation of various sustainability methods in the case study. The use of Building Information Modelling was to measure the solar energy, which contributes to/improves a building's energy performance during operation; using the BIM information of energy analysis improves the building's energy recognition. The case study showed that incorporating BIM into the sustainability and energy analysis process aided the team in delivering a building that is 20% more energy efficient. The cooling load has been found and applied in the calculation system of the applied equipment, and the solar absorption system found as a significant system for use in residential buildings due to the consideration of clean energy. The demand for cooling coincides with the presence of solar radiation in areas, and it is possible to take advantage of solar radiation and invest in electricity generation and dispense with the traditional air conditioning system. In

this study, the third objective was to select an absorption system of vapour pressure using solar energy power and compare two systems to determine the differences. The analysis of the experimental data indicated many observations:

- i. The analysis carried out on the proposed two systems shows that the solar absorption system of LiBr/H₂O is more efficient in energy consumption due to the high used power in Baghdad in Iraq.
- ii. The analytical results show that the solar absorption systems are more efficient than the vapour compression systems. The time period has been calculated to recover the initial cost of the absorption system using the payback period method at all rates of electricity.
- iii. The initial cost for the vapour compression system is \$140,000 over a ten-year period, while the initial cost for the solar absorption system is \$213,000 over a twenty-year period. This means that the initial cost for the vapour compression system is \$14,000 per year and the initial cost for the solar absorption system is \$10,650 per year.
- iv. The operating cost of the absorption system is much lower than the vapour compression system since the maintenance cost of the absorption system is \$2,130, while the maintenance cost of the vapour compression system is \$5,600. In addition, the cost of consuming electricity for the absorption system is much less than the cost of electricity consumption for the vapour compression system, as it represents only 10% of the cost of consuming the vapour compression system, only for pumps.
- v. The payback period at the rate of 0.016\$/kWh is 25 years, while at the rate of 0.092\$/kWh is 17 years, at the rate of 0.066\$/kWh is 9 years, and the rate of 0.1\$/kWh is 6 years. It can be concluded that when electricity consumption is high, the payback periods decrease.
- vi. The results also show that 50% of government support from total investment cost reduces the payback periods of the absorption system. The payback periods of the absorption system have become 12.5 years at the rate of 0.016\$/kWh, 8.5 years at the rate of 0.029\$/kWh, 4.5 years at the rate of 0.066\$/kWh, and 3 years at the rate 0.1\$/kWh. Also, the absorption system performance coefficient was estimated during the summer months (May, June, July, and August) using the EES program.

- vii. The coefficient of performance in May was 0.8048, decreasing to 0.7922 in June, 0.7798 in July, and 0.7676 in August, according to the findings. It may be established that weather factors impacting operation circumstances have an impact on the absorption system's performance coefficient. The maximum coefficient of performance occurs in May at temperatures T_g , T_c , T_{abs} , and T_e of 80, 45, 45, and 7.5, respectively, while the lowest coefficient of performance occurs in August at temperatures T_g , T_c , T_{abs} , and T_e of 110, 60, 60, and 7.5, respectively.

5.3 Limitations of the Study

This study has achieved its objectives which were set out above, and concluded some limitations as described below:

- i. The amount of solar radiation determines how much heat is added to the electrical resources. As a result, it depends on the solar collector's size and the number of solar collectors utilized.
- ii. The results of the study would be better if the correlation between heat resources and material composites could be gathered to provide a better representation of the air conditioning community in Baghdad.

5.4 Recommendations

- i. The main issue in calculating the cooling load of the system is the material type. In this case, it is necessary to develop a database which contains the building material with all characteristics and specifications to use them in BIM as a reference.
- ii. The payback period approach was utilized to analyse the economics of the vapour compression and absorption systems in this study. Other methodologies, such as net present value, can be employed for the economic analysis of refrigeration systems and determining economic benefits (NPV).
- iii. It is feasible to design this system based on theoretical results by utilizing the EES software to create a practical model, compute the practical results, and

compare the theoretical coefficient of performance with the coefficient of performance of practical results.

- iv. The software can generate theoretical findings (excellent pack, MATLAB, and TRANSIS). These results can then be compared with the theoretical results extracted from the EES program.
- v. Solar absorption systems may be designed with evacuated tube collectors instead of flat plate collectors because they are readily accessible on the market and have high efficiency.



REFERENCES

- Abdel-Salam, A. H., Ge, G., & Simonson, C. J. (2013). Performance analysis of a membrane liquid desiccant air-conditioning system. *Energy and Buildings*, 62, 559–569.
- Agrouaz, Y., Bouhal, T., Allouhi, A., Kousksou, T., Jamil, A., & Zeraouli, Y. (2017). Energy and parametric analysis of solar absorption cooling systems in various Moroccan climates. *Case Studies in Thermal Engineering*, 9, 28–39.
- Agyenim, F., Knight, I., & Rhodes, M. (2010). Design and experimental testing of the performance of an outdoor LiBr/H₂O solar thermal absorption cooling system with a cold store. *Solar Energy*, 84(5), 735–744.
- Ali Habeeb, Ahmed Abed, Hasanen Mohammed., & Laith Jaafer .(2019). *How to Use Engineering Equation Solver (EES) Refrigeration and Heat Transfer Applications'* Published by Ohio Publishing and Academic Services, USA Copyright © 2019, ISBN: 9781089429357.
- Al-Alili, A., Islam, M. D., Kubo, I., Hwang, Y., & Radermacher, R. (2012). Modeling of a solar powered absorption cycle for Abu Dhabi. *Applied Energy*, 93, 160–167.
- Al-Alili, Ali, Hwang, Y., & Radermacher, R. (2014). Review of solar thermal air conditioning technologies. *International Journal of Refrigeration*, 39, 4–22.
- Al-Dadah, R. K., Jackson, G., & Rezk, A. (2011). Solar powered vapor absorption system using propane and alkylated benzene AB300 oil. *Applied Thermal Engineering*, 31(11–12), 1936–1942.
- Al-Ugla, A. A., El-Shaarawi, M. A. I., Said, S. A. M., & Al-Qutub, A. M. (2016). Techno-economic analysis of solar-assisted air-conditioning systems for commercial buildings in Saudi Arabia. *Renewable and Sustainable Energy Reviews*, 54, 1301–1310.
- Ali Shirazia, Robert A. Taylor, Graham L. Morrison, Stephen D. White (2018). Solar-powered absorption chillers: A comprehensive and critical review. *Energy Conversion and Management*, 59, 123–132.

- Ali, A. H. H., Noeres, P., & Pollerberg, C. (2008). Performance assessment of an integrated free cooling and solar powered single-effect lithium bromide-water absorption chiller. *Solar Energy*, 82(11), 1021–1030.
- Allouhi, A., Kousksou, T., Jamil, A., El Rhafiki, T., Mourad, Y., & Zeraouli, Y. (2015). Economic and environmental assessment of solar air-conditioning systems in Morocco. *Renewable and Sustainable Energy Reviews*, 50, 770–781.
- Antti Ruuska, A., & Tarja Häkkinen, B. (2014). Material Efficiency of Building Construction. *Buildings*, 4(3), 266-294.
- Arayici, Y., Coates, P., Koskela, L., Kagioglou, M., Usher, C., & O'Reilly, K. (2011). "Technology adoption in the BIM implementation for lean architectural practice", *Automation in Construction*, 20,189-195.
- Asim, M., Dewsbury, J., & Kanan, S. (2016). TRNSYS Simulation of a Solar Cooling System for the Hot Climate of Pakistan. *Energy Procedia*, 91, 702–706.
- Ayou, D.S., & Coronas, A., (2020). New developments and progress in absorption chillers for solar cooling applications. *Applied Sciences*, 10(12), 4073.
- Babylon university, Iraq. (2020). Retrieved from <https://uobabylon.edu.iq>.
- Balghouthi, M., Chahbani, M. H., & Guizani, A. (2008). Feasibility of solar absorption air conditioning in Tunisia. *Building and Environment*, 43(9), 1459–1470.
- Bhamare, D. K., Rathod, M. K., & Banerjee, J. (2019). Passive cooling techniques for building and their applicability in different climatic zones. The state of art. *Energy and Buildings*, 198, 467-490.
- Baniyounes, A. M., Rasul, M. G., & Khan, M. M. K. (2013). Assessment of solar assisted air conditioning in Central Queensland's subtropical climate, Australia. *Renewable Energy*, 50, 334–341.
- Bellos, E., & Tzivanidis, C. (2017). Energetic and financial analysis of solar cooling systems with single effect absorption chiller in various climates. *Applied Thermal Engineering*, 126, 809–821.
- Bellos, E., Tzivanidis, C., & Antonopoulos, K. A. (2016). Exergetic, energetic and financial evaluation of a solar driven absorption cooling system with various collector types. *Applied Thermal Engineering*, 102, 749–759.
- Bellos, E., Tzivanidis, C., Symeou, C., & Antonopoulos, K. A. (2017). Energetic, exergetic and financial evaluation of a solar driven absorption chiller – A dynamic approach. *Energy Conversion and Management*, 137, 34–48.

- Berger M, Weckesser M, Weber C, Döll J, Morgenstern A, Häberle A.(2012). Solar driven cold rooms for industrial cooling applications. *Energy Proc*; 30(90), 4–11.
- Bujedo, L. A., Rodríguez, J., & Martínez, P. J. (2011). Experimental results of different control strategies in a solar air-conditioning system at part load. *Solar Energy*, 85(7), 1302–1315.
- Calise F, d'Accadia MD, Vanoli L.(2011). Thermoeconomic optimization of solar heating and cooling systems. *Energy Convers Manage*;52(15),62–73.
- Cao, X., Dai, X., & Liu, J. (2016). Building energy-consumption status worldwide and the state-of-the-art technologies for zero-energy buildings during the past decade. *Energy and buildings*, 128, 198-213.
- Chang, K. C., Lin, W. M., & Chung, K. M. (2013). Solar thermal market in Taiwan. *Energy Policy*, 55, 477–482.
- Dazhang Yang, Y., & Jing Xie, J. (2022). Research and application progress of transcritical CO₂ refrigeration cycle system: a review. *International Journal of Low-Carbon Technologies*, 17, 245-265.
- Desideri, U., Proietti, S., & Sdringola, P. (2009). Solar-powered cooling systems: Technical and economic analysis on industrial refrigeration and air-conditioning applications. *Applied Energy*, 86(9), 1376–1386.
- Eastman, C., Teicholz, P., Sacks, R. & Liston, K. (2011), *BIM Handbook: A Guide to Building Information Modeling for Owners, Managers, Designers, Engineers and Contractors*, 2nd ed., John Wiley and Sons, Hoboken, NJ.
- Stos Tzivanidis, Ioannis Touris (2014).Effect of thermal mass in the cooling and heating loads of buildings. *International Journal of Engineering Technologies and Management Research*. 51(6), 65-74.
- Eicker, U., Pietruschka, D., & Pesch, R. (2012). Heat rejection and primary energy efficiency of solar driven absorption cooling systems. *International Journal of Refrigeration*, 35(3), 729–738.
- Fabian Schmid, Bernd Bierling, & Klaus Spindler. (2019). Development of a solar-driven diffusion absorption chiller. *Solar Energy*, 84(2), 483–493.
- Facão, J., Oliveira, AC. (2011). Numerical simulation of a trapezoidal cavity receiver for a linear Fresnel solar collector concentrator. *Renewable Energy*, 36, 90–6.
- Farah Kojok. (2016). Performance study of hybrid cooling systems for the utilization in buildings. *Energy and Buildings*, 67, 362–372.

- Fasfous, A., Asfar, J., Al-Salaymeh, A., Sakhrieh, A., Al-hamamre, Z., Al-Bawwab, A., & Hamdan, M. (2013). Potential of utilizing solar cooling in the University of Jordan. *Energy Conversion and Management*, 65, 729–735.
- Fong, K. F., Chow, T. T., Lee, C. K., Lin, Z., & Chan, L. S. (2010). Comparative study of different solar cooling systems for buildings in subtropical city. *Solar Energy*, 84(2), 227–244.
- Garousi Farshi, L., Mahmoudi, S. M. S., Rosen, M. A., Yari, M., & Amidpour, M. (2013). Exergoeconomic analysis of double effect absorption refrigeration systems. *Energy Conversion and Management*, 65, 13–25.
- Gebreslassie BH, Guillén-Gosálbez G, Jiménez L, Boer D.(2012). A systematic tool for the minimization of the life cycle impact of solar assisted absorption cooling systems. *Energy*,35(38) 49–62.
- Gomri, R. (2010). Investigation of the potential of application of single effect and multiple effect absorption cooling systems. *Energy Conversion and Management*, 51(8), 1629–1636.
- Hang Y, Du L, Qu M, Peeta S. (2013). Multi-objective optimization of integrated solar absorption cooling and heating systems for medium-sized office buildings. *Renew Energy*;52,67–78.
- Hang, Y., Qu Ming, M., & Zhao, F. (2011). Economical and environmental assessment of an optimized solar cooling system for a medium-sized benchmark office building in Los Angeles, California. *Renewable Energy*, 36(2), 648–658.
- H M Hashim, E Sokolova¹ , O Derevianko¹ , D B Solovev (2018). Cooling Load Calculations. *International Journal of Engineering Technologies and Management Research*. 5;7(8):70-80.
- Helm, M., Keil, C., Hiebler, S., Mehling, H., & Schweigler, C. (2009). Solar heating and cooling system with absorption chiller and low temperature latent heat storage: Energetic performance and operational experience. *International Journal of Refrigeration*, 32(4), 596–606.
- Herold KE, Radermacher R, Klein SA. *Absorption chillers and heat pumps*. 2nd ed. USA: CRC Press; 2016.
- Hidalgo, M. C. R., Aumente, P. R., Millán, M. I., Neumann, A. L., & Mangual, R. S. (2008). Energy and carbon emission savings in Spanish housing air-conditioning using solar driven absorption system. *Applied Thermal*

- Engineering, 28(14–15), 1734–1744.
- Hu, S., Yan, D., & Qian, M. (2019). Using bottom-up model to analyze cooling energy consumption in China's urban residential building. *Energy and Buildings*, 202, 109352.
- Iranmanesh, A, & Mehrabian, MA. (2014). Optimization of a lithium bromide–water solar absorption cooling system with evacuated tube collectors using the genetic algorithm. *Energy Build*, 85(42) 7–35.
- Iraq metrological. (2021). Retrieved from <https://www.iraqmetrological.gov.iq>
- Iraq weather. (2021). Retrieved from <https://www.accuweather.com/en/iq/iraq-weather>.
- Jain, V., Mullick, S. C., & Kandpal, T. C. (2013). A financial feasibility evaluation of using evaporative cooling with air-conditioning (in hybrid mode) in commercial buildings in India. *Energy for Sustainable Development*, 17(1), 47–53.
- James Muye, Dereje S. Ayou, Rajagopal Saravanan., & Alberto Coronas. (2016). Performance study of a solar absorption power-cooling system. *Applied Thermal Engineering*, 28(11–12), 1556–1564.
- Janowiak, M. K., Iverson, L. R., Mladenoff, D. J., Peters, E., Wythers, K. R., Xi, W., ... Ziel, R. (2014). Forest Ecosystem Vulnerability Assessment and Synthesis for Northern Wisconsin and Western Upper Michigan : A Report from the Northwoods Climate Change Response Framework Project. Gen. Tech. Rep. NRS-136. (August), 247.
- Jelinek, M., Levy, A., & Borde, I. (2008). The performance of a triple pressure level absorption cycle (TPLAC) with working fluids based on the absorbent DMEU and the refrigerants R22, R32, R124, R125, R134a and R152a. *Applied Thermal Engineering*, 28(11–12), 1551–1555.
- Jelinek, M., Levy, A., & Borde, I. (2012). Performance of a triple-pressure level absorption/compression cycle. *Applied Thermal Engineering*, 42, 2–5.
- Jing, Y., Li, Z., Liu, L., Lu, S., & Lv, S. (2018). Exergoeconomic-optimized design of a solar absorption- subcooled compression hybrid cooling system for use in low-rise buildings. *Energy Convers Manage*, 165, 465–76.
- Kim, D. S., & Infante Ferreira, C. A. (2009). Air-cooled LiBr-water absorption chillers for solar air conditioning in extremely hot weathers. *Energy Conversion and Management*, 50(4), 1018–1025.

- Koroneos, C., Nanaki, E., & Xydis, G. (2010). Solar air conditioning systems and their applicability-An exergy approach. *Resources, Conservation and Recycling*, 55(1), 74–82.
- Lim, J. H., & Yun, G. Y. (2017). Cooling energy implications of occupant factor in buildings under climate change. *Sustainability*, 9(11), 2039.
- Lizarte, R., Izquierdo, M., Marcos, J. D., & Palacios, E. (2012). An innovative solar-driven directly air-cooled LiBr-H₂O absorption chiller prototype for residential use. *Energy and Buildings*, 47, 1–11.
- Marc, O., Lucas, F., Sinama, F., & Monceyron, E. (2010). Experimental investigation of a solar cooling absorption system operating without any backup system under tropical climate. *Energy and Buildings*, 42(6), 774–782.
- Martínez, P. J., Martínez, J. C., & Martínez, P. (2016). Comparaison de performances de systèmes solaires autonome et assisté à absorption en Espagne. *International Journal of Refrigeration*, 71, 85–93.
- Mazloumi, M., Naghashzadegan, M., & Javaherdeh, K. (2008). Simulation of solar lithium bromide-water absorption cooling system with parabolic trough collector. *Energy Conversion and Management*, 49(10), 2820–2832.
- Mekhilef, S., Saidur, R., & Safari, A. (2011). A review on solar energy use in industries. *Renewable and Sustainable Energy Reviews*, 15(4), 1777–1790.
- Menezes, A. C., Cripps, A., Buswell, R. A., Wright, J., & Bouchlaghem, D. (2014). Estimating the energy consumption and power demand of small power equipment in office buildings. *Energy and Buildings*, 75, 199-209.
- Monné, C., Alonso, S., Palacín, F., & Serra, L. (2011). Monitoring and simulation of an existing solar powered absorption cooling system in Zaragoza (Spain). *Applied Thermal Engineering*, 31(1), 28–35.
- MoE. (2020). Retrieved from <https://www.moelc.gov.iq>
- Mop.iq. (2019). Retrieved from <https://www.mop.gov.iq/>
- Mukesh Waskel , & Sharad Chaudhary.(2016). Cooling Load Estimation Using CLTD/CLF Method for an Educational Building. *International Journal of Engineering Technologies and Management Research*. 7.8(9):20-30.
- Ortiz, M., Barsun, H., He, H., Vorobieff, P., & Mammoli, A. (2010). Modeling of a solar-assisted HVAC system with thermal storage. *Energy and Buildings*, 42(4), 500–509.
- Paoli Jr, (2012). The HVAC process: changing the properties of air. *Journal of*

- Validation Technology, 18(2),75.
- Pongtornkulpanich, A., Thepa, S., Amornkitbamrung, M., & Butcher, C. (2008). Experience with fully operational solar-driven 10-ton LiBr/H₂O single-effect absorption cooling system in Thailand. *Renewable Energy*, 33(5), 943–949.
- Praene, J. P., Marc, O., Lucas, F., & Miranville, F. (2011). Simulation and experimental investigation of solar absorption cooling system in Reunion Island. *Applied Energy*, 88(3), 831–839.
- Prasartkaew, B., & Kumar, S. (2010). A low carbon cooling system using renewable energy resources and technologies. *Energy and Buildings*, 42(9), 1453–1462.
- Priyadumkol, J., & Kittichaikarn, C. (2014). Application of the combined air-conditioning systems for energy conservation in data center. *Energy and Buildings*, 68(PARTA), 580–586.
- Qu, M., Yin, H., & Archer, D. H. (2010). A solar thermal cooling and heating system for a building: Experimental and model based performance analysis and design. *Solar Energy*, 84(2), 166–182.
- Real D, Johnston R, Lauer J, Schicho A, Hotz N. Novel non-concentrating solar collector for intermediate-temperature energy capture. *Sol Energy* 2014;108:421–31.
- Redmond, A., Hore, A., Alshawi, M. & West, R. (2012). “Exploring how information exchanges can be enhanced through Cloud BIM”, *Automation in Construction*, 24, 175-183.
- Rosiek, S., & Batlles, F. J. (2009). Integration of the solar thermal energy in the construction: Analysis of the solar-assisted air-conditioning system installed in CIESOL building. *Renewable Energy*, 34(6), 1423–1431.
- Said, S. A. M., El-Shaarawi, M. A. I., & Siddiqui, M. U. (2012). Alternative designs for a 24-h operating solar-powered absorption refrigeration technology. *International Journal of Refrigeration*, 35(7), 1967–1977.
- Saleh, A., & Mosa, M. (2014). Optimization study of a single-effect water–lithium bromide absorption refrigeration system powered by flat-plate collector in hot regions. *Energy Convers Manage*, 87, 29–36.
- Samuel, E., Esther, j., & Richard , A. (2016). Optimizing energy consumption in building designs using Building Information Model (BIM). *Slovak Journal of Civil Engineering*, 24, 19-28.
- Sarabia Escriva, E. J., Lamas Sivila, E. V., & Soto Frances, V. M. (2011). Air

- conditioning production by a single effect absorption cooling machine directly coupled to a solar collector field. Application to Spanish climates. *Solar Energy*, 85(9), 2108–2121.
- Shekarchian, M., Moghavvemi, M., Motasemi, F., & Mahlia, T. M. I. (2011). Energy savings and cost-benefit analysis of using compression and absorption chillers for air conditioners in Iran. *Renewable and Sustainable Energy Reviews*, 15(4), 1950–1960.
- Shen, L., Xiao, F., Chen, H., & Wang, S. (2013). Investigation of a novel thermoelectric radiant air-conditioning system. *Energy and Buildings*, 59, 123–132.
- Shirazi, A., Taylor, R.A., Morrison, G.L., & White, S.D. (2017). A comprehensive, multi-objective optimization of solar-powered absorption chiller systems for air-conditioning applications. *Energy Convers Manage*, 132, 281–306.
- Shubbar, R.M., Salman, H.H., & Lee, D.I. (2017). Characteristics of climate variation indices in Iraq using a statistical factor analysis. *International Journal of Climatology*, 37(2), 918-927.
- Solomon G, & Adde YA.(2020). Analytical method to calculate room cooling load. *International Journal of Engineering Technologies and Management Research*. 57(8):56-64.
- Soto, Domínguez-Inzunza, & Rivera, 2018. Preliminary assessment of a solar absorption air conditioning pilot plant. *Case Studies in Thermal Engineering*, 12, 672–676.
- Sultan, M., El-Sharkawy, I. I., Miyazaki, T., Saha, B. B., & Koyama, S. (2015). An overview of solid desiccant dehumidification and air conditioning systems. *Renewable and Sustainable Energy Reviews*, 46, 16–29.
- Suman, S., Khan ,MK., & Pathak, M.(2015). Performance enhancement of solar collectors—a review. *Renew Sustain Energy Rev*; 49, 192–210.
- Tehrani, M. M., Beauregard, Y., Rioux, M., Kenne, J. P., & Ouellet, R. (2015). A predictive preference model for maintenance of a heating ventilating and air conditioning system. *IFAC-PapersOnLine*, 28(3), 130–135.
- Thomas, S., & André, P. (2009). Dynamic simulation of a complete solar assisted conditioning system in an office building using TRNSYS Sébastien Thomas and Philippe André Department of sciences and environmental management , University of Liège 185 Avenue de Longwy , 6700 ARLON , Belgiu. 25–32.

- Tristan, G., Kirti, R., & Malcom, C. (2016). Using BIM capabilities to improve existing building energy modelling practices. *Civil and Building Engineering*, 24, 122-137.
- Tsoutsos, T., Aloumpi, E., Gkouskos, Z., & Karagiorgas, M. (2010). Design of a solar absorption cooling system in a Greek hospital. *Energy and Buildings*, 42(2), 265–272.
- Ullah KR, Saidur R, Ping HW, Akikur RK, Shuvo NH.(2013). A review of solar thermal refrigeration and cooling methods. *Renew Sustain Energy*;24, 499–513.
- United National Development. (n.d.). Retrieved July 20, 2019, from <https://www.undp.org/content/undp/en/home/>
- Wang Ping, Guangcai Gong, Yan Zhou, & Bin Qin (2018). A Simplified Calculation Method for Building Envelope Cooling Loads in Central South China. *Building and Environment*, 66, 54–64
- Xu, S. M., Huang, X. D., & Du, R. (2011). An investigation of the solar powered absorption refrigeration system with advanced energy storage technology. *Solar Energy*, 85(9), 1794–1804.
- Xu, Z. Y., Wang, R. Z., & Wang, H. B. (2015). Experimental evaluation of a variable effect LiBr-water absorption chiller designed for high-efficient solar cooling system. *International Journal of Refrigeration*, 59, 135–143.
- Yin, Y. L., Zhai, X. Q., & Wang, R. Z. (2013). Experimental investigation and performance analysis of a mini-type solar absorption cooling system. *Applied Thermal Engineering*, 59(1–2), 267–277.
- Young, M., Less, B. D., Dutton, S. M., Walker, I. S., Sherman, M. H., & Clark, J. D. (2020). Assessment of peak power demand reduction available via modulation of building ventilation systems. *Energy and Buildings*, 214, 109867.
- Yu, S., Evans, M., & Shi, Q. (2014). Analysis of the Chinese market for building energy efficiency (No. PNNL-22761). Pacific Northwest National Lab.(PNNL), Richland, WA (United States).
- Zhai, X. Q., Qu, M., Li, Y., & Wang, R. Z. (2011). A review for research and new design options of solar absorption cooling systems. *Renewable and Sustainable Energy Reviews*, 15(9), 4416–4423.
- Ziwen, L., Qian, W., Vincent, J.L., Gan, & Luke, P.(2020). Envelope Thermal Performance Analysis Based on Building Information Model (BIM) Cloud

Platform— Proposed Green Mark Collaboration Environment. Automation in Construction, 13, 210-232.



APPENDIX A

A1. Investment cost**(A1.1) For vapour compression system**

VC chiller is 350 kW

VC chiller is \$400/ kW

from Table 3.7

$$I.C = 400 \times 350 = 140,000\$$$

(A1.2) For Absorption system

- i. Flat plate collectors

The flat plate collectors are 100(m²)

The flat plate collectors are \$320/m²

from Table 3.7

$$I.C = 320 \times 100 = 32,000\$$$

- ii. Hot water tank

The Hot water tank is 4(m²)

The Hot water tank is \$100/m²

from Table 3.7

$$I.C = 100 \times 4 = 400\$$$

- iii. Absorption chiller

The absorption chiller is 350kW

The absorption chiller is \$516/kW

from Table 3.7

$$I.C = 350 \times 516 = \$180,600.00$$

A2. Annual operation cost

(A2.1) For vapour compression system

i. Annual Maintenance

The annual maintenance for (VC) was 4% of the investment cost (Al-Ugla et al., 2016)

$$\text{Annual maintenance} = 0.04 \times 140,000 = 5,600\$$$

ii. Annual Electricity

As the building is finished, it has a cooling capacity of 225 kWh

$$225 \times 10 \text{ years} \times 13 \text{ h} = 351,000 \text{ kW}$$

Since it is a system operating at more than 4000 kW at the rate of \$ 0.1/ kWh (**Table 3.6**).

$$351,000 \times 0.1 = 35,100\$$$

(A2.2) For absorption system

i. Annual Maintenance

The annual maintenance of the absorption system was 1% of the investment cost (Alluhi et al., 2010).

$$\text{Annual maintenance} = 0.01 \times 213,000 = \$2,130$$

ii. Annual Electricity

The annual Electricity for the absorption system 10% of (VC) only for pumps.

$$0.1 * 35,100 = \$3,510$$

A3. Payback peredios

(A3.1) Payback peredios at a rate (0.1\$/kWh).

Table 1A3.1: Annual operation cost for VC system and Absorption system at rate 0.1\$/kWh

No	Annual operation cost	VC system (\$)	Absorption system (\$)
1	Electricity	35,100	3,510
2	Maintenance	5,600	2,130
3	Total annual operation cost	40,700	5,640

From table (1A3.1), the total annual operating cost for the vapour compression and absorption systems is (\$40,700 and \$5,640), respectively.

$$\text{Annual cash flow} = \$40,700 - \$5,640 = \$35,060$$

$$\text{PBP} = \text{I.C}/\text{ACF}$$

$$\text{PBP} = 213000/35,060$$

$$\text{PBP} = 6 \text{ Years.}$$

(A3.2) Payback peredios at a rate (0.066\$/kWh).

Table 1A3.2: Annual operation cost for VC system and Absorption system at a rate 0.066\$/kWh.

No	Annual operation cost	VC system (\$)	Absorption system(\$)
1	Electricity	23,166	2,316
2	Maintenance	5,600	2,130
3	Total annual operation cost	28,766	4,446

From table (1A3.2). The total annual operating cost for the vapour compression and absorption systems is (\$28,766 and \$4446), respectively.

$$\text{Annual cash flow} = \$28,766 - \$4,446 = \$24,320$$

$$\text{PBP} = 213000/24,320$$

$$\text{PBP} = 9 \text{ Years.}$$

(A3.3) Payback peredios at rate (0.029\$/kWh).

Table 1A3.3: Annual operation cost for VC system and Absorption system at a rate of 0.029\$/kWh.

No	Annual operation cost	VC system (\$)	Absorption system (\$)
1	Electricity	10,179	1,107
2	Maintenance	5,600	2,130
3	Total annual operation cost	15,779	3,147

From table (1A3.3), the total annual operating cost for the vapour compression and absorption systems is (\$15,779 and \$3,147), respectively.

$$\text{Annual cash flow} = \$15,779 - \$3,147 = \$12,632$$

$$\text{PBP} = 213.000 / 12,632$$

$$\text{PBP} = 17 \text{ Years.}$$

(A3.4) Payback peredios at rate (0.016\$/kWh).

Table 1A3.4: Annual operation cost for VC system and Absorption system at a rate of 0.016\$/kWh.

No	Annual operation cost	VC system (\$)	Absorption system (\$)
1	Electricity	5,616	562
2	Maintenance	5,600	2,130
3	Total annual operation cost	11,216	2,692

From table (1A3.4), the total annual operating cost for the vapour compression system and absorption system is (\$11,216\$ and \$2,642), respectively.

$$\text{Annual cash flow} = \$11,216 - \$2,642 = \$8,524$$

$$\text{PBP} = 213.000 / 8,524$$

$$\text{PBP} = 25 \text{ Years}$$

APPENDIX B

B1. Coefficient of performance for Vapor compression system

First calculate mass flow rate of refrigerant for the system by equation **3-26**

$$m = \frac{225}{(406.7 - 269.6)} = 1.641 \text{ kg/sec}$$

The work of the compressor is calculated from equation **3-23**

$$W = 1.641 (449.2 - 406.7) = 69.73 \text{ kW}$$

The Coefficient of performance is calculated from equation **3-27**

$$C.O.P = \frac{225}{69.73} = 3.227$$

B2. Coefficient of performance for Absorption system in May

$$m_r = \frac{225}{2514 - 188.4} = 0.09674 \text{ kg/sec} \quad \text{From equation 3.20}$$

$$m_{ws} = \frac{0.47 * 0.09674}{0.19} = 0.239 \text{ kg/sec} \quad \text{From equation 3.19}$$

$$m_{ss} = \frac{0.66 * 0.09674}{0.19} = 0.336 \text{ kg/sec} \quad \text{From equation 3.18}$$

$$Q_g = 0.09674 * 2643 + 0.236 * 232.8 - 0.336 * 92.67 = 279.6 \text{ kW} \quad \text{From equation 3.17}$$

$$C.O.P = \frac{225}{279.6} = 0.8048 \quad \text{From equation (3-22).}$$

B3. All parameters exist for the EES soft wear program

Table 1B3: Average temperature during the observant parts of the system during the summer

No.	Q (kW)	May	June	July	August
1	Q_{abs}	255.7	259.6	263.6	267.6
2	Q_{cond}	237.5	239.2	240.9	242.6
3	Q_{cool}	439.1	498.1	504.5	510.2
4	Q_{evap}	225.0	225.0	225.0	225.0
5	Q_{gen}	279.6	284	288.5	293.1

Table 2B3: The enthalpy rate in the absorption system

No	H (kJ/kg)	May	June	July	August
1	h_1	92.67	104.1	115.5	127
2	h_2	232.8	230.3	267.8	285.5
3	h_3	2643	2660	2676	2691
4	h_4	188.4	209.3	230.2	251.2
5	h_5	2514	2514	2514	2514

Table 3B3: The mass flow rate in parts of the Absorption system

No.	\dot{m} (kg/s)	May	June	July	August
1	\dot{m}_r	0.09674	0.09761	0.09851	0.09942
2	\dot{m}_{ss}	0.3311	0.3341	0.3372	0.3402
3	\dot{m}_{ws}	0.2344	0.2365	0.2387	0.2409
4	\dot{m}_{cw}	12.0	12.0	12.0	12.0

Table 4B3: The enthalpy rate in the vapour compression system

No.	H (kJ/kg)
1	406.7
2	449.2
3	269.6
4	269.6

APPENDIX C

C1. Codes of EES program of absorption system and vapor compression system.

```

"-----"
      "Standard VCRS "
"      2019/12/6      "
"      "      "
"-----"

"INPUT DATA "
"===== "

"Refrigerant : R134a"

Qevap=225 [kW]
Tevap= -5
Tc=54.4
Tc_sub=0
T1= 0 [C]
ETA_V=0.9

"Solution"
"===== "

"general pressure"

P_Evap=P_sat (R22,T=Tevap)
Pc=P_sat (R22,T=Tc)

"nood 1"
h1=Enthalpy (R22, P=P_Evap, T=T1)
S1=Entropy (R22, P=P_Evap, T=T1)
V1=Volume (R22,P=P_Evap,T=T1)

"nood 2"
S2=S1
h2=Enthalpy (R22, S=S2, P=Pc)

"nood 3"
h3=Enthalpy (R22, P=Pc, X=0)

"nood 4"
h3=h4

-----"mass flow rates -----"

mass=Qevap/(h1-h4)

----- "mass and energy Balance-----"

----- "Condenser Heat Reject -----"

Q_cond=mass*(h2-h3)

-----"Compressor Power -----"

```

$$\text{Power}=\text{mass}*(\text{h2}-\text{h1})$$

_____ "COP -----"

$$\text{COP}=\text{Q_evap}/\text{Power}$$

"----- _____END -----"

" August"

" 16 / 12 / 2019"

" -----"

"Input Data"

$$\text{Xss}=0.47$$

$$\text{Xws}=0.664$$

$$\text{T_gen}=110$$

$$\text{T_cond}=60$$

$$\text{T_evap}=7.5$$

$$\text{T_abs}=60$$

$$\text{Tw_in}=25 \text{ [C]}$$

$$\text{m_cw}=12 \text{ [kg/s]}$$

$$\text{Q_Evap}=225 \text{ [kW]}$$

" -----"

" Solution"

$$\text{h3}=\text{Enthalpy (Steam, T=T_gen=1)}$$

$$\text{h4}=\text{Enthalpy (Steam, T=T_cond=0)}$$

"Refrigeration Capacity"

$$\text{h5}=\text{Enthalpy (Steam, T=T_evap, X=1)}$$

$$\text{m_dot_r}=\text{Q_Evap}/(\text{h5}-\text{h4})$$

" Generator mass Balance"

$$\text{m_dot_ss}-\text{m_dot_r}=\text{m_dot_ws}$$

"LiBr balance in concentrater"

$$\text{m_dot_ss}*\text{Xss}=\text{m_dot_ws}*\text{Xws}$$

"Lama Calculation"

$$\text{Lamda}=\text{m_dot_ss}/\text{m_dot_r}$$

" COP"

$$\text{Q_Gen}+\text{m_dot_ss}*\text{h1}=\text{m_dot_ws}*\text{h2}+\text{m_dot_r}*\text{h3}$$

$$\text{h1}=\text{h_LiBrH2o (T_abs, Xss)}$$

$$\text{h2}=\text{h_LiBrH2o (T_gen, Xws)}$$

$$\text{COP}=\text{Q_Evap}/\text{Qgen}$$

" Condenser leaving Temperature"

$$\text{Cp_water}=4.18$$

$$\text{Q_abs}+\text{m_dot_ws}*\text{h2}=\text{m_dot_ws}*\text{h2}+\text{m_dot_r}*\text{h3}$$

$$\text{Q_cond}=\text{m_dot_r}*(\text{h3}-\text{h4})$$

$$Q_{\text{cooling}}=Q_{\text{abs}}+Q_{\text{cond}}$$

$$Q_{\text{cooling}}=m_{\text{cw}}*Cp_{\text{water}}*(Tw_{\text{out}}-Tw_{\text{in}})$$

" July"

" 16 / 12 / 2019"

" -----"

"Input Data"

$$X_{\text{ss}}=0.47$$

$$X_{\text{ws}}=0.664$$

$$T_{\text{gen}}=100$$

$$T_{\text{cond}}=55$$

$$T_{\text{evap}}=7.5$$

$$T_{\text{abs}}=55$$

$$Tw_{\text{in}}=25 \text{ [C]}$$

$$m_{\text{cw}}=12 \text{ [kg/s]}$$

$$Q_{\text{Evap}}=225 \text{ [kW]}$$

" -----"

" Solution"

$$h3=\text{Enthalpy (Steam, } T=T_{\text{gen}}, X=1)$$

$$h4=\text{Enthalpy (Steam, } T=T_{\text{cond}}, X=0)$$

"Refrigeration Capacity"

$$h5=\text{Enthalpy (Steam, } T=T_{\text{evap}}, X=1)$$

$$m_{\text{dot}_r}=Q_{\text{Evap}}/(h5-h4)$$

" Generator mass Balance"

$$m_{\text{dot}_{\text{ss}}}-m_{\text{dot}_r}=m_{\text{dot}_{\text{ws}}}$$

"LiBr balance in concentrater"

$$m_{\text{dot}_{\text{ss}}}*X_{\text{ss}}=m_{\text{dot}_{\text{ws}}}*X_{\text{ws}}$$

"Lama Calculation "

$$\text{Lamda}=m_{\text{dot}_{\text{ss}}}/m_{\text{dot}_r}$$

" COP"

$$Q_{\text{Gen}}+m_{\text{dot}_{\text{ss}}}*h1=m_{\text{dot}_{\text{ws}}}*h2+m_{\text{dot}_r}*h3$$

$$h1=h_{\text{LiBrH}_2\text{o}}(T_{\text{abs}}, X_{\text{ss}})$$

$$h2=h_{\text{LiBrH}_2\text{o}}(T_{\text{gen}}, X_{\text{ws}})$$

$$\text{COP}=Q_{\text{Evap}}/Q_{\text{Gen}}$$

" Condenser leaving Temperature"

$$Cp_{\text{water}}=4.18$$

$$Q_{\text{abs}}+m_{\text{dot}_{\text{ws}}}*h2=m_{\text{dot}_{\text{ws}}}*h2+m_{\text{dot}_r}*h3$$

$$Q_{\text{cond}}=m_{\text{dot}_r}*(h3-h4)$$

$$Q_{\text{cooling}}=Q_{\text{abs}}+Q_{\text{cond}}$$

$$Q_{\text{cooling}}=m_{\text{cw}}*Cp_{\text{water}}*(Tw_{\text{out}}-Tw_{\text{in}})$$



```

"      June"
"      16 / 12 / 2019"

" -----"

"Input Data"

Xss=0.47
Xws=0.664

T_gen=90
T_cond=50
T_evap=7.5
T_abs=50
Tw_in=25 [C]
m_cw=12 [kg/s]

Q_Evap=225 [kW]

" -----"
"      Solution"

h3=Enthalpy (Steam, T=T_gen, X=1)
h4=Enthalpy (Steam, T=T_cond, X=0)

"Refrigeration Capacity"

h5=Enthalpy (Steam, T=T_evap, X=1)
m_dot_r=Q_Evap/(h5-h4)

"      Generator mass Balance"
m_dot_ss-m_dot_r=m_dot_ws

"LiBr balance in concentrater"

m_dot_ss*Xss=m_dot_ws*Xws

"Lama Calculation"

Lamda=m_dot_ss/m_dot_r

" COP"

Q_Gen+m_dot_ss*h1=m_dot_ws*h2+m_dot_r*h3
h1=h_LiBrH2o (T_abs, Xss)
h2=h_LiBrH2o (T_gen, Xws)

COP=Q_Evap/Q_Gen

" Condenser leaving Temperature"
Cp_water=4.18

Q_abs+m_dot_ws*h2=m_dot_ws*h2+m_dot_r*h3

Q_cond=m_dot_r*(h3-h4)

Q_cooling=Q_abs+Q_cond

Q_cooling=m_cw*Cp_water*(Tw_out-Tw_in)

```

```

"      May"
"      16 / 12 / 2019"

" -----"

"Input Data"

Xss=0.47
Xws=0.664
T_gen=80
T_cond=45
T_evap=7.5
T_abs=45
Tw_in=25 [C]
m_cw=12 [kg/s]
Q_Evap=225 [kW]

" -----"
"              Solution"

h3=Enthalpy (Steam, T=T_gen, X=1)
h4=Enthalpy (Steam, T=T_cond, X=0)

"Refrigeration Capacity"

h5=Enthalpy (Steam, T=T_evap, X=1)
m_dot_r=Q_Evap/(h5-h4)

"      Generator mass Balance"
m_dot_ss-m_dot_r=m_dot_ws

"LiBr  balance in concentrater"

m_dot_ss*Xss=m_dot_ws*Xws

"Lama Calculation"

Lamda=m_dot_ss/m_dot_r

"  C O P"

Q_Gen+m_dot_ss*h1=m_dot_ws*h2+m_dot_r*h3
h1=h_LiBrH2o (T_abs, Xss)
h2=h_LiBrH2o (T_gen, Xws)
COP=Q_Evap/Q_Gen

"  Condenser leaving Temperature"
Cp_water=4.18
Q_abs+m_dot_ws*h2=m_dot_ws*h2+m_dot_r*h3

Q_cond=m_dot_r*(h3-h4)

Q_cooling=Q_abs+Q_cond

      Q_cooling=m_cw*Cp_water*(Tw_out-Tw_in

```

C2. QUESTION OF HVACS STUDY

This research aims to reduce the costs of systems used in cooling buildings in Iraq, where two commonly used cooling systems are used, the vapour compression system and the absorption system. Since you are the expert in the industry, we require expert opinions to identify which of the listed factors are relevant to the Iraq situation. It would be greatly appreciated if you could contribute your opinion based on your vast experience in the field of air conditioning in Iraq.

Instruction: Please fill in the blanks or mark \checkmark in the box.

1. Name of company/organization: _____

2. Company Address: _____

2. Company Address: _____

3. Type of organization?

Consultant

Contractor

Client

Others please specify _____

4. What is your organization category?

Government

Private

Others please specify _____

5. What type of Projects are undertaken by Your Company?

Residential

Industrial

Commercial

Institutional Care

Educational

Others, please specify _____

6. State the size of projects that you are involved with in terms of contract amount in Iraqi Dinar currency.

S.R. _____

7. What is the highest academic qualification you have achieved?

Diploma

Bachelor Degree

 Master Degree Doctor of Philosophy

8. State your position in the organization.

 Project Manager General Manager Planner Construction Manager Cost Engineer Others, please specify-----

9. State the number of years you have practiced the working in Iraqi air conditioning.

 0 – 5 years 6 – 10 years 11 – 15 Years 16 – 20 Years 21 – 25 Years More than 25 Years

10. How do you classify your company?

 Consultant Contractor Client Others please specify -----

11. How do you describe your company projects?

 Residential Industrial Commercial Institutional Care Educational Others, please specify-----

12. Please state the average project contract amount (in Iraqi Dinar) that your company is usually involved with.

S.R -----

-Thank you for the Contributions

LIST OF PUBLICATIONS

Journal Publications

1. Ali Abduqader, Zamri Noranai & Ahmed imran (2021). Solar absorption cooling systems: A review of International Journal of Thermal Engineering, Vol 7, Issue: 4, pp.970-983. (ISSN: 2148-7847).
2. Ali Abduqader, Zamri Noranai & Ali Habeeb (2019). Study of the coefficient of performance of a solar absorption system during the summer for residential building. Test Engineering and Management. (ISSN: 01934120).



PTTA UTHM
PERPUSTAKAAN TUNKU TUN AMINAH

VITA

The author was born on July 20, 1987, in Baghdad city, Iraq. He went to AL FAROOQ School in ALJAMIMAH district for his primary school education for 6 years. For his secondary school, he studied at ALKINDY School in Baghdad province for 6 years. After completing his secondary school education, he succeeded in getting enrolled in University of Technology in 2006, graduating with the Bachelor of Mechanical Engineering with Honors second class upper in 2010. He started working as a mechanical engineer in Iraq immediately after his graduation in 2010 and he pursued his Master's study in Mechanical engineering under research program in University Tun Hussein Onn Malaysia (UTHM) in February 2018. During his M. Sc. research work, he was actively involved in research and published 2 research papers (2 Journal by Scopus). He is a member of the Iraqi Council of Engineering.



PTTA UTHM
PERPUSTAKAAN TUNKU TUN AMINAH